

MERCURY SPECIATION IN AIR FROM COAL FIRED POWER STATIONS

Lulamile Theo Jongwana

A thesis submitted to the School of Chemistry, Faculty of Science, University of the
Witwatersrand, Johannesburg in fulfilment of the requirement for the degree of Doctor of
Philosophy

Johannesburg, 2014

Declaration

I declare that this thesis is my own, unaided work. It is being submitted for the Degree of Doctor of Philosophy to the University of the Witwatersrand, Johannesburg. It has not been submitted before for any degree or examination to any other university.

.....
(Signature of Candidate)

.....day of..... 2014

ABSTRACT

Mercury occurs naturally and as a result of human activities. One such activity is the combustion of mineral-enriched, sub-bituminous coal to produce electricity—an industry that has existed for over 100 years. Although coal is absolutely necessary to supply the power that South Africa and its neighbouring countries requires, the emitted gases, especially mercury, impact the environment and present a complex array of health-related problems. Controlling the impact of mercury present in the environment depends on the efforts of governments, scientists, business and industry, agriculture, environmental organizations and individuals. Mercury is emitted from the point sources in different forms. Accurate determination of the emitted forms or species of mercury has become a global interest. Determination of the various mercury species requires several well-understood analytical techniques for the confident assessment of potentially contaminated samples.

This study focuses on the development, validation and application of analytical methodologies that are capable of differentiating between the different forms of mercury in environmental samples (air, liquids and solids) from coal-fired power plants. Capillary electrophoresis with amperometric detection, high performance liquid chromatography with amperometric detection, and atomic fluorescence spectrometry methods were developed for mercury speciation. Very low detection limits observed using the methods. For capillary electrophoresis with amperometric detection, the detection limits were $0.005 \pm 0.002 \mu\text{g/l}$ for Hg^{2+} and $0.4 \pm 0.05 \mu\text{g/l}$ for MeHg^+ . Detection limits of $2 \pm 0.04 \text{ ppt}$ and $0.01 \pm 0.02 \mu\text{g/l}$ for Hg^{2+} were observed for high performance liquid chromatography with amperometric detection and atomic fluorescence spectrometry respectively. These detection limits are attractive for the monitoring of mercury in the environment.

Total mercury in solids (coal and ash) was measured by direct mercury measurement using a well-established method, involving the use of the mercury analyzer LECO AMA-254. Total gaseous mercury was measured using the Tekran 2537B system.

On application to environmental samples, very good correlations in results were observed between the different methods. Mercury speciation in South African coal after acid extraction showed that only Hg^{2+} species was detected from the extracts and that 96% of total Hg in acid extracts is in the Hg^{2+} species form.

Different trends in Hg speciation results at the Elandsfontein Air Quality Monitoring (AQM) station were observed over the sampling period. During winter sampling, Hg^{2+} was the predominant species, while Hg^0 was predominant the species during summer sampling. Mercury speciation carried out at Duvha Power Station (units 1 and 2), equipped with fabric filter devices, revealed that the predominant form of Hg after the fabric filter devices was Hg^{2+} , due to oxidation of Hg^0 to Hg^{2+} as the flue gas temperature decreases. Mercury speciation at the Majuba Underground Coal Gasification flare revealed that although mercury is emitted from power plants in the form of different chemical species, with each species have a different fate in the atmosphere, the climate, wind direction and terrain also play roles in the transport of mercury emissions. Therefore, it is difficult to predict the transport patterns of emissions. Nonetheless, with correct measuring equipment and modelling, the patterns of emissions should be able to be predicted.

The patterns observed and data recorded at the Elandsfontein AQM station and Duvha Power Station, respectively, were however, insufficient to permit accurate modelling. This study raised a number of other questions which are too comprehensive for this study to address. Therefore, more comprehensive atmospheric and combustion studies should be done.

ACKNOWLEDGEMENTS

I would like to express my appreciation to:

- Prof. Andrew M. Crouch, for his support, encouragement, guidance and expertise throughout my study.
- Mrs Jenny Reeves, Mr Gerhard Gericke and Mr Siven Naidoo for their valuable advice, guidance and support.
- Eskom, University of Witwatersrand and the National Research Foundation (NRF) for their financial support.
- Mr. B. Botha from the Physics Workshop at Stellenbosch University for constructing the cross hair designs for electrochemical detection.
- My family for their unfailing belief in me.
- To my Saviour, my Healer, my Deliverer, my Friend, my Counsellor my Lord Jesus Christ who made everything possible. I honour You for all the blessings and favours in my life.

CONTENTS

Declaration	i
Abstract	ii
Acknowledgements	iv
List of figures	xi
List of tables	xiv
List of abbreviations	xvi
Publications and conference contributions	xix

CHAPTER 1: BACKGROUND, MOTIVATION AND OBJECTIVES

1.1 Background	1
1.2 Project motivation	2
1.3 Aims and objectives	4
1.4 Layout of the thesis	5

CHAPTER 2: INTRODUCTION AND LITERATURE SEARCH

2.1 Introduction	6
2.2 Literature search	7
2.2.1 Properties of mercury	7
2.2.2 Sources of mercury	7
2.2.3 Uses of mercury	8
2.2.4 Negative influence of mercury in humans	8
2.2.5 Mercury species and transformation in the atmosphere	9
2.2.6 Mercury speciation	12
2.2.7 Modelling mercury atmospheric transport, chemistry and deposition	14
2.3 Problem statement	17
2.4 Regulatory drivers in South Africa and other countries	19

CHAPTER 3: ANALYTICAL METHODOLOGIES FOR MERCURY DETERMINATION

3.1 Analytical techniques for identifying Hg in coal and its products	21
3.2 Methods of sampling and measuring mercury species in flue gases (or air)	22
3.2.1 Gaseous sampling methods	22
3.3 Separation and detection techniques for mercury speciation	25
3.4 Analytical techniques used for Hg speciation in this study	27
3.4.1 Capillary Electrophoresis	27
3.4.1.1 Basic instrument configuration	28
3.4.1.2 Influence applied voltage on migration time	29
3.4.1.3 Electroosmotic	29
3.4.1.4 Injection modes	33
3.4.1.5 Separation modes	34
3.4.1.6 Detection in capillary electrophoresis	34
(a) UV-Visible detection	35
(b) Fluorescence	36
(c) Electrochemical Detection	36
(d) Photodiode-array detection	36
3.4.2 High performance liquid chromatography	37
3.4.3 Atomic Fluorescence Spectrometry	37
3.4.4 LECO automatic mercury analyser (AMA-254)	38

CHAPTER 4: METHOD DEVELOPMENTS FOR CAPILLARY ELECTROPHORETIC SEPARATION AND POST-COLUMN ELECTROCHEMICAL DETECTION OF MERCURY AND METHYL MERCURY AND APPLICATIONS TO COAL SAMPLES

4.1 Reagents and materials	40
4.2 Preparation of standard solutions	42
4.3 Experimental	42
4.3.1 Sample preparation	42
4.3.2 Capillary electrophoresis	43
4.3.3 Electrochemical detector (amperometric detection)	44
4.3.4 Cyclic voltammetry	45
4.4 Results and discussion	46
4.4.1. Cyclic voltammetry	46
4.4.2. Optimization of CE–AD parameters	47
4.5 Method validation	50
4.5.1 Calibration curve	50
4.6 Analysis of coal samples for mercury with CE-UV	53
4.7 Analysis of coal samples for mercury with CE–AD	55
4.8 Hg detection limits with CE	56
4.9 Conclusion	58

CHAPTER 5: MERCURY SPECIATION IN SOUTH AFRICAN COAL

5.1 Reagents	59
5.2 Experimental procedures	60
5.2.1 Coal samples	60
5.2.2 Acid leaching of coal samples and reference materials	61
5.2.3 Capillary electrophoresis	61
5.2.4 LECO automatic mercury analyzer (AMA-254)	62
5.3 Results and discussion	62

5.3.1. Total Hg and Hg species analysis in coal standards and samples using AMA-254 and CE	62
5.3.2 Analysis of coal samples for Hg species with CE-PDA	65
5.4 Calibration curves	68
5.5. Conclusion	69

CHAPTER 6: SAMPLING AND MERCURY SPECIATION WITHIN THE POWER STATION PROCESSES

6.1 Sampling for mercury speciation	71
6.1.1 Sampling reagents	71
6.2 Hg speciation at Duvha Power Station	72
6.2.1 Site descriptions	72
6.2.2 Sampling procedures at the stack at Duvha Power Station	72
6.3 Speciation analysis	75
6.3.1 High performance liquid chromatography coupled with an amperometric detector	75
6.3.1.1 Reagents	75
6.3.1.2 Chromatographic conditions	76
6.3.1.3 Analysis of the samples	76
6.3.2 Atomic fluorescence spectrometry	77
6.3.2.1 Reagents	77
6.3.2.2 Calibration solutions	78
6.3.2.3 Analysis of the samples	78
6.4 Results and discussion	79
6.4.1 High performance liquid chromatography coupled with an amperometric detector	79
6.4.1.1 Optimum conditions for separation	79
6.4.1.2 Linearity and detection limits	80
6.4.1.3 Recovery efficiency and accuracy studies	81
6.4.2 Atomic fluorescence spectrometry	81
6.4.2.1 Linearity and detection limits	81
6.4.2.2 Quality control check and recovery efficiency	82

6.5 Hg speciation in flue gas	83
6.6 Overall mercury balance	85
6.7 Conclusions	87

CHAPTER 7: AIR QUALITY MONITORING OF MERCURY SPECIES AROUND THE POWER PLANTS

7.1 Sampling for mercury speciation	88
7.1.1 Total gaseous Hg measurement	89
7.1.2 Atmospheric Hg speciation	89
7.1.3 Sampling at Majuba UCG flare	90
7.2 Site descriptions of sampling points	90
7.2.1 Elandsfontein Air Quality Monitoring (AQM) station	90
7.2.2 Wind rose at Elandsfontein AQM station	91
7.2.3 Majuba UCG plant flare	92
7.2.4 Wind rose at Majuba UCG flare	93
7.3 Analysis	94
7.4 Results and discussion	95
7.4.1 Hg speciation at Elandsfontein AQM station	95
7.4.2 Hg speciation at the flare of Majuba UCG plant	100
7.5 Conclusions	102
7.5.1 Hg speciation at Elandsfontein AQM station	102
7.5.2 Hg speciation at Majuba UCG flare	102

CHAPTER 8: THE USE OF MODELLING PROCESSES TO PREDICT MERCURY SPECIATION AT DUVHA POWER STATION AND IN AMBIENT AIR

8.1 Modelling of Hg in flue gas at Duvha Power Station	103
8.1.1 Chemked – A program for chemical kinetics of gas-phase reactions	104
8.2 Result of modelling Hg in flue gas	105

8.2.1 Comparison of results obtained in this study to international studies	107
8.3 Modelling of Hg at Elandsfontein Air Quality Monitoring Station	107

CHAPTER 9: SUMMARY, CONCLUSIONS AND

RECOMMENDATIONS FOR FUTURE RESEARCH

9.1 Summary	109
9.2 Conclusions	110
9.3 Recommendations	110

REFERENCES	112
-------------------	-----

APPENDICES

Appendix 1: Electropherograms for analysis of coal samples from different Power stations	127
Appendix 2: Photographs of analytical instruments used	129
Appendix 3: Copyright clearance to use the publications information	131

LIST OF FIGURES

Figure 2.1: Model of interaction between mercury species in the atmosphere	10
Figure 2.2: Explanation of why mercury should be controlled	18
Figure 3.1: Schematic of the Ontario Hydro mercury speciation method impinger train	23
Figure 3.2: Schematic of CE instrument	29
Figure 3.3: Illustration of the origin of the EOF	30
Figure 3.4: Schematic representation of CE separation	33
Figure 4.1a: Schematic representation of the newly developed CE-AD cross hair design	44
Figure 4.1b: Picture of CE–AD cross hair design for Hg speciation	44
Figure 4.2: CE-AD cross hair design for mercury speciation	45
Figure 4.3: Cyclic voltamogram of a Au micro electrode	46
Figure 4.4: Separation of 1.0 $\mu\text{g/l Hg}^{2+}$	47
Figure 4.5: Separation of 100 $\mu\text{g/l MeHg}^+$	49
Figure 4.6: Separation of 50 $\mu\text{g/l MeHg}^+$	50
Figure 4.7a: Calibration curve of Hg^{2+} with CE-AD	51
Figure 4.7b: Calibration curve of MeHg^+ with CE-AD	51
Figure 4.8: Separation of 20 $\mu\text{g/l Hg}^{2+}$ and 10 $\mu\text{g/l MeHg}^+$	52
Figure 4.9: Electropherogram of SARM 20	54
Figure 4.10: Electropherogram of SARM 18	54
Figure 4.11: Electropherogram of coal sample C1632	55
Figure 4.12: Separation of (SARM 20) 0.4 $\mu\text{g/l}$	56
Figure 5.1: Regional power plants	60

Figure 5.2: Comparison of total Hg results in coal samples and acid extracts	65
Figure 5.3: Electropherogram of SARM 20	67
Figure 5.4: Electropherogram of Duvha coal sample	67
Figure 5.5: Calibration curve of Hg ²⁺ with CE-PDA	68
Figure 6.1: Schematic diagram of unit 1 and 2 at Duvha power station	73
Figure 6.2: Sampling at the stack in Duvha Power Station. (A) Sampling personnel; (B) sampling train	74
Figure 6.3: Chromatogram of a standard solution Hg ²⁺ using HPLC-AD	79
Figure 6.4: Calibration curve of Hg ²⁺ determined with HPLC-AD	80
Figure 6.5: Calibration curve of total Hg determined with AFS	81
Figure 6.6: Mercury chemisorption model	85
Figure 7.1: Google map for sampling location and regional power plants around Elandsfontein AQM station	91
Figure 7.2: Wind rose from Elandsfontein AQM station	92
Figure 7.3: Majuba Power Station with UCG plant	93
Figure 7.4 Wind rose from the Majuba pilot plant	94
Figure 7.5 (a): Patterns of speciated Hg and TGM at Elandsfontein AQM station (June 2010)	96
Figure 7.5 (b): Patterns of speciated Hg and TGM at Elandsfontein AQM station (Jan 2011)	97
Figure 7.5 (c): Patterns of speciated Hg and TGM at Elandsfontein AQM station (June 2011)	97
Figure 7.5 (d): Patterns of speciated Hg and TGM at Elandsfontein AQM station (Jan 2012)	98

Figure 7.6: Summary of some of the important physical and chemical transformations of mercury in atmosphere	99
Figure 8.1: Model predictions for the rate of production of the reactions involving HgCl ₂	106
Figure A1.1: Electropherogram of SARM 18	127
Figure A1.2: Electropherogram of Arnot coal sample	127
Figure A1.3: Electropherogram of Lethabo coal sample	128
Figure A1.4: Electropherogram of Hendrina coal sample	128
Figure A2.1: Beckman Coulter P/ACE MDQ instrument for capillary electrophoresis	129
Figure A2. 2: Millennium Merlin atomic fluorescence spectrometer system	129
Figure A2.3: Leco AMA 254 mercury analyser for direct mercury analysis	130

LIST OF TABLES

Table 2.1: Summary of source-based mercury atmospheric models	16
Table 4.1: Chemicals; manufacturer and grade	41
Table 4.2: Parameters for CE-AD	45
Table 4.3: Linear regression data of mercury and methyl mercury cysteine complex	53
Table 4.4 (a): The concentration of reference material and its uncertainty	55
Table 4.4 (b): The average and the standard deviations of experimental results for Hg determination with CE-UV	55
Table 4.5: Comparison of various Hg speciation detection limits by CE	57
Table 5.1: Total Hg and Hg species concentrations for coal standards and samples using AMA-254 and CE	64
Table 5.2: Linear regression data of Hg ²⁺ cysteine complex	69
Table 6.1: Sampling parameters at Duvha Unit 1 and 2	73
Table 6.2: Chromatographic conditions for the HPLC-AD	76
Table 6.3: Linear regression data of Hg ²⁺	80
Table 6.4: Linear regression data of total Hg using AFS	82
Table 6.5: Recovery results of total Hg determined with AFS	82
Table 6.6: Mercury content in coal, bottom ash and fly ash and the relative enrichment factors for units 1 and 2	83
Table 6.7: Hg speciation in the flue gas for unit 1 and 2 (corrected to a 3% O ₂ basis)	84
Table 6.8: Mass balance of Hg at Duvha Power Station unit 1 and 2	86
Table 7.1: Summary of Hg speciation measurements and TGM at Elandsfontein AQM station	95
Table 7.2: Summary of Hg speciation measurements at Majuba UCG plant flare	101

LIST OF ABBREVIATIONS

Abbreviation	Description
AD	Amperometric detection
ADOM	Acid Deposition and Oxidant Model
AES	Atomic emission spectrometry
AFS	Atomic fluorescence spectrometry
AMA	Automatic mercury analyser
APCD	Air Pollution Control Devices
AQM	Air Quality Monitoring
ASTM	American Society for Testing and Materials
ASTRAP	Advanced Statistical Trajectory Regional Air Pollution
CAA	Clean Air Act
CAM	Canadian Modelling
CAMR	Clean Air Mercury Rule
CDCP	Centres for Disease Control and Prevention
CE	Capillary electrophoresis
CE-AD	Capillary electrophoresis with amperometric detection
CE-PDA	Capillary electrophoresis with photo diarray detection
CE-UV	Capillary electrophoresis with Ultraviolet-Vis detection
CRM	Certified reference material
CSIR	Council for Scientific and Industrial Research
CV	Cyclic voltammetry
CYS	Cysteine
DMM	Dimethyl mercury
Dtz	Dithizone

EC	Electrochemical detection
EMEP	Europe Monitoring and Evaluation Programme
EOF	Electro osmotic flow
EPA	Environmental Protection Agency
ESP	Electrostatic precipitator
FAMS	Flue Gas Adsorption Mercury Speciation
FF	Fabric filter
FGD	Flue gas desulphurisation
GAW	Global Atmospheric Watch
GC	Gas Chromatography
Hg	Mercury
Hg ⁰	Elemental mercury
Hg ²⁺	Oxidize mercury
Hg _p	Particulate mercury
Hg _T	Total mercury
HPLC	High performance liquid chromatography
HPLC-AD	High performance liquid chromatography with amperometric detection
ICP-MS	Inductively coupled plasma- mass spectrometers
ICR	Information Collection Request
i.d.	Internal diameter
IUPAC	International Union of Pure and Applied Chemistry
LC	Liquid chromatography
LOD	Limit of detection
LOQ	Limit of quantification

MACT	Maximum achievable control technology
MESA	Mercury speciation adsorption method
MMM	Monomethyl mercury
MW	Mega Watts
OH	Ontario Hydro method
PDA	Photodiode-array detection
PM	Particulate matter
REFs	Relative enrichment factors
RELMAP	Regional Lagrangian Model of Air Pollution
ROME	Reactive and Optics Model of Emissions
RSD	Percentage relative standard deviation
RTI	Research Triangle Institute
SA	South Africa
SAMA	South African Mercury Assessment Program
SARM	South African Reference Materials
STD	Standard deviation
TEAM	Trace Elements Analysis Model
TGM	Total Gaseous Mercury
UCG	Underground Coal Gasification
UNEP	United Nations Environment Program
USGS	United States Geology Survey
USA	United States of America
UV	Ultra violet

PUBLICATIONS AND CONFERENCE CONTRIBUTIONS

Publications:

1. **Jongwana L.T., Crouch A.M. (2012).** Mercury speciation in South African coal. *Fuel*, 94:234–239
2. **Martin L.G, Jongwana L.T, Crouch A.M. (2010).** Capillary electrophoretic separation and post-column electrochemical detection of mercury and methyl mercury and applications to coal samples. *Electrochimica Acta*; 55; 4303–4308
3. Submitted paper: **Jongwana L.T, Crouch A.M.** Air Quality Monitoring of Mercury species at Elandsfontein in South Africa. *South African Journal of Science, SAJS-* 2013-0243

Posters and Talks

1. **Jongwana L.T., Crouch A.M., Gericke G.** Mercury speciation in coal; flue and ambient gas in South Africa, **1st VUT/ESKOM Partnership Colloquium, Vaal University of Technology, Applicable research: Opportunities & Possibilities, 3rd November 2012.** (Invited talk)
2. **Jongwana L.T., Chiloane K.** Ambient mercury monitoring in South Africa, **8th Mercury Emissions from coal (MEC8) working group, Kruger Gate, South Africa, 18 - 20 May 2011.** (Invited talk)
3. **Jongwana L.T., Crouch A.M.,** Mercury speciation in coal, **40th South African Chemical Institute (SACI) National Convention and Federation of African Chemical Societies (FACS) meeting: A prelude event to the International Year of Chemistry, SACI 2011, 16 – 21 January 2011** (Poster).

4. **L.T. Jongwana L.G Martin, A.M Crouch**, Mercury speciation using capillary electrophoresis, **2008 NACA/IUAPPA conference, Nelspruit, South Africa, 1 - 3 October 2008** (Poster)
5. **L.G Martin, L.T. Jongwana, A.M Crouch**, Mercury speciation using capillary electrophoresis with electrochemical detection, **16th International Symposium in Capillary Electromigration Techniques, Catania, Italy, 31 Aug - 3 Sept 2008** (Poster)
6. **L.G Martin, L.T. Jongwana, A.M Crouch**, Post column electrochemical detection for mercury speciation analysis. **1st International Symposium on Electrochemistry, University of the Western Cape, Bellville, South Africa, 9 – 11 July 2008.** (Keynote Speaker)

CHAPTER 1

BACKGROUND, MOTIVATION AND OBJECTIVES

1.1 Background

Mercury (Hg) is a global pollutant; it is a persistent, toxic and bioaccumulative metal [Gupta, 2007]. Due to its high potential risk for toxicity, Hg emitted from coal-fired power plants cause for worldwide health concern. A recent study showed that coal combustion is the main source of anthropogenic Hg emitted into the environment [UNEP, 2008]. In Europe, Hg emissions from stationary combustion facilities represent 53% of the total amount of anthropogenic Hg in the air, whereas in North America they account for 43% [Pirrone *et al.*, 2010]. The most recent estimates suggest that fossil fuel combustion produces 45% of the total Hg emitted from worldwide human activity [Pacyna *et al.*, 2010]. The United Nations Environment Programme (UNEP) recently released figures for the global atmospheric release of Hg in tons per year from 2005 and a status quo scenario for 2020 for each continent [AMAP/UNEP, 2008].

The need to determine different species of trace metals in the environment, air and food is becoming increasingly important because of the toxic effects of an elemental chemical form and its behaviour [Leermakers *et al.*, 2006]. Most analytical methods only deal with the total content of an element in an analysed sample (such as lead, Hg or cadmium). Until recently, analytical methods allowed the analyst to determine total content only; however, it was soon realised that this information was insufficient as a predicting factor for toxicity [Leermakers *et al.*, 2006; Spiro and Stagliani, 1996; Timerbaev, 2002].

Toxicological investigations have shown that, for living organisms, the chemical form of a specific element or oxidation state in which the element is introduced into the environment is

crucial. It is therefore important to not only gain information about the total concentration of an element, but also to determine the individual chemical and physical forms of the element [Spiro and Stagliani, 1996]. According to the official definition given by the International Union of Pure and Applied Chemistry (IUPAC): ‘speciation analysis’ is the process leading to the identification and determination of the different chemical and physical forms of an element existing in a sample. The analytical activity involved in identifying and measuring species is hence defined as ‘speciation analysis’. The determination of the concentration of specific chemical forms, such as organic Hg rather than elemental Hg, is essential for the interpretation of their biochemical behaviour or assessment of the potential danger to humans and organisms [Leermakers *et al.*, 2006].

1.2 Project motivation

Hg and its related compounds are toxic for humans and for the environment. As a natural occurring element, human activities have increased the level of Hg in addition to that already in circulation natural. Pacyna *et al.* (2006) published a global anthropogenic Hg emissions inventory. The inventory was based on the estimates of total Hg emissions derived from gold mining and coal combustion. This inventory placed South Africa (SA) as the second largest Hg emitter in the world behind China. These findings from the inventory about SA led to the formation of South African Mercury Assessment (SAMA) program in April 2006. SAMA drew together the scientist from academia, research institutions, industry and non-governmental organisations.

Several studies [Dabrowski *et al.*, 2008; Leaner *et al.*, 2009] carried out through SAMA program on anthropogenic Hg emissions in SA on coal combustion found that Hg emissions arising from SA coal-fired power plants are lower than Hg emissions suggested by Pacyna *et al.* (2006) (approximately 50 tonnes/year). Leaner *et al.* (2009) reported the assessment

conducted by Pacyna et al. (2006) signal the need for a critical evaluation of the major Hg sources in the country. Work from SAMA helped to inform subsequent global inventory research published by Pacyna et al. (2009). Following the publication of the revised inventory SA was rated as the sixth largest Hg emitter in the world behind China (1st), United State of America (2nd), India (3rd), Russia (4th) and Indonesia (5th) [UNEP, 2008]. Masekoameng et al. (2010) showed that approximately 80 % of the SA emissions are derived from coal-fired generation, with the balance of emissions coming from cement, ferrous, non-ferrous, domestic fuel burning and petrochemical sectors.

Because of the health risks associated with Hg, it is important to clarify many uncertainties regarding the transport, fate and consequences of Hg pollution from fossil fuel burning [Wagner and Hlatshwayo, 2005]. Cases such as the Minamato incident (1950s) and the THOR Chemicals incident (1987) focused attention on the importance of speciation and the toxicity of Hg [Virginia, 2002; www.en.wikipedia.org/wiki/mercury].

With SA's increasing demand for energy, the commissioning of two new coal-fired power plants and the de-mothballing of three existing coal-fired power plants [MRA, 2003], Hg emissions to the environment will inevitably increase over the next decade, unless strict emission control technologies and Hg reduction policies are implemented [Leaner *et al.*, 2009].

This indicates the importance of the requirement for information on the chemical speciation of Hg released from the stacks of coal-fired power plants, which is currently lacking in SA, and requires further research. Relating chemical speciation to anthropogenic sources will help to improve policy decisions relating to the control of Hg in the environment. Therefore, appropriate and reliable methods for sampling; analysis and speciation of Hg species at very low concentrations in gaseous emissions from coal-fired power stations need to be developed.

1.3 Aims and objectives

The fundamental aim of the research was to develop methods and analytical methodologies capable of differentiating between the different forms of Hg in air from coal-fired power plants and produce a practical solution to monitoring Hg species in flue gas.

The following questions were posed regarding this fundamental aim:

- Is there a relationship between the Hg speciation concentration in flue gas and the coal?
- How is this expressed in terms of the different Hg species that exist (as a fraction of the total Hg species) at elevated temperature and at room temperature?
- What is the current legislation in SA, regarding Hg?
- What is the environmental fate of the Hg species?
- Can a predictive model be validated relating the quality of coal used to the Hg species formed?

To answer these questions, the following research objectives were adopted:

- Develop various analytical methods for Hg speciation.
- Compare the developed methods with existing analytical methods for Hg speciation.
- Determine the most suitable method for total Hg analysis in coal.
- Determine the most suitable method for sampling of Hg species in ambient air and in flue gases at coal-fired power plant stacks.

- Apply the developed analytical Hg speciation methods to environmental samples at different coal-fired power stations.
- Compare the results obtained at the different stations with environmental guidelines for the country.
- Develop a predictive model relating the quality of coal used to the Hg species formed.

1.4 Layout of the thesis

The first phase of the study involves analytical method development and validation for Hg speciation in different environmental samples. This was followed by the application of the developed methods to environmental samples: coal, ambient air and elevated temperature gases (flue gas). The obtained data will assist with validation of the method and for use in process prediction of Hg species emission from coal-fired power stations, combustion technologies, flue gas clean-up technologies, coal characterization, and, ultimately selecting the most appropriate Hg control technologies.

CHAPTER 2

INTRODUCTION AND LITERATURE SEARCH

2.1 Introduction

Mercury (Hg) is considered as dangerous pollutant due to its toxicity towards the environment. It is widely dispersed throughout the environment, but in general at very low concentration. Increased global industrialisation has resulted in an elevation of natural levels. Anthropogenic activity, such as fossil fuel combustion, mining, electroplating processes, iron and steel production have all contributed to increased levels of Hg in environmental systems. This has cause for worldwide health concern.

Hg exists in several forms in the environment. The three most important chemical forms of Hg known to be present in the environment are: elemental mercury (Hg^0), which has a high vapor pressure and relatively low solubility in water; mercurous (Hg_2^{2+}) and mercuric Hg^{2+} inorganic cations or oxidised mercury which is far more soluble in water and which have a strong affinity for many inorganic and organic ligands especially those containing sulfur. Their analysis becomes even more difficult due to their transformation between various chemical species.

Each species has its specific biogeochemical property and its toxicity. Thus the total concentration determination is not sufficient for the understanding of their effect on the environment. Only the chemical speciation of the compounds can elucidate the problem.

Currently, speciation data on Hg is in short supply, partly due to the limited or expensive analytical capability required for the production of data. Sampling protocols, sample preparation procedures, analysis and detection methods also pose significant challenges to Hg

speciation analysis. This research project will attempt to answer some, or all, the research questions stated in Section 1.3.

2.2 Literature review

This section describes the chemical nature of Hg as well as its occurrence, fate and transport in the environment, specifically pertaining to Hg transformation during coal combustion. Speciation and the resulting toxicity are also addressed. Modelling Hg, regulatory drivers in South Africa and other countries, and the problem statement (see Section 2.3) are addressed.

2.2.1 Properties of mercury

Hg is a silvery, liquid metal at room temperature. It is sometimes referred to as one of the ‘heavy metals’. Like water, Hg can evaporate and become airborne. Hg can exist in three oxidation states: Hg^0 (metallic), Hg_2^{2+} (mercurous) and Hg^{2+} (mercuric) [<http://www.pca.state.mn.us/>]. The oxidation state strongly influences its properties and chemical behaviour [Jones and Slotten, 1996]. Because Hg is an element, it does not break down into less toxic substances. Once Hg escapes to the environment, it circulates in and out of the atmosphere until it ends up in the bottom of lakes and oceans. The Hg compounds most likely to be found under environmental conditions are the mercuric salts (i.e., HgCl_2 , $\text{Hg}(\text{OH})_2$ and HgS) and methylHg compounds (i.e., CH_3HgCl and CH_3HgOH). Depending on its chemical form, elemental Hg (Hg^0) may travel long distances before it falls to earth with precipitation or dust [<http://www.pca.state.mn.us/>].

2.2.2 Sources of mercury

“Hg is a naturally occurring element. Hg ore, cinnabar (HgS) is mined in Spain, Algeria, Kyrgyzstan and China. Hg is also a by-product of gold and zinc mining. Hg enters the environment from:

- natural sources, such as volcanoes and the weathering of rocks
- intentional uses of Hg
- unintentional releases of Hg from burning fossil fuels and smelting metals.

Hg can also escape to the environment when items containing Hg are broken or thrown away. Whether the items are dumped in sewers, garbage cans or burned, some of the Hg will eventually enter the atmosphere and later end up in lakes or oceans, where it can accumulate in fish. Hg is also a pollutant in air emissions from activities such as burning coal and producing taconite. A number of other possible sources of Hg exist, including cement plants and gasoline combustion, sewage treatment and chlor-alkali plants.

2.2.3 Uses of mercury

- to produce chlorine and caustic soda
- in wiring devices and switches
- for electric lights
- for measuring and control instruments (such as blood pressure gauges and thermometers) [<http://www.pca.state.mn.us>].

2.2.4 Negative influence of mercury in humans

Hg affects the human brain, spinal cord, kidneys and liver. It affects the ability to feel, see, taste and move. It can cause tingling sensations in the fingers and toes, a numb sensation around the mouth, and tunnel vision. Long-term exposure to Hg can result in symptoms that get progressively worse and lead to personality changes, stupor and coma [Thorsrud and Faqi, 2011]. Women who are pregnant should not eat fish with high levels of Hg. Hg affects foetal development, preventing the brain and nervous system from developing normally. Affected children show lowered intelligence, impaired hearing and poor coordination. Their verbal and motor skills may be delayed [EPRI TR-107695, 1996].

The symptoms of Hg poisoning may not readily manifest themselves; they may often be undetected or misdiagnosed, especially in cases of exposure at low doses. As a result, these symptoms are often attributed to other diseases such as rheumatism, senile dementia, emotional instability and psychosis.

While there is no scientific dispute about the hazards of high levels of Hg exposure, concern is emerging that even low levels of exposure may cause subtle and irreversible damage to the brain and central nervous system, particularly among children and during foetal development. In a study conducted on the toxicological effects of methylHg in 2001, the Centers for Disease Control and Prevention (CDCP) estimated that as many as 375 000 US babies being born each year are at risk for developmental disorders [Thorsrud and Faqi, 2011]. However, based on an analysis of the data and measurements of Hg levels in newborns, the US Environmental Protection Agency (EPA) has found that >630 000 babies out of 4 million born each year may have dangerously high levels of the toxin in their bodies [EPRI TR-107695, 1996].

2.2.5 Mercury species and transformation in the atmosphere

“The atmospheric chemistry of Hg involves several interactions, namely

- gas phase reactions
- aqueous phase reactions (in cloud and fog droplets, and in deliquesced aerosol particles)
- partitioning of elemental and oxidized Hg species between the gas and solid phases
- partitioning between the gas and aqueous phases
- partitioning between the solid and aqueous phases in the case of insoluble particulate matter (PM) scavenged by fog or cloud droplets.

Pirrone (2001) summarized the interplay between Hg atmospheric processes and chemistry in Figure 2.1.

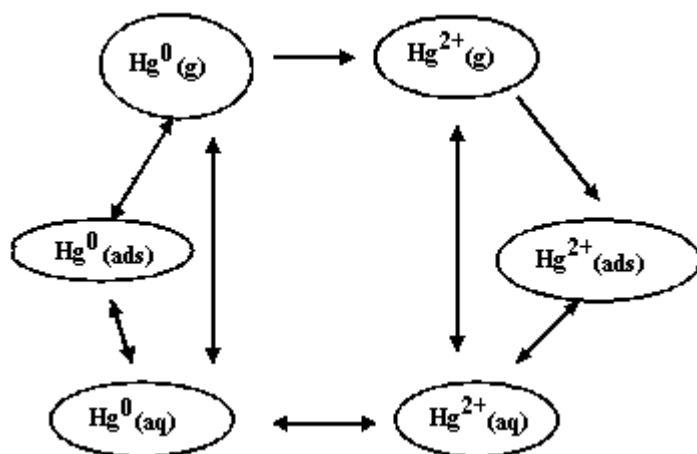


Figure 2.1: Model of interaction between Hg species in the atmosphere [Pirrone, 2001].

Since the first serious attempt at modelling the atmospheric chemistry and speciation of Hg within the framework of a tropospheric photochemical box model that included fog and cloud chemistry as well as PM [Pleijel and Munthe, 1995], a number of additional Hg atmospheric reaction parameters have been measured and two major reviews of atmospheric chemistry have been published by Lin and Pehkonen, (1999) and Schoeder and Munthe, (1998)” [<http://www.pca.state.mn.us>].

The prevailing Hg species is elemental Hg (Hg^0). Due to its physical properties (temperature dependence of saturated vapour pressure), elemental Hg occurs in the atmosphere solely in the form of vapour. Even at the absolute temperature minimum over the earth’s surface (the Antarctic, Siberia) the partial pressure of Hg vapour is several times lower than the pressure of saturated vapour [Lindqvist *et al.*, 1991].

Atmospheric Hg occurs in the form of different compounds-inorganic and organic. Inorganic compounds include Hg chloride (HgCl_2) and Hg hydroxide ($\text{Hg}(\text{OH})_2$). The composition of

gaseous inorganic Hg compounds has not been adequately investigated yet [Ebinghaus *et al.*, 1999; Subir *et al.*, 2012].

Organic Hg is represented in the atmosphere mainly by compounds with one to two methyl groups. The first type of compounds includes CH_3HgCl , CH_3HgOH , CH_3HgBr - name monomethyl Hg (MMM). The second includes $\text{Hg}(\text{CH}_3)_2$ - dimethylHg (DMM).

Hg in the solid phase is incorporated into the composition of aerosol particles. According to Schoeder *et al.* (1991), the solid phase Hg in the atmosphere can be presented by the following compounds: HgO , HgS , HgCl_2 , HgSO_4 , $\text{Hg}(\text{NO}_3)_2$.

In the combustion zone of fuels, most of the emissions occur in the gaseous phase. Hg in fuel coal can be oxidized by flue gas components such as HCl , SO_2 , H_2O and fly ash, forming an oxidized form of Hg (Hg^{2+}) [Lee *et al.*, 2006; Shah *et al.*, 2010]. Hg^{2+} can further react with the particulate in the flue gas and form Hg_p . Hg^{2+} can be easily removed by wet-type scrubbers due to its high solubility in water than Hg^0 .

The reaction of Hg^0 oxidation by halogens (Cl and Br) is important for the atmosphere over the ocean and its reaction rate does not depend on temperature [Holmes *et al.*, 2009; Seigneur *et al.*, 1994]. According to Holmes *et al.* (2009), the major reaction in marine boundary layer is oxidation with Br and reaction with Cl is only of minor importance.

2.2.6 Mercury speciation

Several review studies were conducted by Environmental Protection Agency (EPAs) on Hg speciation and stack measurements using OH method at the inlet and outlet of the pollution devices. These studies were based on the following factors:

- fuel type
- boiler type
- configuration of air pollution control equipment

Hg in coal was vapourized under the combustion conditions of the boiler furnace and was reported that coals with <100 ppm Cl had predominantly elemental Hg at the inlet to the particle-capture device, while coals with >500 ppm Cl had less than 20% elemental Hg [Senior, 2001]. Kolker et al. (2006) conducted a study of USA coal and observed that chlorine content in the coal and coal rank were poorly correlated. Variations in speciation of Hg in emissions was observed to be influenced by the range of operating conditions, type of air pollution control device (APCD), and type/rank of feed coal [Kolker *et al.*, 2006]. A review of the EPA database revealed that, for bituminous-ranked coals, APCDs produce an average decrease of 20% in elemental Hg (Hg^0), while for low-rank coal, there was little change in Hg^0 across an electrostatic precipitator (ESP) and a large decrease across fabric filters (FF) (in the order of 50% average) [Senior, 2001].

Lee et al. (2004) and Pavlish et al. (2003) reported different Hg removal across cold-side ESPs. Lee et al reported 50% different Hg removal across cold-side ESPs compared to 27% reported by Pavlish et al. The later also reported 58% Hg removal by fabric filters. Wet and dry flue gas desulphurization (FGD) remove 80–90% of Hg^{2+} but fail to capture the Hg^0 form

[Pavlish *et al.*, 2003]. These differences in Hg removal suggest that the oxidation of Hg^0 to Hg^{2+} and adsorption of gaseous Hg across particle-capture devices are not simply related to chlorine. Other mechanisms may play a significant role in the process. These mechanisms have been incorporated in attempts to develop a combined homo- and heterogeneous model for Hg speciation [Niksa *et al.*, 2002; Sable *et al.*, 2008].

Comparison measurements of Hg speciation at the ESP outlet in coal-fired power station equipped with ESP were conducted by He *et al.* (2007) and Wang *et al.* (2009) using both a semi-continuous monitoring method and the OH method. He *et al.* (2007) found that the Hg concentrations were about $1.285 \pm 0.808 \mu\text{g Nm}^{-3}$ post-ESP. Wang *et al.* (2009) found that Hg mainly exited as Hg^0 and Hg^{2+} in flue gas. Hg^0 was in the range $0.77\text{--}13.57 \mu\text{g Nm}^{-3}$ post-ESP/FF, and Hg^{2+} was in the range $0.02\text{--}21.2 \mu\text{g Nm}^{-3}$ post-ESP/FF. Hg_p measured was $0\text{--}0.54 \mu\text{g Nm}^{-3}$.

In 2010, Pavlish *et al.* reported that Hg concentrations depending upon the coal type and flue gas chemistry have an impact on Hg speciation. They change Hg reactivity and potential for capture. Low Hg concentrations in the flue gas affect mass-transfer reactions, limiting kinetic reactions in systems that typically have short residence times. The high halogen concentrations (e.g., chlorine) present in the flue gas result in higher ratios of Hg oxidation than low-halogen coal. In addition, coal/flue gas constituent chemistry, particulars of the generation system will also affect the amount of Hg emitted. Just as each type of coal is unique and will result in slightly different flue gas constituents compared to others in its respective rank, each coal-fuelled unit will also result in different Hg speciation and emissions as a result of system type, configuration and operation of the unit (temperature, pressure and other operational parameters such as level of unburned carbon). Elemental Hg is

generally not captured and emitted, whereas oxidized Hg tends to be soluble in water and frequently becomes particulate bound, aiding in its capture by pollutant control devices such as those currently used for SO_x, NO_x and PM [Pavlish *et al.*, 2010].

These chemical-physical properties have placed Hg on the priority list of an increasing number of International, European and National conventions, and agreements, aimed at the protection of the ecosystems including human health. This interest, in turn, stimulates a significant amount of research including measurements of gaseous elemental mercury reaction rate constant with atmospheric oxidants, experimental and modelling studies in order to understand the cycling of Hg and its impact to these ecosystems.

2.2.7 Modelling the atmospheric transport, chemistry and deposition of mercury

The most efficient means to determine the atmospheric transport and deposition pathways is through numerical modelling. Models can link emission sources with deposition at receptors and thus be used to identify which sources contribute to most insensitive areas and how deposition rates might vary across the region [Pai *et al.*, 1996]. Therefore, Hg modelling depends on source characteristics, environmental conditions (local and regional meteorology, terrain, nearby structures), as well as atmospheric chemistry, and removal and deposition processes (precipitation, dry deposition).

“Although measurements of Hg speciation in the atmosphere and in stack gases are limited, the most significant emitted species from a deposition perspective are thought to be Hg⁰, Hg²⁺ and Hg_p. The overwhelming majority of the Hg in air is Hg⁰, but the much higher wet scavenging and/or dry deposition rates for Hg²⁺ and Hg_p can impact significantly on Hg deposition rates near sources of these compounds. Petersen *et al.* (1991; 1995) have described a simplified aqueous phase chemistry and scavenging scheme for elemental and particulate phase Hg, which was incorporated into the Europe Monitoring and Evaluation Programme

(EMEP) model [Eliassen and Saltbones, 1983]. This model was applied in Europe to estimate Hg air concentration and deposition gradients. An effective washout ratio for elemental Hg was derived to include the aqueous chemistry proposed in those studies”.

A more detailed treatment of the aqueous chemistry of Hg, as well as the in-cloud and below-cloud scavenging processes, can be performed in a comprehensive Eulerian model. The Acid Deposition and Oxidant Model (ADOM) was adapted to examine Hg transport, chemical transformation and deposition, including aqueous phase oxidation of elemental Hg. This model has been applied in some preliminary model simulations over eastern North America using the best available information on scavenging and dry deposition processes for elemental, divalent and particulate Hg. Sensitivity runs were then performed to delineate the most important input data and then model physics/chemistry parameters in terms of predicted air concentrations and deposition. This model is currently being adopted for European applications. Tests on the Hg aqueous chemistry scheme were performed using a stand-alone version of the cloud mixing, scavenging and aqueous chemistry modules of ADOM” [http://www.eqb_dqe.cciw.ca/ modelling]. A summary of the atmospheric models being used to address Hg is given in Table 2.1.

Therefore, the choice of a modelling technique’s sophistication level is dictated by the precision of the input information and the desired accuracy of the results.

Table 2.1: Summary of source-based Hg atmospheric models, with references

Model	ADOM	ASTRAP	CAM	ROME	RELMAP	TEAM
Emissions (Sources)	Point and area source	Point and area source	Area source	Point source	Point and area source	Point and area source
Transport	Eulerian. Horizontal advection and diffusion.	Langrangian	-	Advection with mean wind trajectory	Puff advection with vertically averaged wind field	Eulerian. Horizontal advection using a semi-Langrangian scheme
Hg transformation	Hg ⁰ oxidation by O ₃ assumed balanced by reduction reaction; HgCl ₂ scavenged using Henry's Law scavenging coefficient; Hg _p scavenged by nucleation	Slow net conversion of Hg ⁰ to Hg _p at rate 0.05%/h	Aqueous chemistry. Detailed chemistry of Hg, oxidants and inorganic ligands	Gas-phase and aqueous chemistry	Hg ⁰ -Hg ²⁺ redox: O ₃ oxidation and sulphate reduction; considers Hg ²⁺ adsorption by soot particles	Gas-phase and aqueous chemistry
Dry deposition	Deposition to forest	Deposition velocity of Hg ²⁺ and Hg _p . Includes Hg ⁰	No deposition for Hg. Deposition for reactants	Deposition velocities for gases and particulates	Deposition velocities for Hg ⁰ (g), Hg ²⁺ (g), Hg _p , and carbon soot	Deposition velocities for gases and particulates calculated for each grid cell based on land use and input meteorology
Wet deposition (including cloud & precipitation)	(See Hg transformation above)	Deposition to surface, and redistribution from mixed layer to free troposphere	No	Cloud microphysics, rainout and the washout	Precipitation scavenging of Hg ²⁺ , Hg _p and soot; clouds assumed at top layers when precipitating	Wet deposition flux calculated as the product of cloud water concentration of Hg species and precipitation amount
Major applications	Eastern North America episodes; sensitivity analyses	Great Lakes Region deposition loading	Sensitivity analysis of chemistry	Power plant plume simulations	United States	Simulated the transport and fate of Hg emissions in the contiguous United States; includes detailed model evaluation
References	ERT 1984	Shannon, 1985	-	Constantinou and Seigneur, 1993	Eder <i>et al.</i> , 1986	Pai <i>et al.</i> , 1997

ADOM: Acid Deposition and Oxidant Model; **ASTRAP:** Advanced Statistical Trajectory Regional Air Pollution; **CAM:** Canadian model; **ROME:** Reactive and Optics Model of Emissions; **RELMAP:** Regional Lagrangian Model of Air Pollution; **TEAM:** Trace Elements Analysis Model

2.3 Problem statement

Coal combustion provides the largest source of energy to South Africa, yet the information on Hg emissions from this source is scarce. Many households, particularly in rural areas, burn coal for heating and cooking purposes, and the emissions of various pollutants, including Hg, pose a risk to human health. Due to South Africa's reliance on coal as a primary energy source, it is inevitable that emissions of compounds such as sulphur dioxide (SO₂), nitrogen oxides (NO_x) and Hg will increase unless improved control measures are applied or more renewable energy sources are used.

With South Africa's increasing demand for energy, the commissioning of two new coal-fired power plants and the de-mothballing of three existing coal-fired power plants [MRA, 2003], Hg emissions to the environment will inevitably increase over the next decade, unless strict emission control technologies and Hg reduction policies are implemented [Leaner *et al.*, 2009].

Eskom is compelled by South African policy on pollution prevention, waste minimization, impact management and remediation to maintain heavy metal concentrations emitting from their power stations below a certain mandated level as stated in the Air Quality Act, Act 39 of 2004. Any violation of this policy must be reported to the Department of Water Affairs. Multiple violations by a particular power station can result in financial penalties, costly remediation and even forced closure.

In South Africa, coal provides about 75% of the country's primary energy needs, and over 90% of its electricity is coal derived. Because of the health risks associated with Hg, it is important to clarify the much improbability regarding the transport, fate and consequences of Hg pollution from fossil fuel burning in South Africa and to map these for mitigation purposes. Figure 2.2 clearly illustrates why Hg emissions should be controlled [Kohl, 2011].

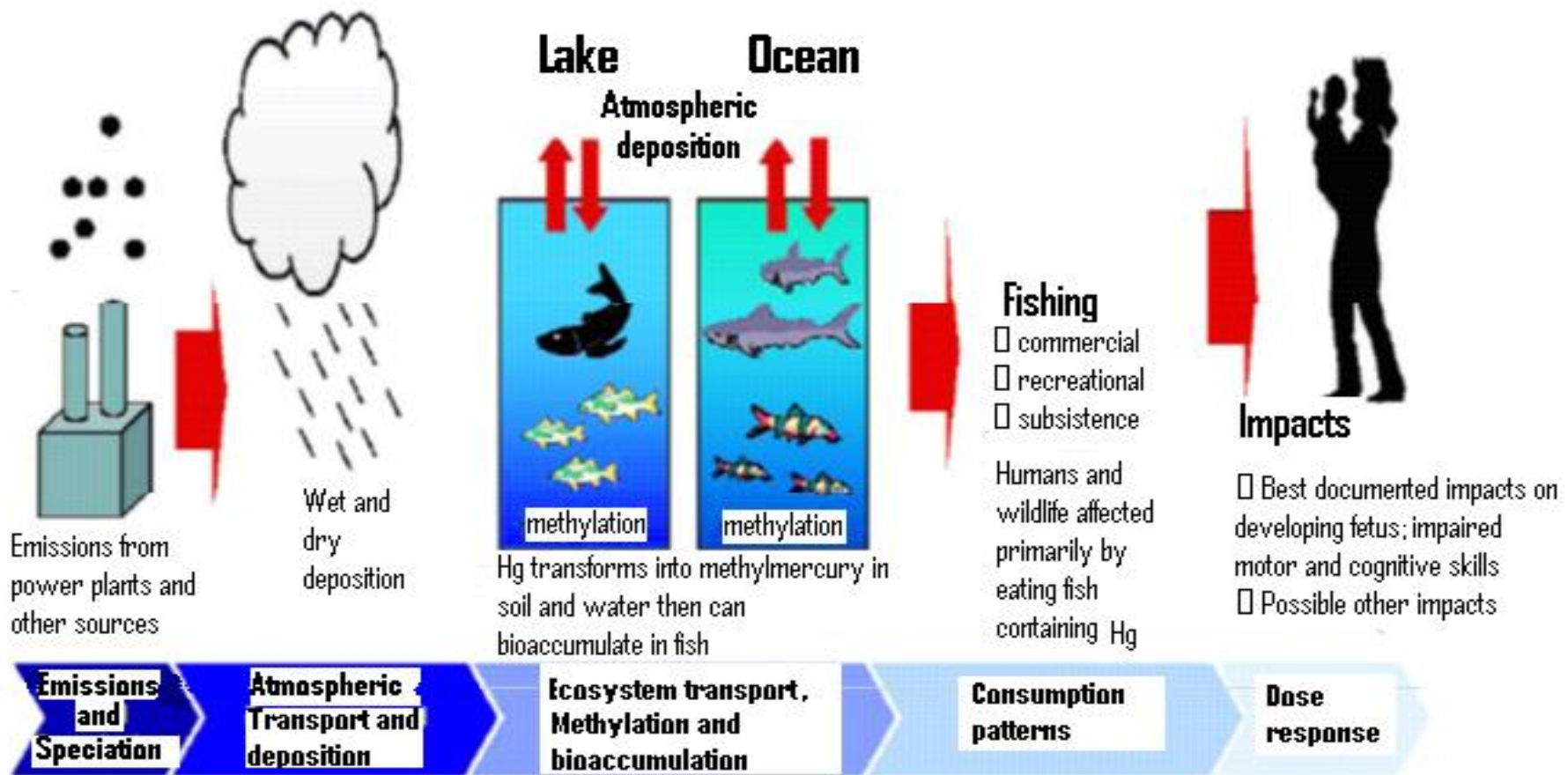


Figure 2.2: Explanation of why Hg should be controlled [Kohl, 2011].

2.4 Regulatory drivers in South Africa and other countries

Worldwide Hg reductions are being sought either by regulations that are specific and targeted at Hg emissions from coal-fired power plants or by regulations that seek more strict multi-pollutant control of SO₂, NO_x and PM [Palvish *et al.*, 2010].

In USA, the EPA announced in 2000 the need to regulate Hg emissions from coal-fired electric-generating units under the 1970 Clean Air Act (CAA). At that time, a dedicated effort was already underway in both the USA and Canada to better understand the fate and formation of Hg, including native capture in existing coal-fired power plants, most of which are pulverized coal-fired units. The world's first Hg control regulation was released by the EPA on 18 March 2005: the Clean Air Mercury Rule (CAMR) [US EPA, 2005a]. A sister rule promulgated just prior to the CAMR, the Clean Air Interstate Rule, was crafted concurrently to provide early multi-pollutant control of Hg by controlling SO_x, NO_x and PM [US EPA, 2005b]. Despite earlier expectations that the EPA would release a rule that called for maximum achievable control technology (MACT) standards, the CAMR called for a cap-and-trade approach. After significant input from both the private and public sectors, a lawsuit was brought against the EPA. The recent outcome of that suit is that the District Court of Appeals revoked the CAMR on 8 February 2008, leaving the EPA with instruction to draft a new regulation, which means that utilities in the United States will soon be required to comply with MACT standards.

Canadians have also been evaluating Hg control options for their power plants and gathering data from existing units, especially through the efforts of the Canadian Electricity Administration [Palvish *et al.*, 2010]. In 2006, the Canada-wide Standards were released, which set a federal Hg cap requiring a 70% overall reduction in Hg from coal-fired power plants.

Japan, China, Australia, Mexico, Russia and the European countries are evaluating and estimating Hg emissions from their coal-fired sources but to date have not issued regulations directly targeting Hg reductions. However, many of these countries are pursuing/achieving reductions in Hg emissions through implementation of improved control of SO₂, NO_x and PM.

Currently, the South African government has no enforced legislation on Hg levels. Recently, in April 2006, the South African Mercury Assessment programme (SAMA) was established. The aim of this programme is to monitor Hg and develop new analytical techniques to determine Hg in the environment and help government set up proper protocols for Hg determination.

Atmospheric monitoring of Hg concentrations in South Africa to date has mostly been made at Cape Point's Global Atmospheric Watch (GAW) Station in the Western Cape. Measurements of total gaseous Hg have been recorded since 1995 at the Cape Point GAW Station [Leaner *et al.*, 2009] and these have recently been supplemented with additional atmospheric Hg sampling. The average yearly concentrations of total gaseous Hg in the atmosphere between 1995 and 2004 ranged between 1 and 1.5 ng m⁻³, similar to those measured on board ship in the South Atlantic, and only slightly elevated compared to those measured at Neumayer on the Antarctic Peninsula [Baker *et al.*, 2002; Slemr *et al.*, 2003].

Initial atmospheric Hg studies are currently underway at the Elandsfontein Air Quality Monitoring (AQM) station situated in the Mpumalanga Highveld and at the Council for Scientific and Industrial Research (CSIR), Pretoria, Gauteng. While these studies are only now commencing, there is evidence that the concentrations of total gaseous Hg are occasionally elevated (2 ng m⁻³), especially during the day; some concentrations are lower at night [Leaner *et al.*, 2009].

CHAPTER 3

ANALYTICAL METHODOLOGIES FOR MERCURY

DETERMINATION

This chapter is divided into two sections. The first section presents a comprehensive overview of the analytical methods used for Hg analysis in environmental samples (solids, liquid and gases). The second section focuses specifically on analytical methods used in this study.

3.1 Analytical techniques for identifying Hg in coal and its products

It has been observed that there are no international standard methods for the determination of Hg in coal [Dale and Riley, 1995]. Therefore, there is a need to develop accurate and reliable methods for the determination of Hg in coal and its products. It is apparent that a major consideration in the determination of Hg in coal and other materials is the sample preparation technique [Wagner and Hlatshwayo, 2005]. Further, it should be acknowledged that it is difficult to obtain repeatable results for Hg in coal due to the nature of Hg occurrence as well as the low levels, of the order of parts per million, in which it occurs. The heterogeneity of coal further complicates matters; it is often difficult to repeat experiments with similar coal samples that have the same concentrations of Hg.

According to Huggins (2002), analytical methods for the analysis of inorganic components in coal can be divided into the following categories:

- methods that measure elemental concentration in coal (or ash)
- methods that determine mineralogical component
- methods that determine modes of occurrence.

Hg concentrations and modes of occurrence in coal can be determined by using direct Hg analyser instruments for Hg analysis in liquid and solid samples or using chromatographic systems. In a chromatographic system, coal cannot be directly injected into a system, extraction of Hg species from the coal sample should be done. The Hg species are either leached out from coal sample or digested in acidic or alkaline media. Methods such as alkaline dissolution, acid leaching, microwave digestion, aqueous distillation or solvent extraction [Liang *et al.*, 1996; Uria and Sanz-Medel, 1998] can be used to leach out Hg species. Pyrolysis can also be used [Liu *et al.*, 2010]. During the pre-treatment, stringent precautionary measures are important to avoid contamination. Each step in an analysis may contribute to errors therefore it is important that the procedure include as few steps as possible.

In this study, the following analytical techniques were used to determine Hg and its species in coal:

- direct Hg analysis using an automatic mercury analyzer (AMA 254 Mercury Analyzer)
- acid extraction (ASTM D6414-99) followed by capillary electrophoresis (CE) analysis
- pyrolysis followed by CE analysis.

3.2 Methods of sampling and measuring Hg species in flue gases (or air)

3.2.1 Gaseous sampling methods

Sampling and measuring of Hg species in air from coal facilities is challenging. The two major challenges are the lack of qualitative sampling methods and the lack of analytical techniques that can analyse and separate Hg species at very low concentrations. It is critical

to identify the Hg species, elemental form (Hg^0), oxidized forms (Hg^{2+}) and particle-bound forms (Hg_p), at various locations throughout the air pollution control device (APCD) train. However, such analysis is not an easy task.

As discussed in Section 2.2.6, the most commonly used sampling and analytical method is the Ontario Hydro (OH) Hg speciation method, but it has its limitations. This method was developed by Keith Curtis and other researchers at Ontario Hydro Technologies in late-1994. Since tests carried out using the EPA method 29 appeared to show that some of the Hg^0 was captured in the nitric acid-hydrogen peroxide impingers, an attempt was made to more selectively capture the Hg^{2+} by substituting three aqueous 1 N KCl impinger solutions for one of the $\text{HNO}_3\text{-H}_2\text{O}_2$ solutions. A schematic of the impinger train is shown Figure 3.1. A complete description of the OH method can be obtained from American Society for Testing and Materials (ASTM), number ASTM D6784-02.

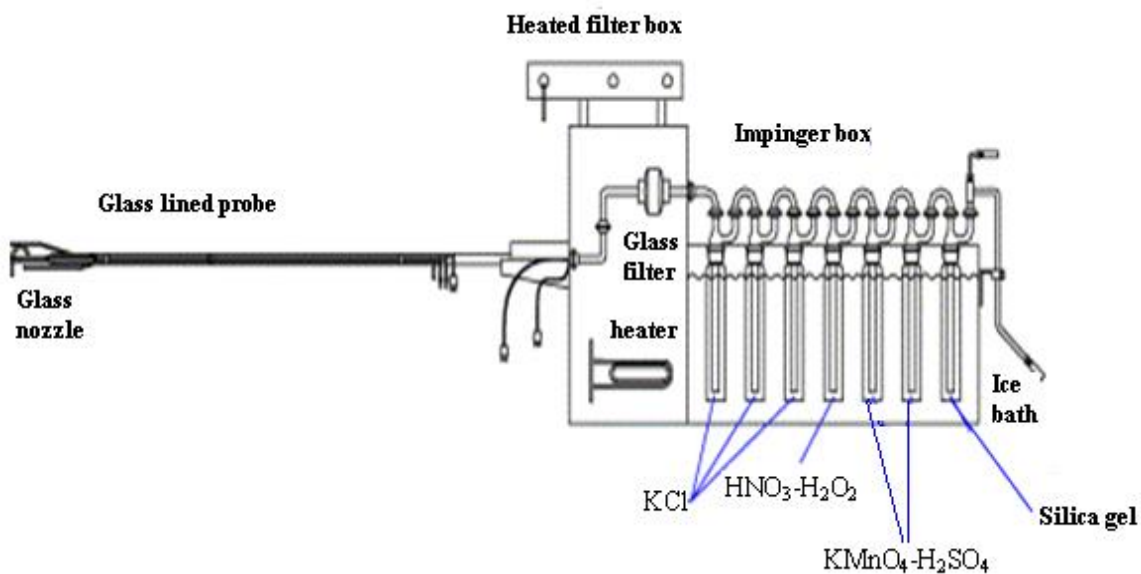


Figure 3.1: Schematic of the Ontario Hydro Hg speciation method impinger train [Kellie *et al.*, 2004].

Hg emissions from stationary combustion sources can be determined by several different sampling procedures. The boiler maximum achievable control technology (MACT) allows the use of either of two EPA methods (Method 29 or Method 101A) or the ASTM D 6784-02 'Ontario Hydro' method. The EPA promulgated an additional Hg sampling method, Method 324, which offers several advantages, provided the test objective requires quantification of only total Hg. The flue gas adsorbent mercury speciation (FAMS) method, a dry sorbent trap technique based on Method 324, yields results for speciated Hg similar to those of the ASTM OH method.

The choice of method/s should be primarily based on the test objectives. If only Hg needs to be quantified (no other elements), then it is not necessary to use Method 29. If speciated Hg data is not required, or if it is not necessary to distinguish between particle-bound Hg and gaseous Hg, then Method 101A or Method 324 is recommended. The choice of method/s should take into consideration the relative ease of use of the method/s and potential problems that may arise due to such problems as, for example, handling strong acids.

Although the analytical cost per sample for the dry sorbent trap methods is higher than for the wet sample methods, the overall test programme cost for a dry sorbent trap based test programme is likely to be less than for a wet test method due to the requirement for less field sampling labour effort associated with the dry sorbent trap sampling train setup and recovery.

For total gaseous Hg, sampling and analysis of atmospheric Hg is often made as total gaseous mercury (TGM), which is an operationally defined fraction that includes species passing through a 0.45- μm filter or some other simple filtration device such as quartz wool plugs and which are collected on gold. TGM is mainly composed of elemental Hg vapour with minor fractions of other volatile species such as HgCl_2 , CH_3HgCl or $(\text{CH}_3)_2\text{Hg}$. At remote locations, where particulate Hg concentrations are usually low, TGM constitutes the main part (>99%)

of the total Hg concentration in air. Over the past few years, new automated and manual methods have been developed to measure TGM and particulate Hg [Lu *et al.*, 1998; TEKRAM, 1998].

In this study, the OH Hg speciation method and ‘clean hands/dirty hands’ basic sampling procedure (from EPA Method 1669), were chosen for gaseous sampling for Hg speciation. Automated Tekran gas-phase Hg analyser was used to measure TGM.

3.3 Separation and detection techniques for Hg speciation

Review papers have been published describing the determination of total Hg concentrations in environmental and biological samples [Morita *et al.*, 1998]. Various detection methods have been used to detect Hg selectively and with good sensitivity.

Chromatographic separation and spectrometric detection techniques can be used to detect Hg species. In chromatographic separation, separation by gas chromatography (GC), CE, or high performance liquid chromatography (HPLC) and liquid chromatography (LC) [Harrington, 2000] are often applied. Spectrometric detection methods such as cold vapour atomic absorption spectrometry [Balarama Krishna *et al.*, 2005], atomic fluorescence spectroscopy (AFS) and inductively coupled plasma-mass spectrometry (ICP-MS) are often applied.

A method for Hg speciation can include many steps but the original species composition in the sample must be preserved throughout the analysis. If species are transformed or lost during storage, pre-treatment and analysis the determined concentration will not represent that of the original in the sample. Accurate results in the speciation analysis can be obtained if the integrity of Hg species is retained or if the degree of transformation, for example alkylation and dealkylation, can be quantified and corrected for. By understanding mechanisms and conditions for various possible reactions which might take place during the

analysis, analytical errors might be avoided by choosing suitable conditions during sample work-up, or compensated for, by taking into account redistribution, transformation or losses of Hg species [Qvarnström and Frech, 2002]

In most situations empirical procedures are used for quality assurance. By comparing results obtained from several methods based on different sample preparation procedures and detection techniques it is often possible to evaluate the performance of the methods with respect to accuracy and precision. If several independent methods give agreeable results the data have a larger probability to be accurate than if only one method has been used. Each method has its own precision which is determined by repeated analyses of aliquots from the same sample. But if results differ, which is a common problem for speciation analysis, a 'true' value cannot be given. For speciation of Hg, most laboratories have only one method available and they therefore have to resort to certified reference materials (CRMs). Often CRMs with an appropriate matrix composition and concentration of the species of interest are not available and in this situation recovery tests have to be performed for quality assurance. Analytical recovery is defined as the fraction or percentage of a species residue recoverable following extraction and analysis of a matrix containing the species [Holland, 1996]. In practice, the recovery is determined from analyte amounts added to the sample and this might not reflect the recovery of the incipient analyte of the sample.

In this study, chromatographic separation (CE and HPLC) and spectrometric detection techniques (AFS) were used. Several methods for separation and detection for Hg speciation were developed. The developed methods are:

- CE coupled with electrochemical detector
- CE coupled with photodiode array (PDA) detector

- AFS
- HPLC coupled with electrochemical detector

3.4 Analytical techniques used for Hg speciation in this study

3.4.1 Capillary electrophoresis

Recently, there has been increasing interest in the separation and determination of metal species using CE [Martin *et al.*, 2010; Silva da Rocha *et al.*, 2000]. This analytical technique is attractive for a variety of applications due to its simplicity, speed, resolving power and minimal sample reagent requirements [Vogt and Conradi, 1994].

Ultraviolet (UV) absorption is the simplest detection mode in CE; it is the detection system of choice for general analysis. For Hg detection with CE-UV, a derivatization step is required, for which sulphur-containing ligands such as cysteine and dithizone sulphonate have been used in the past [Hardy and Jones, 1997; Medina *et al.*, 1993].

Although relatively good detection limits have been achieved, the ongoing problem faced by many researchers is the relatively poor sensitivity of UV absorption for use in ultra-trace analysis [Martin *et al.*, 2010]. There is therefore the need for more sensitive detection modes for CE, such as mass spectroscopy, laser-induced fluorescence or electrochemical detector (EC), to overcome this problem [Lai *et al.*, 1998]. Originally described by Wallingford and Ewing in 1988, EC has an advantage over UV-Vis detection in that it is much more economical, provides better selectivity and higher sensitivity without the need for a derivatization step [Wallingford and Ewing, 1988]. EC detection in CE can be operated in a variety of modes: amperometric, potentiometric, voltammetric and conductometric. Most CE coupled with EC analyses employ amperometric detection (AD), where the working electrode is kept at a fixed potential. Electroactive compounds are either reduced or oxidized upon contact with the working electrode and the resulting current flowing as a result of analyte

oxidation or reduction at that potential is measured [Baldwin, 2000; Timerbaev and Shpigun, 2000]. Despite these attractive features, the success in EC is strongly dependent on the choice of the working electrode material. Different electrodes such as carbon, nickel, platinum and gold have been used in the past for CE-AD [Hua and Tan, 2000; Zhou and Lunte, 1995]. To date, only two articles have been published dealing with the speciation of Hg by CE with AD [Lai *et al.*, 1998; Martin *et al.*, 2010]. Lai *et al.* (1998) used reductive voltammetry at a gold electrode for the detection of Hg complexes. They were able to separate inorganic Hg, methylHg and ethylHg in a separation electrolyte composed of 0.1 M creatinine at pH 4.8 (adjusted by acetic acid). The limits of detection (LODs) achieved were excellent: 0.2 µg/l for inorganic Hg and 3 µg/l for methylHg [Lai *et al.*, 1998; Martin *et al.*, 2010].

3.4.1.1 Basic instrumental configuration

The basic components of a CE instrument are shown in Figure 3.2. CE is a family of related techniques that employ narrow-bore capillaries to perform high efficiency separation of both large and small molecules. In CE, electrophoresis is performed in a narrow-bore, polyimide-coated, fused silica capillary (typically 25–75 µm i.d., 365 µm outer diameter, 20–100 cm length). High voltage (10–30 kV) and high electric fields (100–500 V/cm) are applied across the capillary after injection, while both end of the capillary are submerged in the buffer vials. The voltage is applied to the inlet electrolyte vial using a Pt or other inert electrode and the outlet end is grounded in the same way. Capillary detection features a detection window, some distance before the electrolyte outlet reservoir, with a UV-Vis or fluorescence detector [Landers 1997; Weinberger 2000].

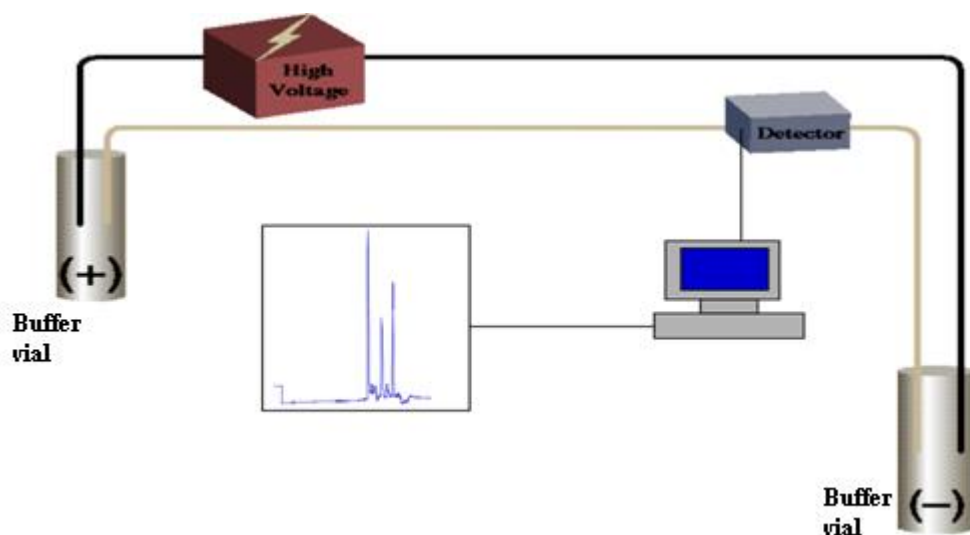


Figure 3.2: Schematic of a CE instrument [<http://www.ceandcec.com/> accessed June 2012].

3.4.1.2 Influence of applied voltage on migration time

The applied voltage produces an electric field gradient that causes positive ions to migrate toward the negatively charged end of the capillary. Negative ions migrate towards the positively charged end of the capillary. The rate at which the anions move is directly proportional to the applied electric field. Neutral species are not affected; only ions move with the electric field. If two ions are the same size, the one with greater charge will move fastest. For ions of the same charge, the smaller particle has less friction and an overall faster migration rate. This bulk movement of solution is termed electroosmotic flow (EOF) [Landers, 1997; Weinberger, 2000].

3.4.1.3 Electroosmotic flow

EOF is due to the ionic double layer that forms near the inner surfaces of the capillary when a voltage is applied between the ends of an insulating tube that contains a liquid. EOF and laminar flow will influence migration times. The flow rate of EOF is proportional to the voltage and the buffer viscosity, and depends on the charge at the inner surface of the

capillary. Control of EOF is essential to obtain reproducible results in CE. The origin of EOF is illustrated in Figure 3.3

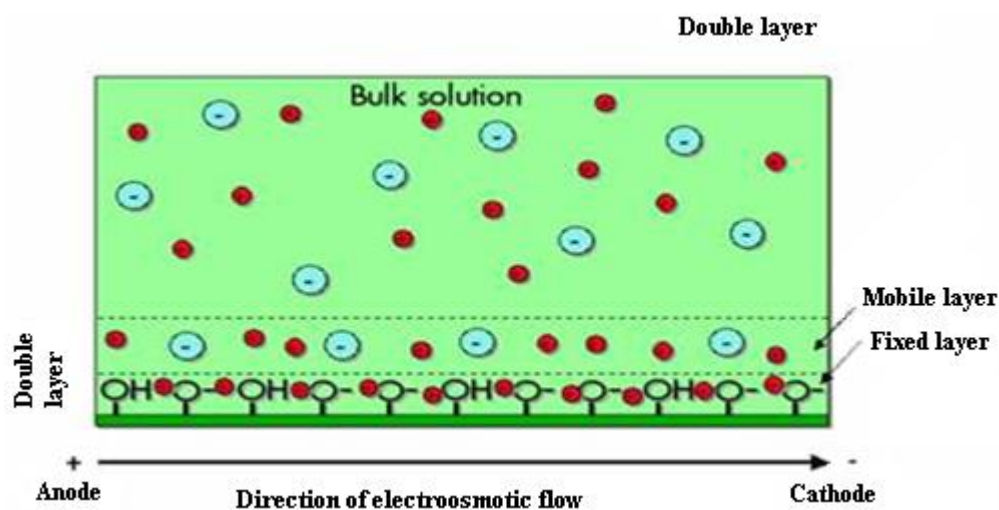


Figure 3.3: Illustration of the origin of the EOF [Weinberger, 2000].

The electroosmotic flow is defined in terms of velocity or mobility by

$$V_{\text{EOF}} = (\varepsilon\zeta / \eta)E$$

$$\mu_{\text{EOF}} = (\varepsilon\zeta / \eta)$$

Where ε is the dielectric constant, η is the viscosity of the buffer, and ζ is the zeta potential measured at the plane of shear close to the liquid-solid interface. V_{EOF} is velocity and μ_{EOF} is EOF mobility.

Buffer pH is one of the most significant factors influencing the EOF in a fused-silica capillary because of the development of charge at the silica wall surface due to dissociation of the residual silanol sites on the capillary. The pK_a for the silanol group is about 5.9, depending on the solution composition in contact with the fused silica wall. Typically, EOF for the fused silica capillary is high in basic buffer, it decreases significantly at about pH 6 and is low in a more acidic buffer solution. Even with an acidic buffer, analyte migration is

towards the negative electrode, but is sharply decreased because of the low EOF under the acidic conditions. Depending on the specific conditions, the EOF can vary by more than an order of magnitude between pH 2 and 12. Also, a change in EOF is dependent on buffer composition and on the experimental process used to condition the fused-silica capillary wall [Landers, 1997].

Other experimental variables can be changed to optimise EOF and improve resolution, alter analyte migration time or direction, and/or change analysis time. Increasing the buffer ionic strength decreases the EOF while an EOF change can also be correlated to the viscosity, dielectric properties, solvent composition and temperature of the buffer solution [Timerbaev, 2013]. Coating the fused-silica capillary wall and/or derivatisation of the wall silanol sites, can mask or alter the influence of the residual silanol sites. While these techniques often minimise analyte capillary wall interactions, they will also affect capillary wall surface charge and viscosity and also therefore, the EOF. Adding ionic or non-ionic surfactants to the buffer below critical micelle formation affects the EOF due to interactions between the surfactant and capillary wall surface. For example, for quaternary ammonium salts the decrease in EOF is dependent on the concentration and alkyl chain length of the tetra-alkyl ammonium cation [Heiger *et al.*, 1990]. For long alkyl chain lengths an EOF reversal is observed.

Modification of the fused-silica capillary wall with a highly ionised group, compared to silanol group, should offer several advantages. Extensive ionisation, which is less sensitive to buffer pH, whether due to anionic or cationic groups, should lead to a more constant surface charge. The dependence of the EOF on pH should be minimised and therefore, should result in a more constant, reproducible EOF, which should lead to better reproducibility in CE separations. In addition, wall-analyte interactions should be minimised, depending on the analyte and type of charged wall modification. These advantages have been realised in

studies where anionic surface are generated attaching a sulphate group or a boranate group on fused-silica capillary wall and where cationic surfaces are generated via the introduction of cationic groups on the wall [Maa *et al.*, 1991; Swedberg, 1990]

A unique feature of EOF in the capillary is the flat profile flow. This flow is beneficial since it does not directly contribute to the dispersion of solute zones. This is in contrast to that generated by external pump, which yields a laminar or parabolic flow due to the shear forces of the wall.

The flow rate drops rapidly at the wall. This gentle solution layer is caused by friction against flow at the surface. Since this layer extends a short way into the solution, it is relatively unimportant to the wall separation process. Further, the flow rate and profile are generally independent of capillary diameter. The profile will be disrupted, however, if the capillary internal diameter is too wide (≥ 200 to $300 \mu\text{m}$).

One great benefit of having electroosmotic flow present is that electrophoretic separations and detection can be run for anions and cations simultaneously. Without EOF, either only anions or only cations would migrate toward the detector. The oppositely charged ion would migrate back out of the injection end, and the neutral ions would remain and spread by diffusion. Under normal conditions (that is, negatively charged capillary surface), the flow is from the anode to the cathode. Anions will be flushed towards the cathode since the magnitude of the flow can be more than an order of magnitude greater than their electrophoretic mobilities. Thus cations, neutral ions, and anions can be electrophoresed in a single run since they all “migrate” in the same direction. Cations migrate fastest since the electrophoretic attraction towards the cathode and the EOF are in the same direction, neutrals are all carried at the velocity of the EOF but are not separated from each other, and anions

migrate slowest since they are attracted to the anode but are still carried by EOF toward the cathode. This is illustrated in Figure 3.4

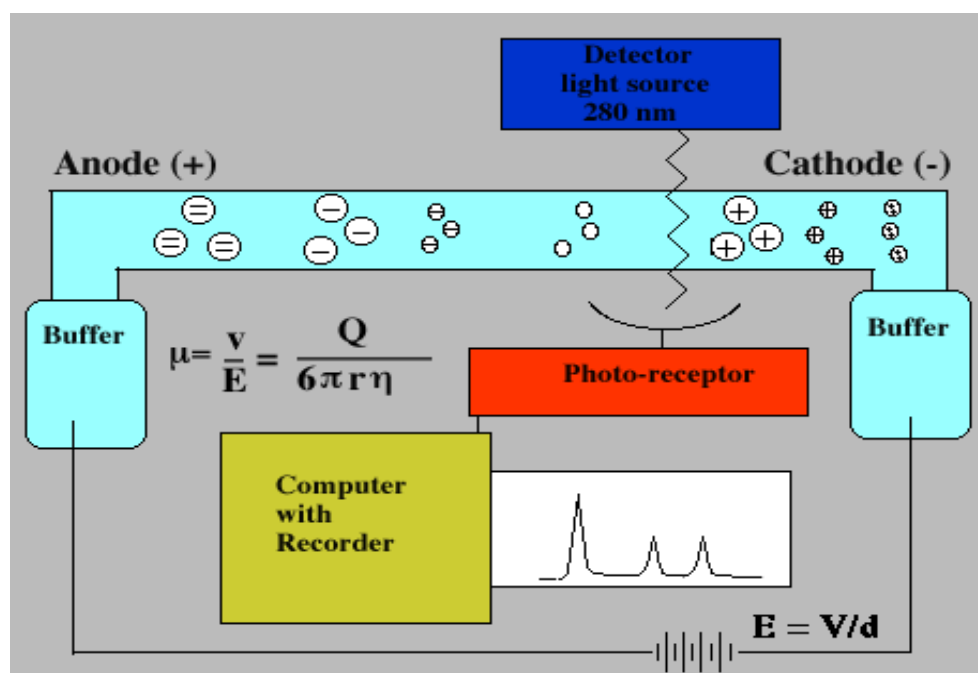


Figure 3.4: Schematic representation of CE separation [Li, 1992].

For the analysis of small ions (for example, sodium, potassium, chloride) the magnitude of EOF is usually not greater than the solute mobilities. In addition, modification of the capillary wall charged can decrease the EOF while leaving solute mobility unaffected. Under these circumstances, anions and cations can migrate in the opposite direction. While the EOF is usually beneficial, it often needs to be controlled.

3.4.1.4 Injection modes

There are two methods of sample injection in CE: hydrodynamic and electrokinetic injection. Hydrodynamic injection can be accomplished by application of pressure at the injection end of the capillary and vacuum at the exit end of the capillary, or by a siphoning action obtained by elevating the injection reservoir relative to the exit reservoir. With hydrodynamic injection, the quantity of sample loaded is virtually independent of the sample matrix.

Electrokinetic injection is performed by replacing the injection-end reservoir with a sample vial and applying voltage. The inlet end of the capillary is placed into the sample vessel. A small voltage is applied between the sample solution and the outlet end of the capillary for a short amount of time. The voltage is then turned off and then the inlet end of the capillary is taken out of the sample vessel and placed into the running buffer vial. In this mode of injection the amount of analyte injected is dependent on the mobility of the analyte ion. If the analyte has a high mobility, a larger quantity will be injected than an analyte with a low mobility. If the charge on the analyte is neutral or opposite the charge near the capillary inlet, no analyte will be injected. The main advantage of this mode of injection is that it's possible to preconcentrate analytes improving sensitivity and detection limits [Landers, 1997].

3.4.1.5 Separation modes

CE comprises a family of techniques that have dramatically different operative and separative characteristics. The techniques are capillary zone electrophoresis capillary gel electrophoresis, micellar electrokinetic capillary chromatography capillary isoelectric focusing, capillary electrochromatography isotachopheresis as well as the newly developed microchip CE

3.4.1.6 Detection in capillary electrophoresis

Detection in CE is a significant challenge because it is not a 'trace' analysis technique. Concentrated analyte solutions or pre-concentration methods are often necessary. A number of detection methods have been used in CE to meet this challenge [Landers, 1997]. Choosing suitable detectors will increase the selectivity of a separation if the analytes can be detected with greater sensitivity. The selection of detection systems is somewhat limited. UV-Vis detection is the most used detection method.

(a) UV-Visible detection

(i) Direct detection

The direct detection mode refers to an analytical signal related directly to the chemical or physical properties of the metal ion itself (e.g., the energy of emitted X-rays). Measuring the UV-Vis absorption of the analyte directly provides some specificity, when entire spectra are obtained. The optical path length through the separation capillary is very small and, therefore, the direct measurement of absorption is limited to compounds that have relatively high molar absorptivities.

(ii) Indirect detection

The indirect detection mode refers to signals that are non-specific for the metal ion and are obtained from transformed species containing the metal ion (e.g., the UV-Vis spectrum of a complexed metal ion) or from a species containing no metal ion from the sample (e.g., the signal from the background electrolyte in indirect UV-Vis detection). This method provides a means of detecting an analyte that shows little or no detector response. Indirect detection in CE holds greater potential because of its high sensitivity and broad applicability [Dabek-Zlotorzynska *et al.*, 1998; Timerbaev and Shpigun, 2000].

CE-UV-Vis is still the simplest and most widely used detection mode in CE but the LOD values reported with CE-UV-Vis spectroscopy are not suitable for ultra-trace analysis [Lia *et al.*, 1998]. In speciation analysis, the choice of the detector strongly depends on the chemical form to be determined and the mode of separation used [Dabek-Zlotorzynska *et al.*, 1998; Lia *et al.*, 1998].

(b) Fluorescence

Laser-induced fluorescence is a very sensitive detection technique currently available for CE [Medina *et al.*, 1993; Landers, 1997; Weinberger, 2000]. In this form of detection, radiation from a lamp or laser source is focused onto the capillary and the resulting fluorescence is collected at right angles to the excitation beam. For compounds having a strong natural fluorescence, this mode of detection is more sensitive than UV absorbance detection. It is much easier to detect a small signal above a 'zero' background (as in the case of fluorescence) than to detect a difference between two large signals (as in the case of absorption). Although detection limits are excellent in fluorescence, the technique itself is highly selective. Few compounds naturally fluoresce and a limited number of laser wavelengths are available for excitation. In most cases there is the need for derivatization of the sample with a fluorophore [Landers, 1997; Weinberger, 2000].

(c) Electrochemical detection

An alternative method is to use EC [Landers, 1997]. As an alternative to conventional spectroscopic methods, this method is ideally suitable for CE. Its rapid speed, high separation efficiency, high selectivity and sensitivity, and variety of configurations and materials that can be employed make this method suitable for Hg detection at ultra-trace levels [Landers, 1997; Weinberger, 2000].

(d) Photodiode array detection

Photodiode array detection (PDA) is an alternative to single or multiple wavelength detection. It offers detection limits, sensitivity, and a linear detection range that is equal to or exceeds that of single- or multiple-wavelength detectors. Like UV detector, PDA uses the absorbance of light to detect the presence of the sample as they pass the detection window. It

simplifies the analysis by selecting number of wavelength, for example from 190-600 nm with the bandwidth of 400 nm. This allows for the optimal wavelength(s) to be selected for actual analysis. In single analysis, all the solutes absorbing with this range will be detected.

3.4.2 High performance liquid chromatography

The use of High performance liquid chromatography (HPLC) for Hg speciation has the advantage of simplified sample preparation [Bettmer *et al.*, 1993]. Another advantage of using HPLC is the relatively low cost of analysis. Aqueous buffers are used as mobile phase. Combining HPLC with spectroscopic detection provides a simple and selective method for metal speciation [Hempel *et al.*, 1992].

For Hg speciation with HPLC, Hg species are usually mixed with sulphur containing reagents to form a complex, which improves the chromatographic separation properties of the species. Cysteine and dithizone [Cammann *et al.*, 1994; Harrington and Catterick, 1997] were successfully used as complexing agents for Hg speciation. There is however also some disadvantages using HPLC for metal speciation. Some of these disadvantages are the poor retention reproducibility, tailing of peaks, the use of hazardous organic solvent, time consuming extractions to remove interfering compounds [Cammann *et al.*, 1994] and decomposition of diphenylmercury [Bettmer *et al.*, 1993].

3.4.3 Atomic fluorescence spectrometry

Several articles have appeared on the determination of Hg using AFS [Craig, 1986; Gao *et al.*, 2012]. Most of the early work used flame atomization. This technique was later further developed by using an electrothermal atomization or cold vapour atomization [Bloom and Fitzgerald, 1988]. This technique makes use of Hg autofluorescence, the narrow band emission of UV radiation by Hg⁰ atoms during relaxation to the ground state after absorption

of radiation of wavelength 253.7 nm. The result is a sensitive and selective detection of mercury in the picogram range [Cai, 2000, Hill and Fisher, 1999]. Hg is liberated by aeration or reduction and trapped on an Au filament. The Au filament is then heated to 700 °C to liberate Hg⁰ which is then introduced to a flow type atomic fluorescence cell. The detection limit is 5 pg Hg with a relative standard deviation of 3%. Using an atomic fluorescence instrument that uses ICP as an atomization cell and a pulsed Hg hollow cathode lamp can produce a detection limit of 0.5 ng/l [Brenner, 2010].

3.4.4 LECO automatic mercury analyser (AMA-254) for total Hg analysis

The LECO automatic mercury analyzer (AMA-254) is a unique atomic absorption spectrometer that is specifically designed to determine total Hg content in various solids and liquids without sample pre-treatment or sample pre-concentration. Designed with a front-end combustion tube that is ideal for the decomposition of difficult matrices like coal, combustion residues, soils, and fish, the instrument's operation may be separated into three phases during any given analysis: decomposition, collection and detection.

“The first stage of the analysis is known as the decomposition phase. During this phase, a sample container with a nominal amount of the matrix is placed inside a pre-packed combustion tube. This combustion tube heated to ~750 °C through an external coil provides the necessary thermal decomposition of the sample into a gaseous form. The evolved gases are then transported (via an oxygen carrier gas) to the other side of the combustion tube. The portion of the tube, pre-packed with specific catalytic compounds, represents the area in the instrument where all interfering impurities (i.e., ash, moisture, halogens and minerals) are removed from the evolved gases.

Following decomposition, the cleaned, evolved gas is transported to the amalgamator for the collection phase of the system. The amalgamator, a small glass tube containing gold-plated

ceramics, collects all of the Hg in the vapour. With a strong affinity for Hg and a significantly lower temperature than the decomposition phase, the amalgamator is capable of trapping all Hg for subsequent detection. When all the Hg has been collected from the evolved gases, the amalgamator is heated to ~900 °C essentially releasing all Hg vapour to the detection system.

The released Hg vapour is transported to the final phase of the analysis, the detection phase. During the detection phase, all vapour passes through two sections of an apparatus known as a cuvette. The cuvette is positioned in the path length of a standard atomic absorption spectrometer. This spectrometer uses an element-specific lamp that emits light at a wavelength of 253.7 nm, and a silicon UV diode detector for quantitative determination of Hg”[<http://www.leco.com>]. The results generated are presented in both absolute amount of Hg and in concentration.

CHAPTER 4

METHOD DEVELOPMENTS FOR CAPILLARY ELECTROPHORETIC SEPARATION AND POST-COLUMN ELECTROCHEMICAL DETECTION OF MERCURY AND METHYL MERCURY, AND APPLICATIONS TO COAL SAMPLES

The content of this chapter has been published: Martin L.G, Jongwana L.T, Crouch A.M. (2010). Capillary electrophoretic separation and post-column electrochemical detection of mercury and methyl mercury and applications to coal samples. *Electrochimica Acta*, 55: 4303–4308. Permission to use the content was obtained from Elsevier Limited (see Appendix 3). This chapter describes the development of a selective, sensitive and inexpensive capillary electrophoresis with amperometric detection (CE-AD) method for the detection of Hg in coal at ultra-trace levels. It also explains the experimental setup used in this project, and how methods were validated and applied in environmental samples.

4.1 Reagents and materials

All reagents used were of HPLC or analytical grade. All chemicals and reagents were purchased commercially and used as received. Ultra-pure water was prepared in a Milli-Q water purification system (Millipore, Eschbron, Germany).

Hg stock solutions were obtained by dissolving the appropriate quantity of its chloride (Merck) in 0.5% HCl solution to a concentration of 0.368 mM (100 ppm). MethylHg chloride was obtained by dissolving the salt in the minimum volume of methanol and diluting the final volume with 0.5% HCl to give solutions of 100 ppm. All the organo-Hg solutions were stored at 4 °C when not in use. The cysteine (CYS) stock solution (100 mg/25 ml) of 4000 ppm was prepared by dissolving L-cysteine (Fluka) with 0.01 M HCl. The stock solution was stored

into the refrigerator for a maximum of one week. All complex formation was carried out with solutions that were either freshly prepared or from dilutions of the relevant stock solution.

The electrodes were polished prior to use with various grades of alumina slurry, rinsed thoroughly with Milli-Q water and allowed to dry. After running the experiments, the electrodes were cleaned by removing the deposits using electrochemical oxidation, holding them at a fixed positive potential value ($E = +0.5V$ versus $Ag | AgCl$) for a period of 15 min and then immersing in 6 M nitric acid to remove any Hg that might have formed as an amalgam on the electrode surface.

Table 4.1: Chemicals used during development of the CE-AD method

Chemicals	Manufacturer
Boric acid	Fluka
L-Cysteine	Fluka, Ultra
Hydrochloric acid	Sigma-Aldrich
Hydrogen peroxide	Associated Chemical Enterprises
Methanol	ChromaSolv, Sigma-Aldrich
MethylHg chloride	Merck
Mercuric chloride	Merck
Nitric acid	Sigma-Aldrich
Potassium chloride	Associated Chemical Enterprises
Potassium permanganate	Associated Chemical Enterprises
Sodium hydroxide solution for (1M)	Hewlett Packard
Sodium hydroxide, 20–40 mesh beads	Sigma-Aldrich
Sulphuric acid	Sigma-Aldrich

4.2 Preparation of standard solutions

Preparation of borate buffer solution, 0.025 M NaBO₃: 0.155 g of boric acid was weighed and diluted with distilled water in a 100 ml volumetric flask. The pH was adjusted to 9.3 with NaOH.

Preparation of cysteine solution, 0.033 M cysteine: 100 mg of cysteine was weighed and diluted with 0.01 M HCl in a 25 ml volumetric flask.

Preparation of Hg standard solutions (Hg²⁺, MeHg⁺): 100 mg of HgCl₂ was weighed and diluted with distilled water in a 100 ml volumetric flask, giving a final concentration of 3.28×10^{-4} M.

10 mg of MethylHgCl was weighed and dissolved in 5 ml of MeOH and diluted with distilled water in a 100 ml volumetric flask.

4.3 Experimental

4.3.1 Sample preparation

Hg standards for injection were prepared by mixing 200 µl of the relevant Hg stock solution with 300 µl cysteine made up to 2 ml with a water:methanol (1:1) solvent. One millilitre of this solution was placed in the sample vial and injected in the CE instrument.

Certified reference standards of coal Hg (SARM 18 and SARM 20) were used to evaluate the CE method for Hg detection and formed part of the validation process for this method. Eight grams of reference standard was placed in a quartz tube in a furnace and heated for 1 h at 790 °C in an oxygen atmosphere. At 600 °C, the majority of Hg will evaporate from the coals [Liu *et al.*, 2010]. Higher heating promoted the release of Hg, enhanced the Hg²⁺. The sample was purged with oxygen gas connected from the one side of the quartz tube while the other side was connected to seven chilled impingers. The first three impingers contained 200 ml KCl (1 M) solution. These impingers capture Hg²⁺ from coal. The fourth impinger contained

200 ml of a mixture of 5% (v/v) HNO₃ and 10% (v/v) H₂O₂. The fifth and sixth impingers contained 200 ml of the mixture of 4% KMnO₄ and 10% H₂SO₄. These impingers (5 and 6) capture Hg⁰ from coal. The last impinger contained silica gel to capture the remaining moisture from the coal. This sample trapping procedure is known as the Ontario Hydro method [ASTM D6784].

After each sampling event, the samples were transferred to amber/brown glass bottles using the 'clean hands dirty hands procedure' [EPA method 1669] chilled to 4 °C. A 1 ml aliquot from each of the traps were analysed for Hg species and methylHg by CE. The sampling train glassware and tubing were cleaned following the OH procedure to avoid trace metal contamination.

4.3.2 Capillary electrophoresis

CE-AD experiments were performed on a Waters Quanta 4000 CE system capable of delivering an applied potential of between 0 kV and 30 kV. Experiments were carried out using fused silica capillaries (Composite Metal Services Ltd., Worcester, UK) of 50 µm i.d. and 65 cm length (50 cm effective length). Data analysis was carried out with DAX 32 software (Eindhoven, Netherlands). All experiments were performed at 25 °C. The sample was introduced into the capillary by hydrodynamic injection of 0.5 psi for 5 s. Before use, the capillaries were washed with Milli-Q triple distilled water followed by 1 M NaOH and the separation buffer. The electrolyte and samples were sonicated and filtered through a 0.45-µm membrane filter prior to use.

CE-UV analyses were performed on a HP 3D CE system (Agilent Technologies, Waldbronn, Germany). The instrument is equipped with diode array detection at wavelengths between 190 nm and 820 nm. Data analysis was carried out with ChemStation (REV 6.01) software. The same operating conditions used for CE-AD were applied for CE-UV analysis.

4.3.3 Electrochemical detector (Amperometric detection)

The AD cell (Figure 4.1) was a 40 mm × 40 mm × 20 mm cuvette with four small holes drilled through in the form of a cross hair. The holes were large enough to pass a gold (Au) microwire working electrode and a capillary through it. A silver microwire was used as the reference electrode and fitted into the third leg of the cross hair. As no commercial sources were available to supply the right size Au microelectrode, the working electrode was made in-house by sealing a 60 µm diameter Au wire (Goodfellow Metals, Cambridge, UK) in a 125 µm i.d. fused silica capillary. The one end of the micro electrode was sealed using an inert polymer; the other end was filled with silver epoxy for contact with a copper wire. All electrodes and capillaries were aligned under a microscope (B# Zeiss KF2 Nikon). The Au microelectrode was set at a distance 20 µm from the end of the capillary and kept in position with PEEK ferrules and screws modified to fit the electrochemical cell. The cross-hair design system was placed inside the CE Faraday cage and kept in position by a support system. Amperometric detection was performed at a constant potential of 0.5 V with a BAS LC-4CE amperometric detector (West Lafayette, IN, USA).

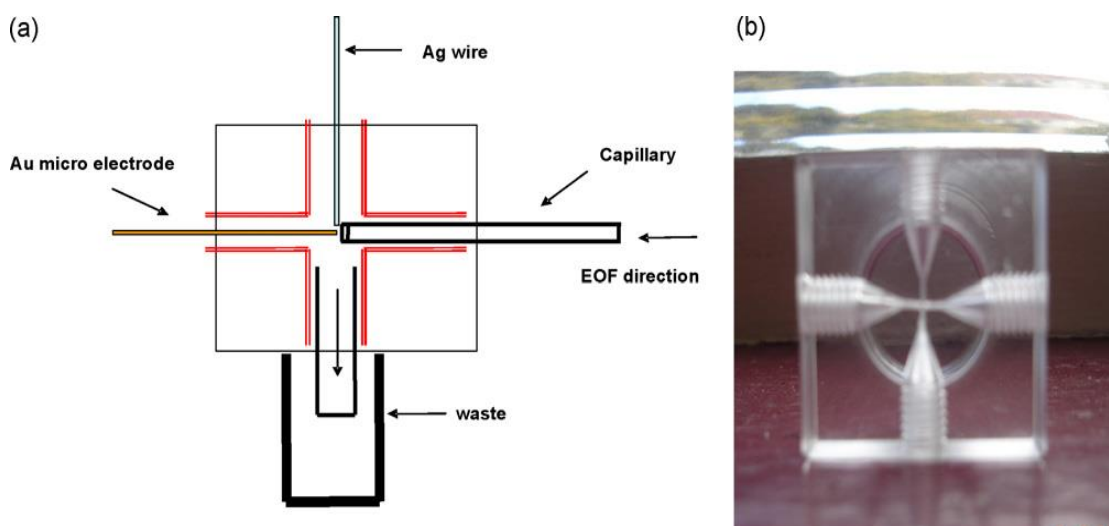


Figure 4.1: (a) Schematic representation of the newly developed CE-AD cross-hair design.

(b) Photograph of CE-AD cross-hair design for Hg speciation.

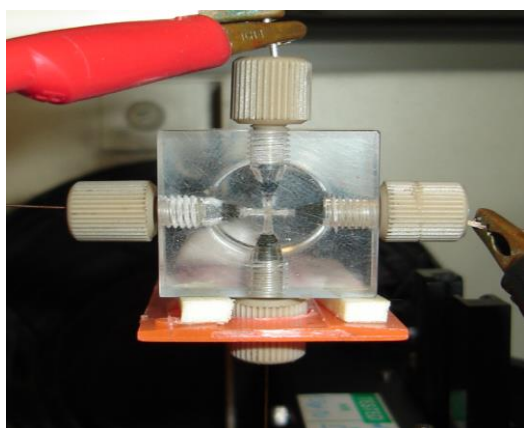


Figure 4.2: CE-AD cross-hair design for Hg speciation.

End-column detection was employed by making use of the newly developed Au microelectrode cross-hair construction. The following parameters were used during electrochemical detection of the respective Hg cysteine complexes.

Table 4.2: Parameters used for CE-AD of Hg cysteine complexes

Amperometric		CE	
Potential	0.5 V	Potential	25 kV
Filter	0.2 Hz	Injection time	5 sec
Range	5 μ A	Hydrodynamic injection	0.5 psi

4.3.4 Cyclic voltammetry

All electrochemical measurements were performed with a BAS CV-50W instrument. The experiments were carried out in a three-electrode cell at room temperature under a nitrogen atmosphere. The counter electrode was a platinum wire and Ag/AgCl (3 AuKCl) was used as the reference. A Au micro-disks electrode was used as the working electrode. Cyclic voltammetry (CV) was the technique applied to study the Hg complexes. The scans took

place at potentials between -500 mV and 600 mV. All potentials were measured vs. Ag/AgCl (3 M KCl).

4.4 Results and discussion

4.4.1 Cyclic voltammetry

The home-made Au microelectrode was tested for activity by successively sweeping a 0.1 M Fe_3CN_6 and 0.1M KCl solution between -400 mV and 400 mV at a scan rate of 50 mV/s, testing its electrochemical activity. Figure 4.3 shows the resulting voltammogram. The electrochemical properties of inorganic and methylHg cysteine complexes were studied by CV, using a Au microelectrode as working electrode. The study found that for amperometric detection of these complexes an applied potential of 0.5 V is needed to detect the Hg complexes with CE-AD.

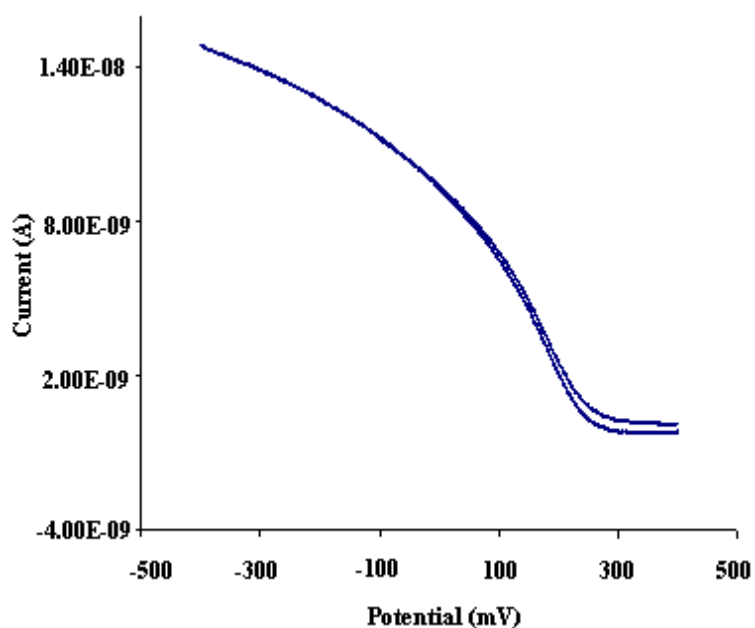


Figure 4.3: CV of a Au microelectrode in 0.1 M Fe_3CN_6 and 0.1 M KCl solution.

4.4.2 Optimization of CE-AD parameters

Medina *et al.* (1993) were the first to demonstrate the separation of four Hg species (Hg^{2+} , MeHg^+ , EtHg^+ and PhHg^+) in alkaline borate buffer (pH 8.35) with 10% methanol. The sample was derivatized with 0.1% CYS prior to CE separation. Very low detection limits were achieved when they studied fish and mussel samples by making use of a modified Westöö extraction method [Kubán *et al.*, 2007; Medina *et al.*, 1993].

In this study inorganic Hg and methylHg were studied using the method developed by Medina *et al.* (1993) and modified by Páger and Gáspár (2000) [Kubán *et al.*, 2007; Páger and Gáspár, 2000]. Firstly, the electrochemical properties of inorganic and methylHg cysteine complexes were evaluated at different metal:ligand ratios by CV. From the experimental data, it was found that for amperometric detection of the Hg cysteine complexes at a gold microelectrode an applied potential of 0.5 V is needed to detect the Hg cysteine complexes with CE-AD. Figure 4.4 shows the separation of inorganic Hg cysteine complex.

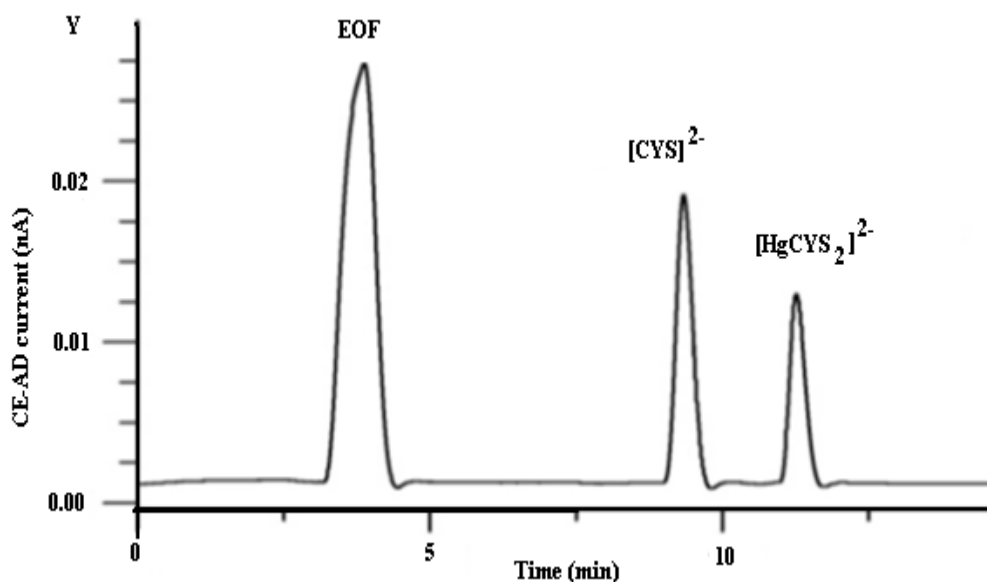


Figure 4.4: Separation of 1.0 $\mu\text{g/l}$ Hg^{2+} complexed with 33mM cysteine: buffer 25mM sodium borate, pH 9.35, voltage = +25 kV, CE-AD detection at 0.5 V.

For CE-AD, an oxidative mode was chosen, making electrode cleaning easier when the negatively charged Hg cysteine complex is formed on the surface of the electrode. Cysteine was added in excess at a 1:4 metal:ligand ratio, thereby ensuring that all the Hg in solution was complexed. This improved the detection limits, as the oxidation of the amino group of Hg cysteine complex is detected rather than the reduction of Hg cations [Kubán *et al.*, 2007]. Before each CE run, the Au microelectrode was kept at -500 mV for 5 min to ensure that all deposited Hg and impurities were reduced and stripped from the Au microelectrode surface. The Hg complex is well separated from the excess cysteine. All components were separated within <12 min and very symmetrical peaks were observed. The background noise was minimal in CE-AD, therefore improving the detection limits for the Hg complexes. The separation was found to be reproducible ($n = 3$) after electrode cleaning of 5 min between runs.

MethylHg showed very complex but interesting electrochemical reactions when studied by CV. This complexity is due to the formation of the methylHg radical species [Agraz *et al.*, 1995]. When a relatively high concentration of methylHg was injected into the CE instrument and studied using CE-AD some new peaks appeared (Figure 4.5). These could be attributed to the formation of different radical species of methylHg.

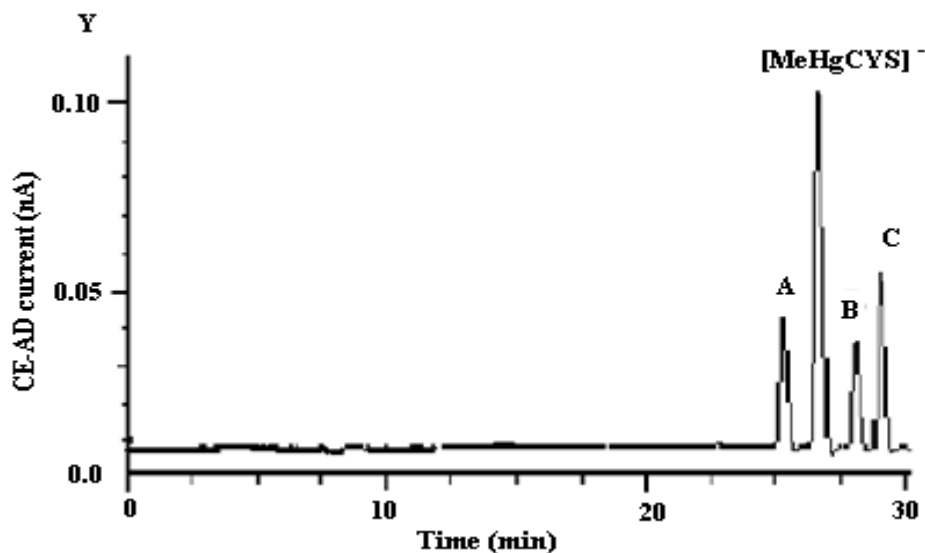


Figure 4.5: Separation of 100 $\mu\text{g/l}$ MeHg^+ complexed with 33 mM cysteine: buffer 25 mM sodium borate, pH 9.35, Voltage = +25 kV, CE-AD detection at 0.5 V. (A,B,C are radical species which could not be identified)

These peaks were not detected when a UV detector was used. These new peaks were detected up to a concentration of 100 $\mu\text{g/l}$. At lower concentrations, only one peak was found. It was assigned to the methylHg cysteine complex (see Figure 4.6). For the separation of methylHg, the increase in the retention time was very high compared with CE-UV analysis. The complex appeared after 20 min. The reason for the increase in retention time is as yet unknown, but the long retention time was consistent throughout when methylHg was studied

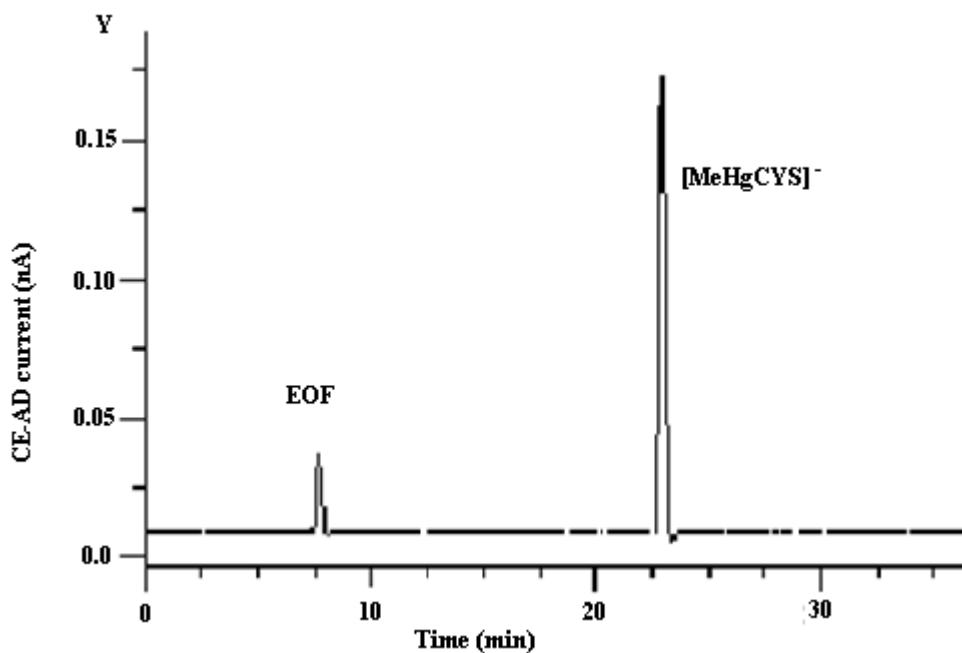


Figure 4.6: Separation of 50 $\mu\text{g/l}$ MeHg^+ complexed with 33 mM cysteine: buffer 25 mM sodium borate, pH 9.35, Voltage = +25 kV, CE-AD detection at 0.5 V.

4.5 Method validation

The performance of an analytical method is tested using several parameters. A measurement should be linear in a certain range of concentration; this is confirmed by undertaking a calibration curve. The method should allow the determination of very low concentrations (to enable good estimation of environmentally relevant levels). This is given by limit of detection (LOD) and limit of quantitation (LOQ).

4.5.1 Calibration curve

The CE-AD system was calibrated with a series of Hg^{2+} standards, up to 100 $\mu\text{g/l}$. For high concentrations of Hg, very broad peaks were observed, making the separation of Hg from the excess cysteine very difficult due to overloading of the capillary. A linear range was observed for Hg^{2+} from 0.01 $\mu\text{g/l}$ to 10 $\mu\text{g/l}$. There were no visible signs of system performance degradation after several hours of CE-AD operation. The repeatability was determined by

injecting the different standard mixtures three times for analysis. Figures 4.7a and 4.7b show the calibration curves for Hg^{2+} and MeHg^+ , respectively. Figure 4.8 is an electropherogram of the mixture of $20 \mu\text{g/l Hg}^{2+}$ and $10 \mu\text{g/l MeHg}^+$ standards.

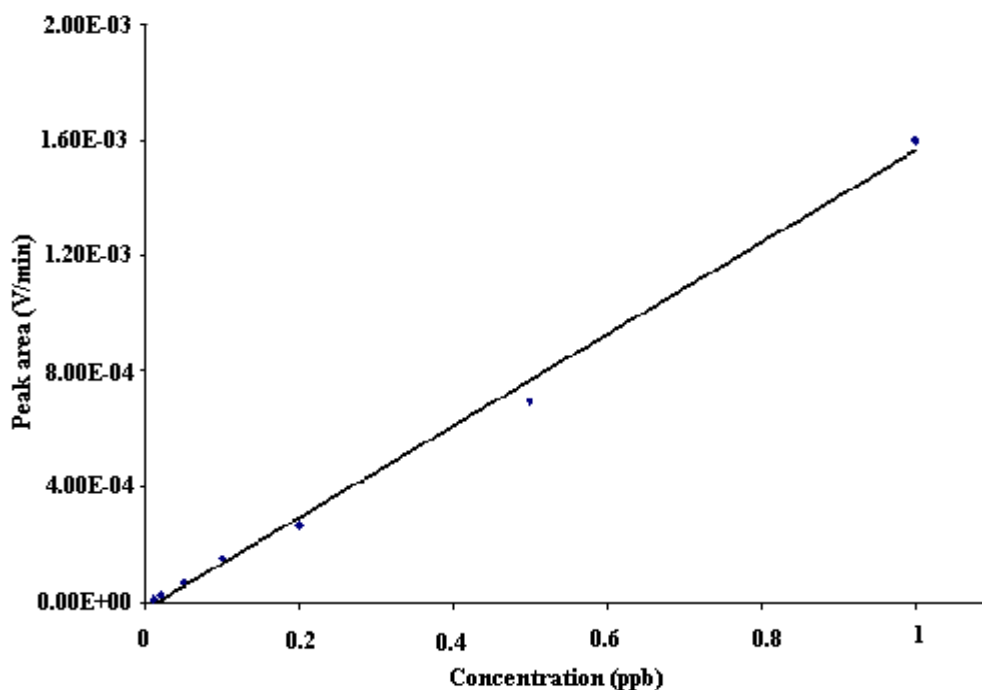


Figure 4.7a: Calibration curve of Hg^{2+} with CE-AD.

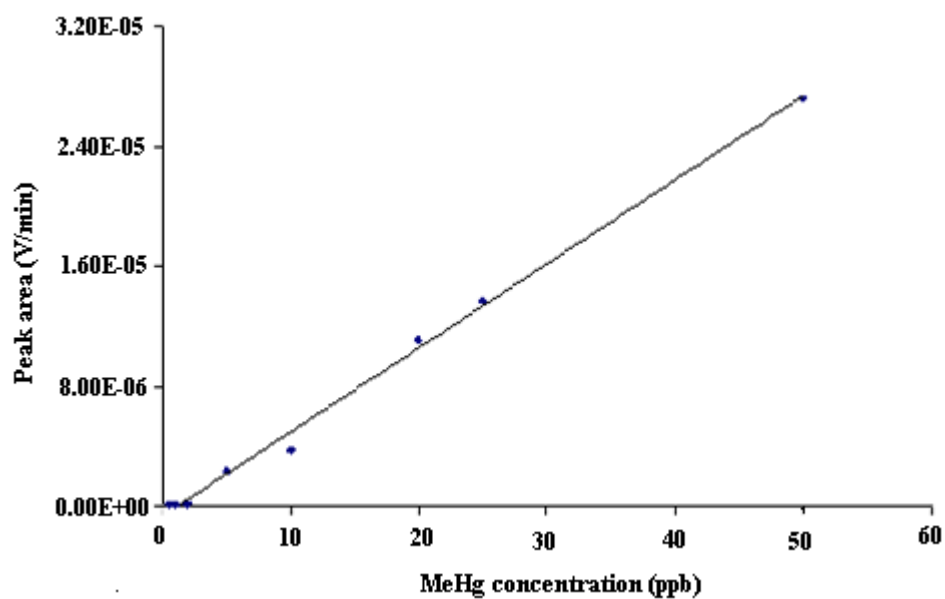


Figure 4.7b: Calibration curve of MeHg^+ with CE-AD.

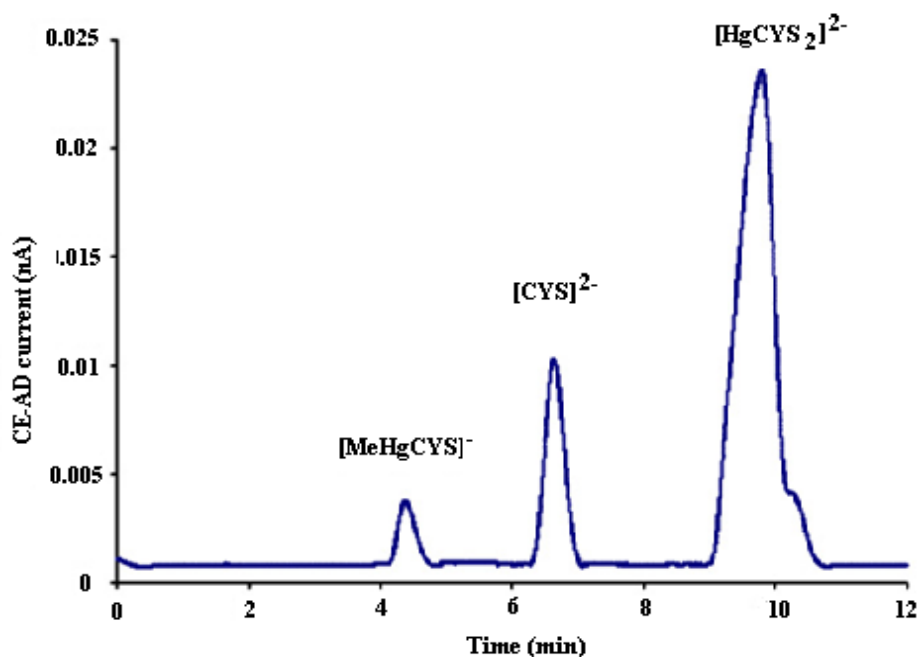


Figure 4.8: Separation of 20 $\mu\text{g/l}$ Hg^{2+} and 10 $\mu\text{g/l}$ MeHg^+ complexed with 33mM cysteine: buffer 25mM sodium borate, pH 9.35, voltage = +25 kV, CE-AD detection at 0.5 V.

Calibration graphs (concentration vs. peak area) were constructed at seven concentration levels. Good linearity and reproducibility was observed from calibration curves. The LOD and LOQ were calculated based on 3 and 10 times the noise level, respectively. The LOD for Hg^{2+} was found to be $0.005 \pm 0.002 \mu\text{g/l}$. This performance is made possible by regular electrode cleaning of the microelectrode before analysis and also proper alignment of the Au microelectrode for end channel detection.

For methylHg, a linear range was observed for MeHg^+ from 0.5 $\mu\text{g/l}$ to 50 $\mu\text{g/l}$. The LOD for MeHg^+ was found to be $0.40 \pm 0.5 \mu\text{g/l}$. The results obtained by CE-AD were found to be comparable and in good agreement with work done by Lai et al. (1998). The results of the linear regression data of the Hg cysteine complex are summarized in Table 4.3.

Table 4.3: Linear regression data of Hg²⁺ and methyl mercury cysteine complex

	Range (µg/l)	Linear regression	Correlation coefficient	LOD (µg/l)	LOQ (µg/l)	% RSD
Hg ²⁺	0.01–1	$1.6E^{-03}x - 2E^{-05}$	0.9958	0.005 ± 0.002	0.01	1.58
MeHg ⁺	0.5–50	$6.6E^{-5}x + 7E^{-07}$	0.9838	0.40 ± 0.05	1	5.21

4.6 Analysis of coal samples for Hg with CE-UV

CE-UV was first used to investigate the concentration range of the different Hg samples and standards giving an indication if a more sensitive detecting system was needed for detection. This proved to be very helpful seeing that the CE-AD system is very sensitive and very high concentrations of Hg foul the electrode surface producing very broad peaks that could not be analysed.

Coal naturally contains Hg and other chemical elements, which differ for the different types of coal and places of origin; typically, the Hg content in coal ranges from 0.01 to 0.48 mg/kg. The CE method was applied to an unknown coal sample (C1632), but was first tested on a Hg certified reference material SARM 18 and SARM 20. Most of the Hg in coal was oxidized to inorganic Hg (Hg²⁺); therefore, no organic Hg was detected. No Hg was detected in the HNO₃-H₂O₂ and the H₂SO₄-KMnO₄ traps [US EPA 1997; 1999; 2000]. The results of the certified reference material, SARM 18 and SARM 20 and coal sample (C1632) are summarized in Figures 4.9, 4.10 and 4.11, respectively. The concentrations of the reference materials and coal sample are summarized in Table 4.4.

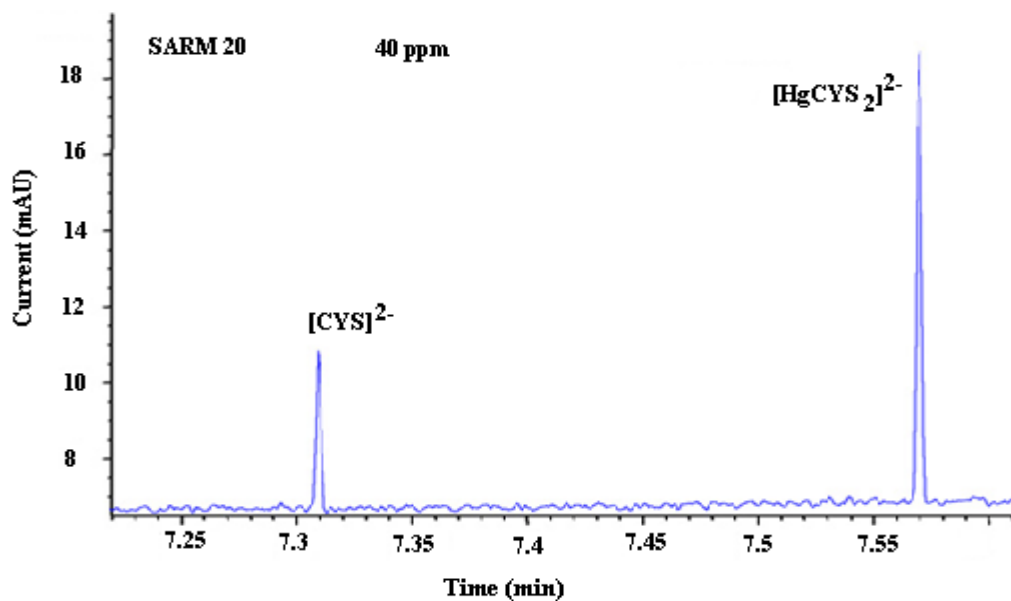


Figure 4.9: Electropherogram of mercury certified reference standard (SARM 20): buffer 25mM sodium borate, pH 9.35, Voltage = +25 kV, UV = 200 nm

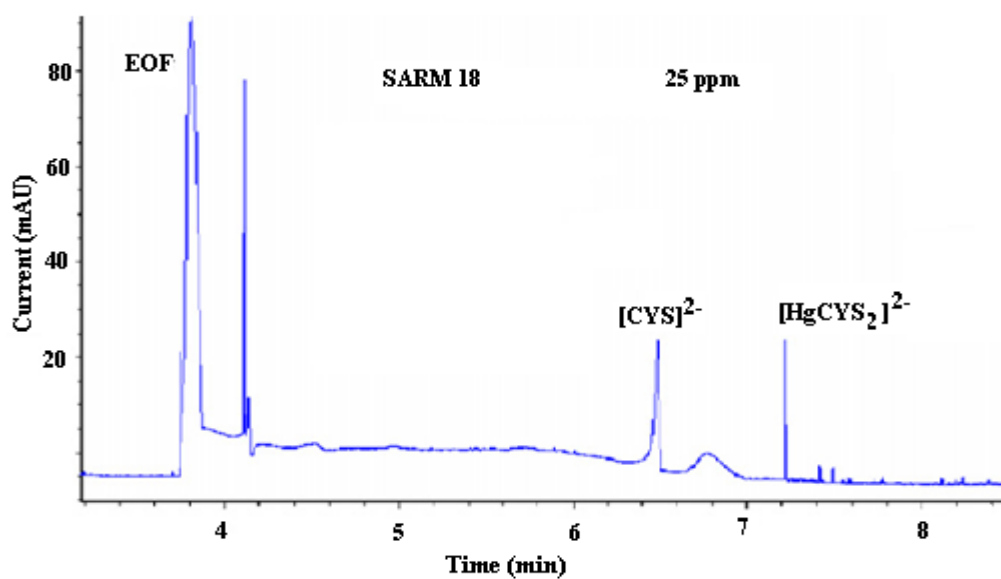


Figure 4.10: Electropherogram of SARM 18 complexed with cysteine: buffer 0.025 M sodium borate, pH 9.35, Voltage = +25 kV, UV = 200 nm.

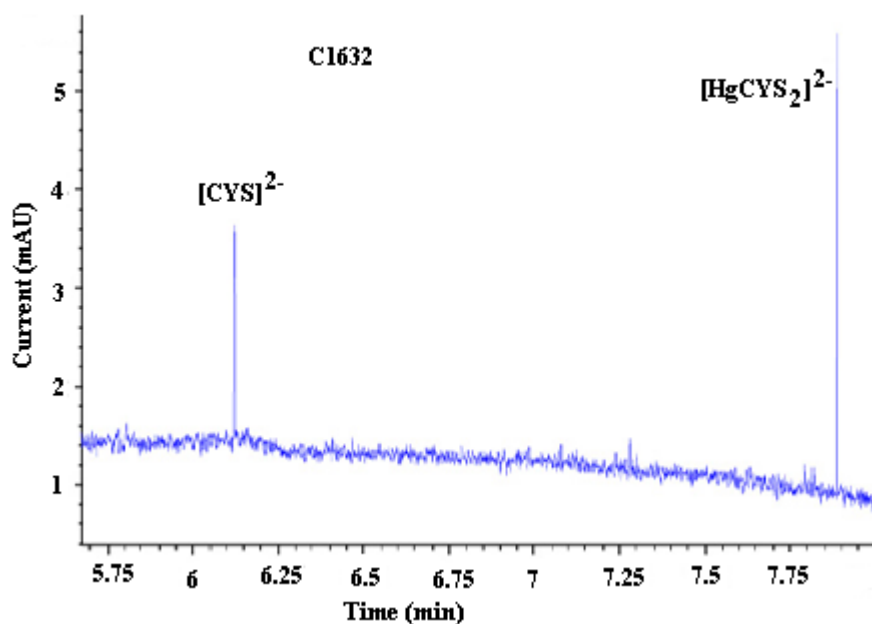


Figure 4.11: Electropherogram of C1632 complexed with cysteine: buffer 0.025 M sodium borate, pH 9.35, Voltage = +25 kV, UV = 200 nm.

Table 4.4: (a) The concentration of reference material and its uncertainty are given
(b) The average and the standard deviations of experimental results for Hg determination with CE-UV

Sample name	(a) Concentration of reference material ($\mu\text{g/g}$)	(b) Experimental data (mg/l)	% RSD
SARM 18	25.0 ± 0.55	23.26 ± 2.18	7.18
SARM 20	40.0 ± 0.98	38.95 ± 1.03	4.03
C1632	unknown	5.25 ± 1.87	6.07

4.7 Analysis of coal samples for Hg with CE-AD

The optimized CE method was applied for the determination of Hg^{2+} in coal samples. Certified reference material SARM 20 was used. Prior to CE analysis, it was treated using the Ontario Hydro (OH) Method (described earlier) and diluted to a final concentration of 0.4

$\mu\text{g/l}$. The result obtained for Hg^{2+} was $0.397 \pm 0.072 \mu\text{g/l}$, with ($n = 3$) and was comparable to the value of $0.4 \mu\text{g/l}$. Figure 4.12 shows the resulting separation obtained using CE-AD. The results obtained indicate that the proposed method can be applied to the analysis of Hg in coal samples.

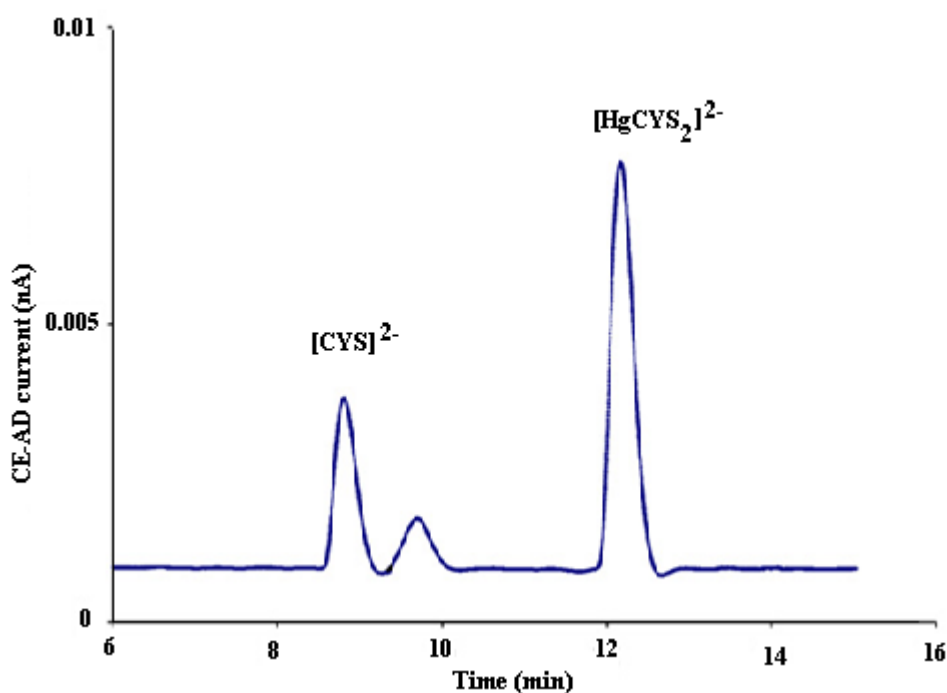


Figure 4.12: Separation of (SARM 20) $0.4 \mu\text{g/l}$ complexed with 33mM cysteine: buffer 25mM sodium borate, pH 9.35, voltage = +25 kV, CE-AD detection at 0.5 V.

4.8 Hg detection limits with CE

Although CE has not been used extensively for Hg speciation, there is a growing interest, as evident from Table 4.5. Comparing the detection limits of various detection modes used in CE found in the literature, the LODs achieved in this study by direct injection of standards are much lower, and are competitive with well-established methods like cold vapour atomic absorption detection methods developed for Hg detection by the United States Environmental Protection Agency (US EPA, Method 245.6) [Lai *et al.*, 1998; Scifres *et al.*, 1995].

Table 4.5: Comparison of various Hg speciation detection limits achieved using CE

Hg species	Separation buffer	Detection	LOD	Reference
Hg ²⁺ , MeHg ⁺ , EtHg ⁺ , PhHg ⁺ complexed with L-cysteine	100 mM sodium borate, pH 8.35	UV 200 nm	0.130 mg/l	[Medina <i>et al.</i> , 1993]
Hg ²⁺ , MeHg ⁺ , EtHg ⁺ , PhHg ⁺ complexed with L-cysteine	25 mM sodium borate, pH 9.3	UV 200 nm	0.50–1.50 mg/l	[Páger and Gáspár, 2000]
Hg ²⁺ , MeHg ⁺ , EtHg ⁺ , PhHg ⁺ complexed with DZS	10 mM sodium acetate, pH 4.5	UV 480 nm	5.0–10 µg/l	[Hardy and Jones, 1997]
Hg ²⁺ , MeHg ⁺	25 mM CaCl ₂	ICP-MS	6.0–14 µg/l	[Tu <i>et al.</i> , 2000]
Hg ²⁺ , MeHg ⁺ , EtHg ⁺	100 mM creatinine acetic acid, pH 4.8	Amperometric	0.2–3.0 µg/l	[Lai <i>et al.</i> , 1998]
Hg ²⁺ , MeHg ⁺ , complexed with L-cysteine	25 mM sodium borate, pH 9.3	Amperometric	0.005–0.4 µg/l	This work

4.9 Conclusions

Capillary electrophoresis with amperometric detection is simple to implement and it provides very good sensitivity for the detection of Hg. The detection limits of 0.005 $\mu\text{g/l}$ for Hg^{2+} and 0.4 $\mu\text{g/l}$ for MeHg^+ are attractive for the monitoring of Hg in coal. Correct alignment and proper electrode cleaning is of the utmost importance to achieve very low and accurate detection levels. The preparation and alignment of the microelectrode is important for the optimum performance of the electrochemical detector for end-column detection. A comparison of the LODs achieved in this study with established literature values shows that the developed electrochemical detector achieves lower LODs and is therefore better suited for environmental Hg determination [Wallingford and Ewing, 1988]. Overall, CE-AD is a quick, inexpensive and sensitive detection mode for Hg, and definitely warrants further exploration.

CHAPTER 5

MERCURY SPECIATION IN SOUTH AFRICAN COAL

The content of this chapter has been published: Jongwana L.T. and Crouch A.M. (2012). Mercury speciation in South African coal. *Fuel*, 94:234–239. Permission to use the content was obtained from Elsevier Limited (see Appendix 3). This study presents total Hg (Hg_T) and Hg speciation in coal samples from different South African power stations. The main objective was to compare the quantified results for Hg_T and Hg species using the in-house established methods [Martin *et al.*, 2010], an automatic Hg analyser (LECO Hg analyzer, AMA-254) and capillary electrophoresis (CE) coupled with a photodiode array detector (CE-PDA).

Although a very sensitive CE-AD method was developed, CE-PDA analysis were performed first using the same operating conditions used in CE-AD in order to investigate the concentration range of coal samples. This was done because high Hg concentrations foul the CE-AD electrode surface and produce broad peaks that could not be analyzed. Good separation results within the detection limits of CE-PDA were observed for coal samples. Based on results observed and time consumed during preparation and alignment of microelectrodes in CE-AD, the CE-PDA method was used for the rest of this study.

5.1 Reagents

All reagents used were of HPLC or analytical grade. Ultrapure water was prepared in a Milli-Q water purification system (Millipore, Eschbron, Germany). Nitric acid (65%) and HCl (32%) were obtained from Merck. The calibration standards and buffers for CE were prepared as explained in Chapter 4. The coal standards were obtained from Industrial Analytical (Pty) Ltd (SA).

5.2 Experimental procedures

5.2.1 Coal samples

Coal samples were obtained from six different power stations in South Africa: Arnot, Camden, Duvha, Hendrina, Lethabo and Tutuka. Permission was obtained from Eskom via Deidre Herbst (Generation Division Environmental Manager then). Figure 5.1, adopted from Lourens *et al.* (2011), shows the regional power plants where coal samples were obtained. Before acid leaching, the coal samples were pulverized and sieved to 120-mesh, then dried in a drying oven at 60 °C for 2 h. After that, they were sealed under N₂ and packed for analysis.

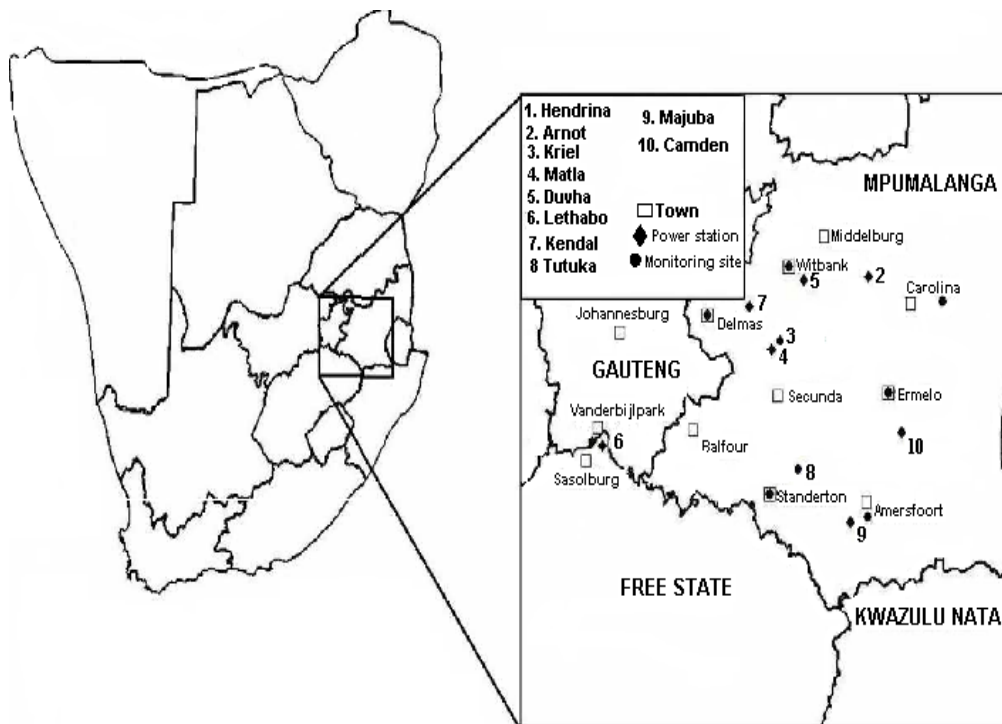


Figure 5.1: Regional power plants where coal samples were obtained, adopted from Lourens *et al.*, 2011.

5.2.2 Acid leaching of coal samples and reference materials

A measured amount of approximately 1 g of coal sample or standard (SARM 18 and 20) was placed in a 250 ml round-bottom flask. To this was added 6 ml of concentrated HCl (32%) and 2 ml of concentrated HNO₃ (65%). The flask was placed in an oil bath at 80 °C for 1 h, then removed and allowed to cool to room temperature. Once the sample was cooled, 20 ml of Milli-Q water was added to dilute the acid sample. The sample was filtered and the filtrate was analysed for Hg speciation using CE and total Hg, using AMA-254. The residue was air dried in a drying oven at 60 °C and weighed, followed by total Hg measurement using AMA-254. The mass of the residue was used in AMA-254 as a requirement for total Hg measurement.

5.2.3 Capillary electrophoresis

To study Hg speciation and the assignment of different Hg species to specific anions, a commercially available Beckman Coulter P/ACE MDQ CE instrument using a PDA detector was used. Experiments were carried out using fused silica capillaries (Composite Metal Services Ltd., Worcester, UK) of 50 µm i.d. and 65 cm length (50 cm effective length). Before use, the capillaries were washed with Milli-Q triple distilled water followed by 1 M NaOH and the separation buffer. The electrolyte and samples were sonicated and filtered through a 0.45-µm membrane filter prior to use. Data analysis was carried out with 32 Karat™ 8.0 software. All experiments were performed at 25 °C. Between each injection, the capillary was filled with the buffer solution and flushed for 5 min. The sample was introduced into the capillary by hydrodynamic injection for 5 s. Random error (precision) was used for measurement of quality.

5.2.4 LECO automatic Hg analyzer (AMA-254)

The coal samples were pulverized to less than 150 μm . The samples were weighed and introduced into the sample boat. In AMA-254, the samples were initially dried and then thermally decomposed in a continuous flow of oxygen. Combustion products were carried off and further decomposed in a hot catalyst bed. Hg vapours were trapped on a gold amalgamator and subsequently desorbed for quantification. The Hg content was determined using an atomic absorption spectrophotometer at 253 nm wavelength. Random error (precision) was used for measurement of quality.

5.3 Results and discussion

5.3.1 Total Hg and Hg species analysis in coal standards and samples using AMA-254 and CE-PDA

The results obtained for total Hg for reference materials (see Table 5.1) show good agreement with the respective certified values provided for reference materials. Hg from coal samples and reference materials was successfully extracted and then detected by AMA-254 and CE-PDA. Total Hg analysis in acid extracts showed that 80% of Hg was extracted with the respective certified values provided for reference materials as well as coal samples. This is also demonstrated in the comparison of total Hg results in coal samples and acid extracts (see Figure 5.2).

According to literature [Wagner and Hlatshwayo, 2005], Hg in South African coal is associated with pyrite, followed by the organic fraction and then carbonate. Pyrite is linked to the content of sulphur in the coal [Goodarzi, 2002]. Pyrite is soluble in HCl and HNO₃, hence 80% recovery of Hg and 20% of Hg can be associated with insoluble forms that are organic matter; volatiles and silicates, which are insoluble in HCl and HNO₃. The results for the residue show

that more than 10% of total Hg in coal standards and samples was not extracted. According to the United States Geological Survey (USGS) leaching protocol 1990 [Hoffart *et al.*, 2006], it is stated that if Hg is in organic matter, its concentration in the HNO₃/HCl solution will be low because HNO₃/HCl solution does not release Hg from organic matter. Feng and Hong (1999) found Hg to have a good correlation with sulphur, but determined a negative correlation between Hg and organic matter present in coal.

Table 5.1: Total Hg and Hg species concentrations obtained for coal standards and samples determined using AMA-254 and CE-PDA

Samples		Total Hg in coal standards and samples (ppm)	Total Hg in acid extracts (ppm)	Hg ²⁺ in acid extracts (ppm)	Total Hg in residue (ppm)	Total Hg extracted in coal (%)	Total Hg in residue (%)	Hg ²⁺ in acid extracts (%)
SARM 20	Replicate 1	0.21	0.18	0.16	0.024	85.71	11.43	88.89
	Replicate 2	0.301	0.19	0.17	0.032	63.12	10.63	89.47
	Replicate 3	0.221	0.18	0.16	0.033	81.45	14.93	88.89
	Certified value	0.250 (0.2–0.3)^a						
SARM 18	Replicate 1	0.037	0.027	0.025	0.006	81.08	16.22	96.67
	Replicate 2	0.036	0.028	0.026	0.006	77.78	16.67	94.44
	Replicate 3	0.037	0.029	0.027	0.005	78.38	13.51	91.89
	Uncertified value	0.040^a						
SRM 1632C	Replicate 1	0.0918	0.0725	0.0695	0.0121	78.98	13.18	95.86
	Replicate 2	0.0916	0.0733	0.0702	0.0131	80.02	14.3	95.77
	Replicate 3	0.0917	0.0724	0.0691	0.0123	78.95	13.41	95.44
	Certified value	0.0938^a						
BCR180	Replicate 1	0.12	0.0944	0.0909	0.0158	78.67	13.17	96.29
	Replicate 2	0.119	0.0937	0.0894	0.0159	78.74	13.36	95.41
	Replicate 3	0.118	0.0927	0.0888	0.016	78.56	13.56	95.79
	Uncertified value	0.123^a						
Duvha	Sample	0.11	0.093	0.09	0.013	84.55	11.82	96.77
Lethabo	Sample	0.141	0.113	0.11	0.021	80.14	14.89	97.35
Camden	Sample	0.14	0.11	0.108	0.016	78.57	11.43	98.18
Arnot	Sample	0.121	0.097	0.093	0.015	80.17	12.4	95.88
Hendrina	Sample	0.141	0.11	0.107	0.024	78.01	17.02	97.27
Tutuka	Sample	0.142	0.116	0.11	0.02	81.69	14.08	94.83
Percentage quality uncertainty		± 0.203%	± 0.203%	± 0.305%	± 0.203%			

^a Certified value with the acceptable ranges in brackets.

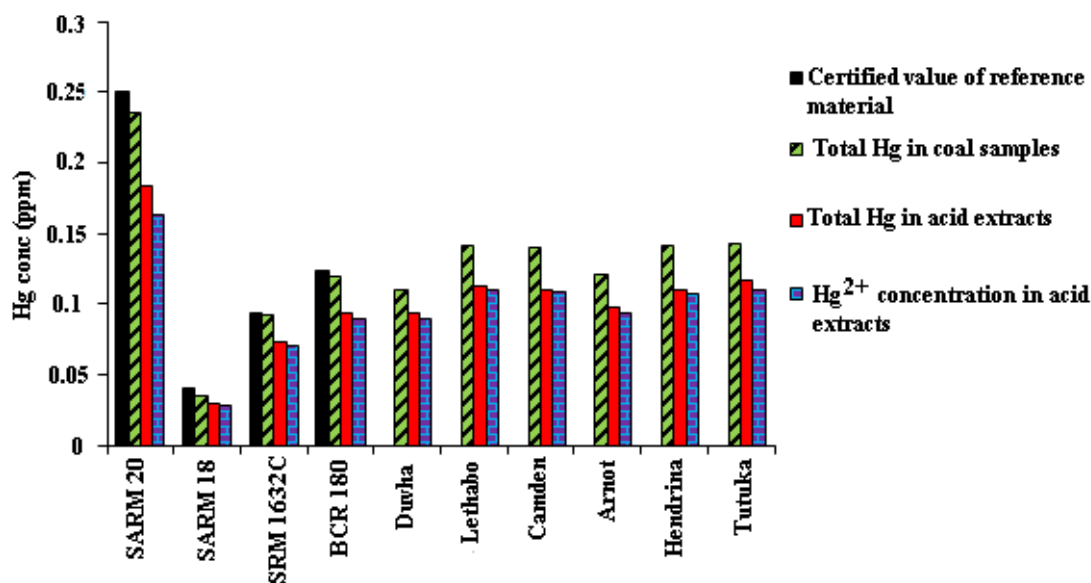


Figure 5.2: Comparison of total Hg results in coal samples and acid extracts determined using AMA-254 as well as Hg²⁺ concentration in acid extracts.

5.3.2 Analysis of coal samples for Hg species using CE-PDA

Figures 5.3 and 5.4 show the electropherograms that were obtained using CE-PDA for certified standard material (SARM 20) and Duvha coal sample extracts, respectively. The electropherograms obtained for other certified standard materials and power station coal sample extracts are included in Appendix A1. The electropherograms show that only Hg²⁺ species was detected from the extracts in all coal samples. The concentration of Hg²⁺ species for coal samples and certified standard materials are shown in Table 5.1. The comparison of results in Figure 5.2 and Table 5.1 clearly shows that 96% of the total Hg in acid extracts is Hg²⁺ species. From this result, and the discussion on acid extraction in coal, it can be assumed that 4%, which was not detected in CE, is unleachable Hg in the organic matter that is probably bound to humic acids and/or other refractory organic material. Based on these studies and results obtained in this study, it can be concluded that although the coal samples contain mainly inorganic Hg, small amounts of organic Hg are also present.

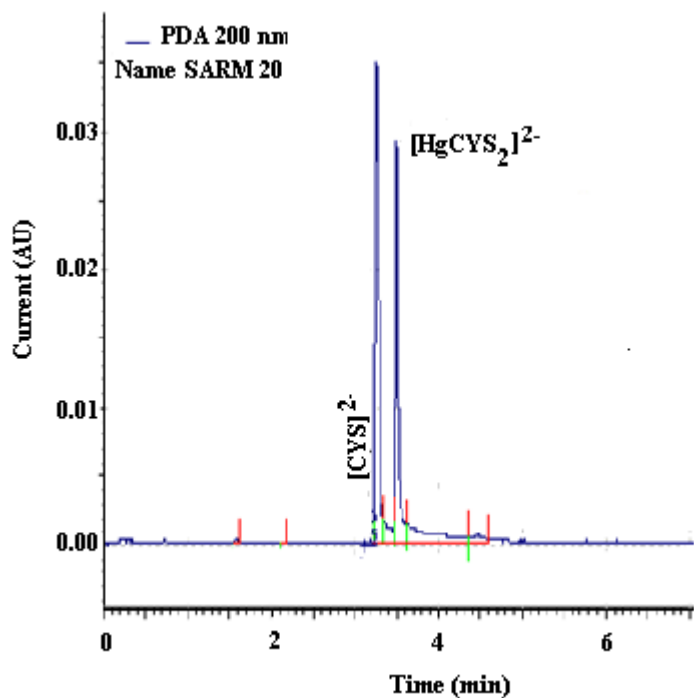


Figure 5.3: Electropherogram of SARM 20 complexed with cysteine: buffer 0.025 M sodium borate, pH 9.35, voltage = +25 kV, UV = 200 nm.

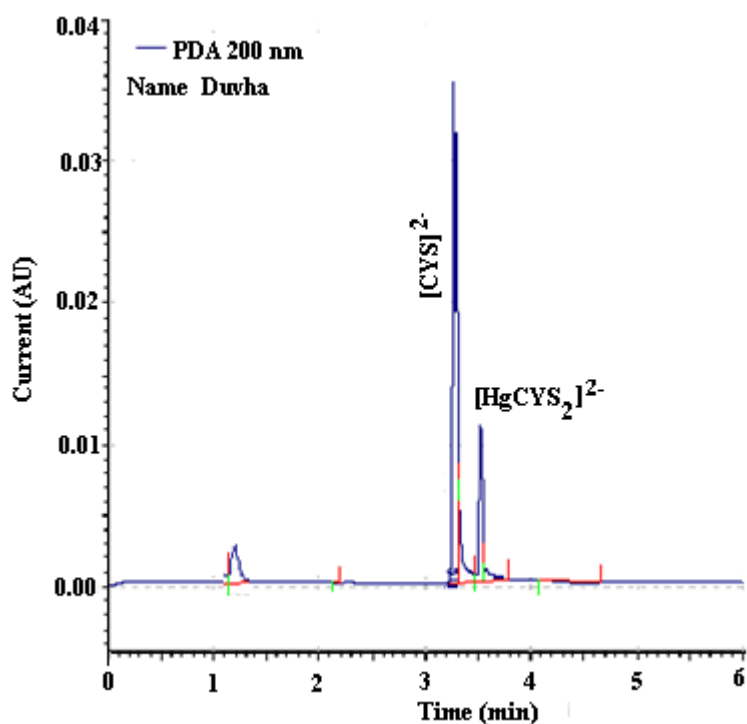


Figure 5.4: Electropherogram of Duvha coal sample complexed with cysteine: buffer 0.025 M sodium borate, pH 9.35, voltage = +25 kV, UV = 200 nm.

5.4 Calibration curves

The CE-PDA system was calibrated with a series of Hg^{2+} standards up to a concentration of 100 $\mu\text{g/l}$. A linear range was observed for Hg^{2+} from 0.01 to 20 $\mu\text{g/l}$. The repeatability was determined by injecting the different standards three times into the CE-PDA instrument. Good linearity (Figure 5.5) and reproducibility were observed during the experiments. The LOD was determined with a signal-to-noise ratio of 3:1. A correlation of 0.9757 of eight measurements was obtained. Results for standard deviations (STD) and percentage relative standard deviations (% RSD) were calculated with Microsoft Excel for all CE experiments. The LOD for Hg^{2+} was found to be $0.01 \pm 0.007 \mu\text{g/l}$. The results of the linear regression data of Hg^{2+} cysteine complex are summarized in Table 5.2.

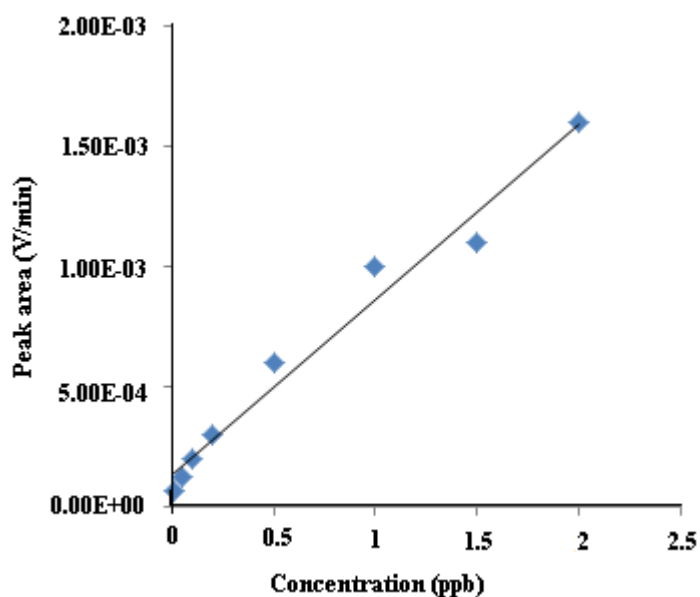


Figure 5.5: Calibration curve of Hg^{2+} with CE-PDA.

Table 5.2: Linear regression data of Hg²⁺ cysteine complex

	Range (µg/l)	Linear regression	Correlation coefficient	LOD (µg/l)	LOQ (µg/l)	% RSD
Hg ²⁺	0.01–20	$7.0E^{-04}x+1E^{-05}$	0.9757	0.01 ± 0.007	0.02	1.74

5.5 Conclusions

In this study, total Hg concentration in coal samples, reference materials and acid extracts were analyzed using a LECO automatic Hg analyzer (AMA-254). Hg speciation in acid extracts was analyzed by CE. Only 80% recovery of total Hg concentration from coal samples and reference materials after acid extraction was obtained, and 96% of that 80% was found to be the Hg²⁺ species. Based on results obtained in this study, it can be concluded that although the coal samples contain mainly inorganic Hg, small amounts of organic Hg are also present.

CHAPTER 6

SAMPLING AND MERCURY SPECIATION WITHIN THE POWER STATION PROCESSES

This chapter describes sampling and Hg speciation measured at the stack in Duvha Power Station for units 1 and 2. The sampling for Hg speciation was conducted in accordance with the ASTM method of Ontario Hydro (OH) sampling (ASTM D6784). The experimental section in this chapter has been submitted for publication: Jongwana L.T. and Crouch A.M. Air Quality Monitoring of Mercury species at Elandsfontein in South Africa. South African Journal of Science, SAJS-2013-0243

The main objectives were as follows:

- determine the Hg species present under operating conditions using recently established techniques (Jongwana and Crouch, 2012; Martin *et al.*, 2010)
- compare the observed Hg species results measured using recently established techniques with the results obtained using other analytical techniques, such as high performance liquid chromatography with an amperometric detector (HPLC-AD) and atomic fluorescence spectrometry (AFS)
- carry out an overall Hg mass balance.

6.1 Sampling for Hg speciation

6.1.1 Sampling reagents:

(i) KCl absorbing solution (1 M)

KCl (74.56 g) was dissolved in 500 ml Milli-Q triple distilled water in a 1000 ml volumetric flask and diluted to the volume with Milli-Q triple distilled water. A new batch of solution was prepared prior to each sampling test.

(ii) HNO₃-H₂O₂ absorbing solution (5% (v/v) HNO₃, 10% (v/v) H₂O₂)

Fifty millilitre of concentrated HNO₃ (55%) was added slowly, with stirring, to a 1000 ml volumetric flask containing approximately 500 ml of Milli-Q triple distilled water, and then 333 ml of (v/v) H₂O₂ (30%) was added. The solution was diluted to volume with Milli-Q triple distilled water. A new batch of solution was prepared prior to each sampling test.

(iii) H₂SO₄-KMnO₄ absorbing solution (4% (w/v) KMnO₄, 10% (v/v) H₂SO₄)

Fifty millilitre of concentrated H₂SO₄ (97%) was carefully mixed into approximately 800 ml of Milli-Q triple distilled water and made to 1000 ml by adding Milli-Q triple distilled water, to afford a 10% (v/v) H₂SO₄. Forty grams of KMnO₄ was dissolved into approximately 800 ml of 10% (v/v) H₂SO₄, and made to 1000 ml by adding 10 % (v/v) H₂SO₄. To prevent autocatalytic decomposition of the permanganate solution, the solution was filtered through filter paper. A new batch of solution was prepared prior to each sampling test.

(iv) Saturated potassium permanganate solution (5% w/v)

Five grams of KMnO_4 were mixed into 50 ml Milli-Q triple distilled water and diluted to 100 ml with Milli-Q triple distilled water.

6.2 Hg speciation at Duvha Power Station

6.2.1 Site description

Duvha Power Station is a coal-fired power plant operated by Eskom. It is located approximately 15 km east of Witbank in Mpumalanga. Its chimneys, 300 m (980 ft) tall, are the tallest free standing concrete structures in Africa [http://en.wikipedia.org/wiki/Duvha_Power_Station]. It has six units and an installed capacity of 3600 MW. Units 1–3 of its six units are retrofitted with fabric filters and units 4–6 are retrofitted with electrostatic precipitators.

6.2.2 Sampling procedures at the stack at Duvha Power Station

Coal, bottom ash, fly ash and flue gas samples were collected from Duvha Power Station units 1 and 2. The flue gas sampling was conducted in accordance with the OH method (11–14 June 2011). Figure 6.1 is the schematic diagram of units 1 and 2 at Duvha Power Station. Table 6.1 presents the sampling parameters at Duvha unit 1 and 2. The OH method was used to take Hg^0 , Hg^{2+} and Hg_p samples from the flue gas. The samples were taken from the flue gas stream isokinetically, through a glass-lined probe and a glass fibre filter at 120 °C, followed by a series of seven impingers immersed in an ice bath. The filters that were used were Pall Life Science glass fibre filters with a typical 0.3 μm di-octyl phthalate aerosol retention of 99.98%. After sampling, the filter was digested according to the OH method. The Hg content in the particles captured by filter was reported as Hg_p .

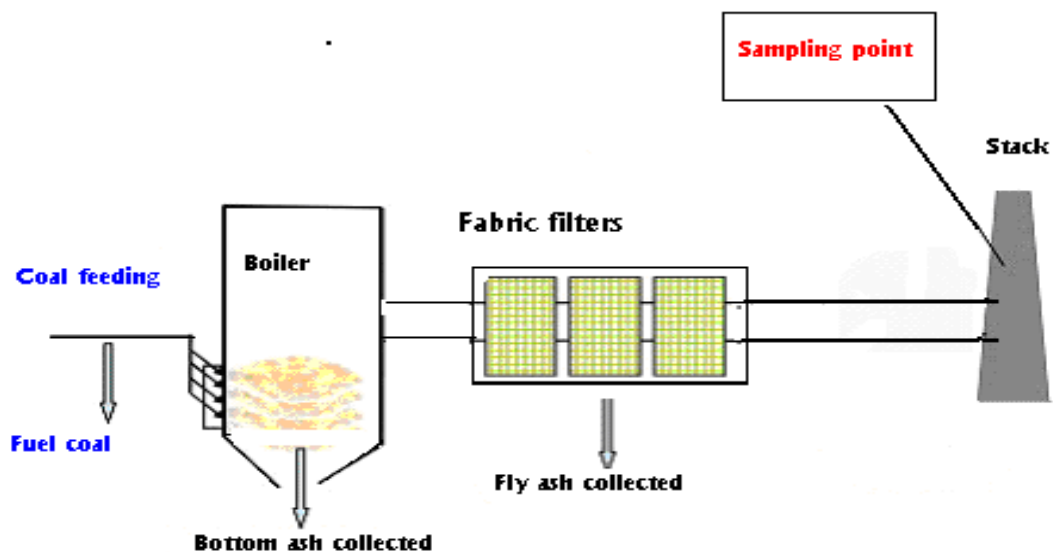


Figure 6.1: Schematic diagram of units 1 and 2 at Duvha Power Station [Park *et al.*, 2008].

Table 6.1: Sampling parameters at Duvha Unit 1 and 2

Parameter	units	Unit 1	Unit 2
Gas volume sample at dry STP	m ³	2.4	2.6
Gas Temperature	°C	120.0	120.1
Oxygen	%	9.1	9.4
Sample Time	min	150.0	150.0
Moisture concentration	%	11.4	11.5
Isokineticity	%	97.8	97.8
Velocity	m/s	36.2	35.4
Volumetric flow rate at STP (3% O ₂)	Nm ³ /s	880.39	854.39

The impinger train was cooled by placing it into an ice bath to reduce the flue gas temperature to below the boiling point of Hg. The first three impingers contained 100 ml KCl (1 M) solution. These impingers capture Hg²⁺ from flue gas. The fourth

impinger contained 100 ml of a mixture of 5% (v/v) HNO_3 and 10% (v/v) H_2O_2 . The fifth and sixth impingers contained 100 ml of the mixture of 4% KMnO_4 and 10% H_2SO_4 . These impingers capture Hg^0 from flue gas. The last impinger contained silica gel to capture the remaining moisture from the flue gas. The flue gas samples were taken at a height of 300 m at the stacks of units 1 and 2, equipped with pollution control devices (fabric filters), while the boiler operated at full load. Approximately 7 l/min of flue gas sample passed through the impingers over a period of 2.5 h. After each sampling event, the samples were transferred to amber/brown glass bottles using the ‘clean hands dirty hands procedure’ (US EPA method 1669) and preserved as required for the OH method. The sampling train glassware and tubing were cleaned following the OH procedure to avoid trace metal contamination. Figure 6.2 shows a photograph of the sampling personnel and sampling train at the stack in Duvha Power Station.



Figure 6.2: Sampling at the stack in Duvha Power Station: (A) Sampling personnel;
(B) Sampling train.

6.3 Speciation analysis

Concentrations of Hg in coal, bottom ash and fly ash samples were determined by the in-house method (LECO AMA-254) that was explained in Chapter 5 (Section 5.2.4). Analysis of the Hg content from the impingers was conducted using the following methods:

- the developed capillary electrophoresis (CE) technique published by Jongwana and Crouch (2012)
- high performance liquid chromatography coupled with an amperometric detector
- atomic fluorescence spectrometry

6.3.1 High performance liquid chromatography coupled with an amperometric detector

In this method, the Hg compounds were complexed with cysteine and separation of the Hg species was carried out on an Agilent 1100 series coupled with amperometric detector. The separation was achieved on a reversed-phase Synergi Hydro-RP C₁₈ column (15 cm × 4.6 mm i.d.) using aqueous 0.1% w/v CYS and 0.1% w/v L-cysteine mobile phase at a flow rate of 0.8 ml/min at ambient temperature.

6.3.1.1. Reagents

The chemicals used were reagent grade purity and purchased from Merck. The water used to prepare the aqueous solution was ultrapure and purified by a Milli-Q system. A stock solution of Hg²⁺ was prepared by dissolving its chloride salt (Sigma-Aldrich)

in 0.1% HCl. The stock solution was stored in a refrigerator. The standard solutions were prepared daily by appropriate dilutions with purified water.

6.3.1.2 Chromatographic conditions

The operating conditions used for the determination of Hg are listed in Table 6.2. The mobile phase was prepared by volume and consisted of aqueous 0.1% w/v CYS and 0.1% w/v L-cysteine. The mobile phase was filtered through a 0.45- μm Durapore membrane and sonicated before use. The mobile phase and the standards were prepared daily.

Table 6.2: Chromatographic conditions used for the HPLC-AD analysis of Hg

HPLC		Amperometric	
Column	Phenomenex Synergi Hydro-RP	Potential	0.5 V
Column temperature	Ambient temperature	Filter	0.2 μm
Injection volume	20 μl	Range	5 μA
Flow rate	0.8 ml min^{-1}		
Pump mode	Isocratic		
Mobile phase	0.1% w/v CYS + 0.1% w/v L-cysteine		
Run time	12 min		

6.3.1.3 Analysis of the samples

The samples obtained from the impingers were complexed with cysteine. Analyses were carried out in duplicate and samples injected into the HPLC in triplicate.

6.3.2 Atomic fluorescence spectrometry

In AFS, an aliquot of the acidified sample was digested using chemically generated bromine, which is known to break down all commonly occurring organo-Hg species to Hg^{2+} . Elemental Hg vapour was generated from the digested sample by reduction with stannous chloride, followed by purging of the elemental Hg with the argon carrier gas (spectrographic grade), at a regulated pressure of >700 kPa. The Hg vapour was detected using a Millennium Merlin AFS system.

6.3.2.1 Reagents

As reagents may contain Hg as impurity, ultra-pure reagents were used. The following solutions were used:

(i) 1000 mg/l Hg stock solution

Hg stock solution (1000 mg/l) was obtained from Merck

(ii) Hydrochloric acid (33% v/v))

HCl (33% v/v) was prepared by diluting 167 ml of high purity HCl (36%) to 500 ml in water.

(iii) Stannous chloride (SnCl_2) solution (2% m/v)

SnCl_2 (2% m/v) was prepared by dissolving 10 g of SnCl_2 salt (Merck) in 225 ml of the 33% HCl (ii), while heating. The solution was allowed to cool and then transferred to a 500 ml volumetric flask and make up with Milli-Q water.

(iv) Potassium bromate-bromide stock solution (0.1N)

Ready-made ampoules of potassium bromate-bromide solution were purchased from Merck.

6.3.2.2 Calibration solutions

Hg calibration solutions (10 mg/l) were prepared by pipetting 5 ml of Hg stock solution (1000 mg/l) into 500 ml volumetric flasks. Ten millilitre of potassium bromate-bromide (0.1 N) solution was added followed by 75 ml of the HCl (33% v/v) and then made up to the volume with Milli-Q water.

From the prepared 10 mg/l Hg solution, 50 ml was pipetted into a 500 ml volumetric flask. 10 ml of potassium bromate-bromide (0.1 N) solution was added, followed by 75 ml of the HCl (33% v/v) and then made up to the volume with Milli-Q water.

The calibration standards of 1 µg/l, 2 µg/l and 5 µg/l of Hg were prepared from 1 mg/l Hg solution. Appropriate quantities (1 ml, 2 ml and 5 ml, respectively) of 1 mg/l were pipetted into 1000 ml volumetric flasks. To each flask, 20 ml of potassium bromate-bromide (0.1 N) solution and 150 ml of the HCl (33% v/v) were added and then made up to the volume with Milli-Q water.

The blank solution was prepared by adding 2 ml of 0.1 N potassium bromate-potassium bromide solution and 15 ml of the 33% v/v HCl (33%) to 70 ml Millipore water in a 100 ml volumetric flask. The solution was made up to the volume with Milli-Q water.

6.3.2.3 Analysis of the samples

The samples from the impingers were digested using chemically generated bromine and reduced with stannous chloride to form elemental Hg vapour. The generated Hg vapour was purged with the argon carrier gas and detected by AFS. Analysis was carried out in duplicate.

6.4 Results and discussion

6.4.1 High performance liquid chromatography coupled with an amperometric detector

6.4.1.1 Optimum conditions for separation

Figure 6.3 shows the chromatogram of a standard solution of Hg^{2+} determined with HPLC-AD. The calibration graph containing the information for the determination of the Hg^{2+} is illustrated in Figure 6.4. The optimum conditions for separation given in Table 6.2 were used to obtain the required data.

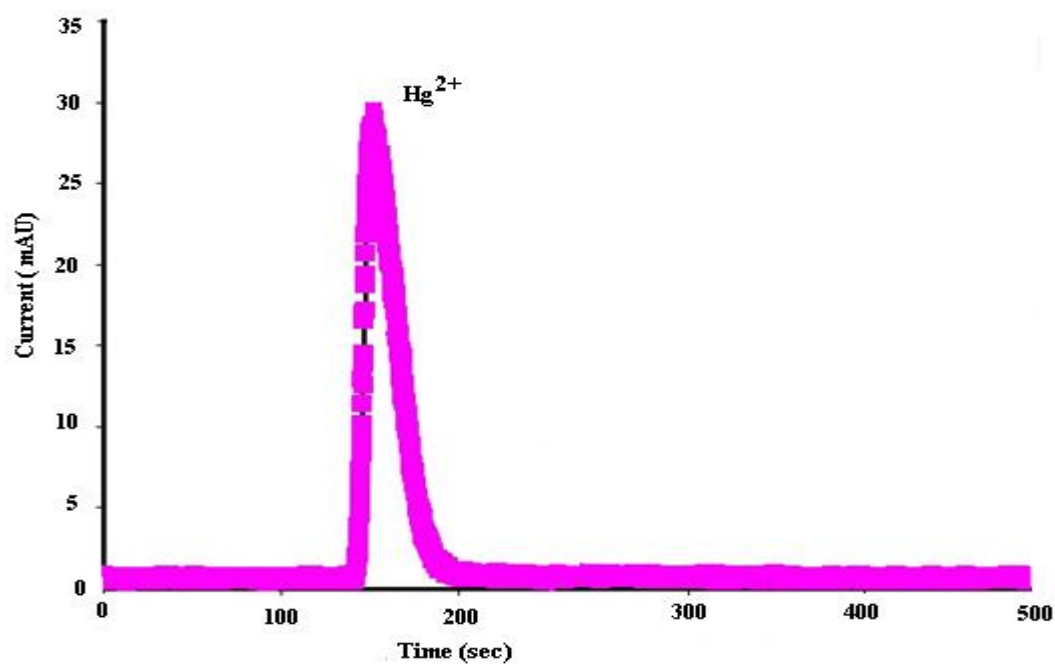


Figure 6.3: Chromatogram of a standard solution of Hg^{2+} with the mobile phase as mentioned above determined with HPLC-AD.

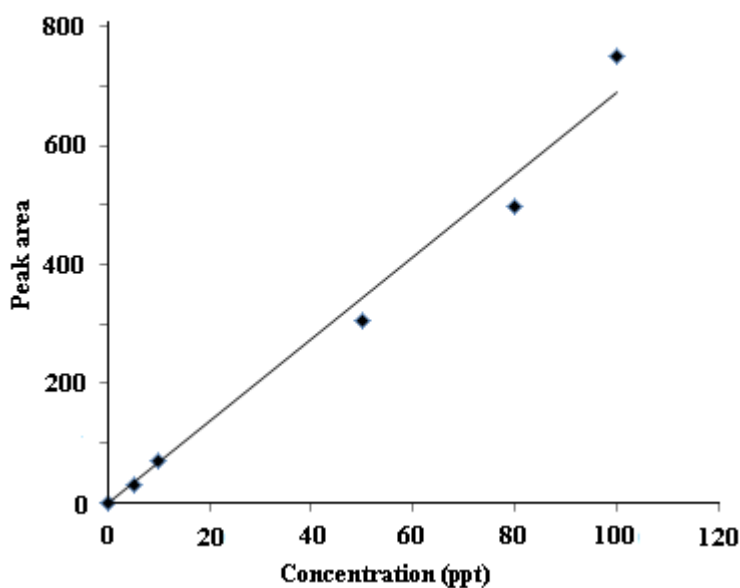


Figure 6.4: Calibration curve of Hg^{2+} determined with HPLC-AD under optimum conditions.

6.4.1.2 Linearity and detection limits

Linear regression data for Hg^{2+} are shown in Figure 6.4. A calibration curve was obtained from six standards and the correlation coefficient was 0.9822. The detection limit was defined as the calculated amount of the analyte that corresponds to a signal equal to three times the standard deviation of six representative blank samples [Malesuik *et al.*, 2006]. The limit of detection (LOD) and limit of quantification (LOQ) values were determined using a signal-to-noise ratio of 3 and 10, respectively.

Table 6.3: Linear regression data for Hg^{2+}

	Range (ppt)	Linear regression	R^2	LOD (ppt)	LOQ (ppt)
Hg^{2+}	10–120	6.8841x	0.9822	2 ±0.04	7

6.4.1.3 Recovery efficiency and accuracy studies

The samples were spiked with known quantities of the Hg species in order to determine the recovery efficiency. The analyte recoveries from the spiked samples were 97.54–119.9%. The accuracy of the method was determined by analysing a standard solution. The recovery value obtained from the standard solution was 98.2%.

6.4.2 Atomic fluorescence spectrometry

6.4.2.1 Linearity and detection limits

The calibration graph containing information that was later to be used for the determination of the total Hg is illustrated in Figure 6.5.

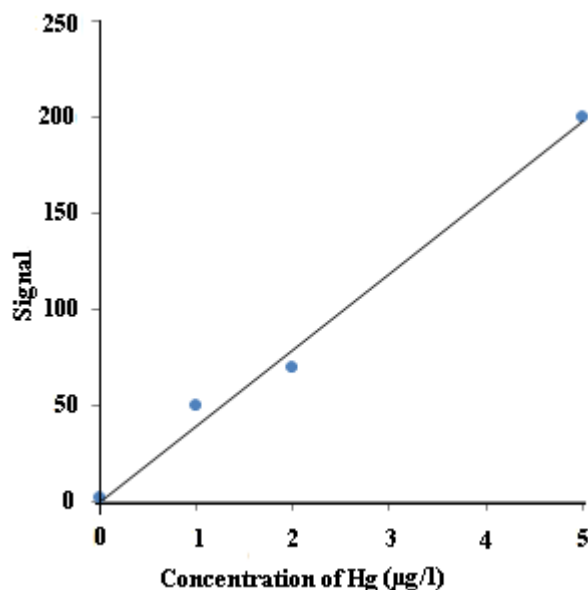


Figure 6.5: Calibration curve of total Hg determined with AFS.

A calibration curve was obtained from three standards and the blank sample. The correlation coefficient was than 0.99073 of four measurements. The detection limit is defined as the calculated amount of the analyte that corresponds to a signal equal to three times the standard deviation of six representative blank samples. The LOD and LOQ values were determined using a signal-to-noise ratio of 3 and 10, respectively.

Table 6.4: Linear regression data of total Hg determined using AFS

	Range (µg/l)	Linear regression	R²	LOD (µg/l)	LOQ (µg/l)
Total Hg	1–5	39.667x	0.9907	0.01±0.02	1

6.4.2.2 Quality control check and recovery efficiency

A process similar to that used for the preparation of the calibration solutions was used, but here the 1000 mg/l Hg stock solution was from Spectrascan Solution Standards provided by Industrial Analytical (Pty) Ltd (SA). For recovery efficiency, the samples were spiked with known quantities of the Hg standard (2 µg/l) in order to determine the recovery efficiency. Analysis was carried out in duplicate. The recoveries from the spiked samples were 94.52–98.21%, as tabulated in Table 6.5. The accuracy of the method was determined by analysing a standard solution. Recovery values obtained from the standard solution was 98.9%.

Table 6.5: Recovery results of total Hg determined using AFS

Sample	Total Hg without spike (µg/l)	Spike (µg/l)	Total Hg after spiking (µg/l)	Spike recovery (%)
1	0.6962	2.0	2.5866	94.52
1	0.6961	2.0	2.5864	94.52
2	0.6981	2.0	2.6201	96.10
2	0.6980	2.0	2.6204	96.12
3	1.2620	2.0	3.1862	96.21
3	1.2620	2.0	3.1856	96.18
4	1.1110	2.0	3.0536	97.13
4	1.1108	2.0	3.0528	97.10
5	0.7051	2.0	2.6693	98.21
5	0.7050	2.0	2.6688	98.19
6	0.4040	2.0	2.3641	98.01
6	0.4040	2.0	2.3642	98.01
% quality uncertainty	± 0.82%			

6.5 Hg speciation in flue gas

Table 6.6 shows the total Hg in coal, bottom ash and fly ash and the relative enrichment factors (REFs) measured at Duvha unit 1 and 2. REFs were used to express the volatility of trace elements during combustion in power station. Introduced by Meij (1994), the REFs in the context of trace elements in coal combustion products is defined below:

$$REF = \left(\frac{\text{TE content in ash}}{\text{TE content in coal}} \right) \times \left(\frac{\% \text{ ash content in coal}}{100} \right)$$

where TE: trace element.

The volatility of trace elements can be classified according to the REFs [Meij, 1994]. Hg was mostly volatile, escaping with flue gas through the stack. Therefore, to be able to understand emissions of Hg from a coal-fired power station, it is important to conduct flue gas sampling. After the REFs of fly ash were compared, it appears that Hg enrichment in fly ash from both units is the same.

Table 6.6: Mercury content in coal, bottom ash and fly ash and the relative enrichment factors for Duvha Power Station units 1 and 2

Unit	Hg ($\mu\text{g}/\text{kg}$) at Duvha Power Station			Relative enrichment factors	
	Coal	Bottom ash	Fly ash	bottom ash	fly ash
1	113 \pm 3.2	1.1 \pm 0.15	22.1 \pm 0.9	0.003	0.065
2	110 \pm 3.1	1.2 \pm 0.16	22.4 \pm 0.9	0.003	0.067

Previous studies suggest that Hg is adsorbed on the un-burnt carbon particles in the fly ash [Guo *et al.*, 2007; Lu *et al.*, 2007]. Carbon particles act as adsorbents for Hg; particles capture the volatile Hg in the post-combustion cooling zone [Sable *et al.*, 2008]. Hence, higher Hg concentrations were measured in fly ash than in bottom ash.

Hg speciation results in the flue gas for the stacks of unit 1 and 2 are shown in Table 6.7. These results show a clear transition of Hg speciation at the sampling point. Hg^{2+} was the predominant species measured at the stack for both units. This could be explained by the fact that Hg compounds could be oxidized through fabric filters (which are designed to remove particulates) because an increase in contact time in the flue gas and fly ash and/or acidic gas components enhances the Hg oxidation rate [Pavlish, 2011].

Table 6.7: Hg speciation in the flue gas for unit 1 and 2 (corrected to a 3% O_2 basis)

	Unit 1			Unit 2		
	Hg^0	Hg^{2+}	Hg_p	Hg^0	Hg^{2+}	Hg_p
	$(\mu\text{g}/\text{Nm}^3)$			$(\mu\text{g}/\text{Nm}^3)$		
CE	0.431	3.388	0.031	0.433	3.398	0.035
HPLC-AD	0.427	3.392	0.027	0.437	3.402	0.031
AFS	0.427	3.388	0.035	0.437	3.398	0.035

South African coal contains very low concentration of chlorine which means that the dominant oxidizing agent in the flue gas is SO_2 . Therefore, during the contact time of flue gas and fly ash in the fabric filters, the Hg compounds are oxidized by SO_2 (in flue gas) to Hg^{2+} . Some of the Hg^{2+} then reacts with NO_2 (also a component of flue gas) to form the Hg nitrate salt ($\text{Hg}(\text{NO}_3)_2$). $\text{Hg}(\text{NO}_3)_2$ is then released to the fly ash. This explanation is clearly demonstrated by the Hg chemisorption model shown of Pavlish (2011), in Figure 6.6.

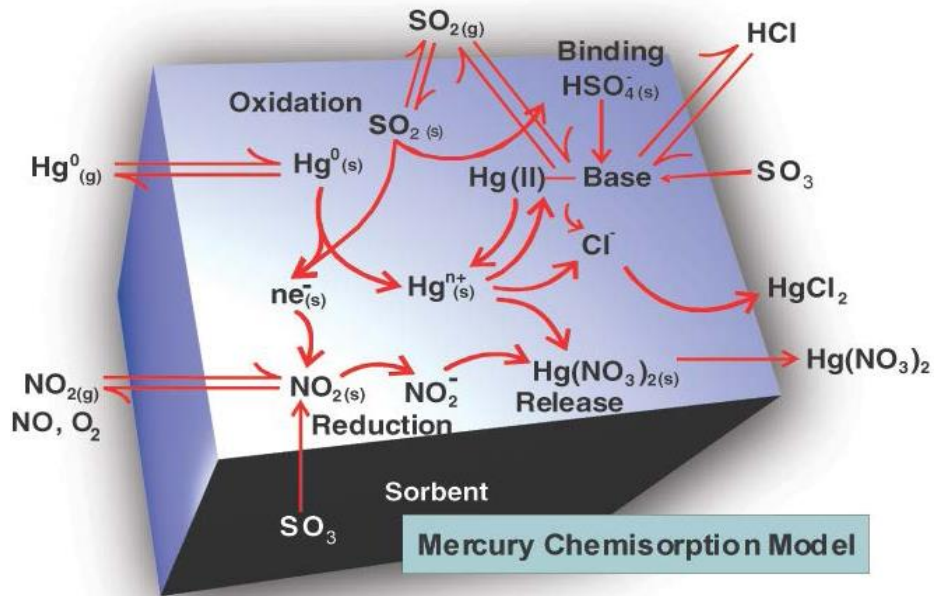


Figure 6.6: Hg chemisorption model [Pavlish, 2011].

6.6 Overall mercury balance

During combustion, most of the coal Hg is first released as the elemental Hg (Hg^0) form. As the flue gas temperature decreases, part of the Hg^0 is oxidized to Hg^{2+} , either by gas-phase oxidation or catalytic oxidation [Galbreath and Zygarlicke, 2000]. As the flue gas temperature drops further, part of the Hg^0 and Hg^{2+} in the gas phase condenses on, or is adsorbed by, fly ash particles. The material of the fabric filters may also alter the Hg partitioning in the flue gas since it removes a substantial amount of the Hg^{2+} . The Hg balances for both units varied from 74.36% to 74.57% of the input coal Hg as shown in Table 6.8

Table 6.8: Mass balance of Hg at Duvha Power Station unit 1 and 2

	Hg content	Flow rate	Total Hg flow (g/h)	Mass balance (%)
<u>Unit 1</u>				
Coal	113 µg/kg	~ 41 kg/s	0.277980	
Bottom ash	1.1 µg/kg	~ 0.5 kg/s	0.000033	74.36
Fly ash	22.1 µg/kg	~ 2.5 kg/s	0.003315	
Flue gas	3.8 µg/Nm ³ /s	880.39 Nm ³ /s	0.203370	
<u>Unit 2</u>				
Coal	110 µg/kg	~ 41 kg/s	0.27060	
Bottom ash	1.2 µg/kg	~ 0.5 kg/s	0.00004	74.57
Fly ash	22.4 µg/kg	~ 2 kg/s	0.00336	
Flue gas	3.87 µg/Nm ³	854.39 Nm ³ /s	0.19839	

About 22.1–22.4 µg/kg of Hg was collected from the fabric filter’s fly ash storage hopper and 3.8 -3.87 µg/Nm³ of Hg was measured at the sampling point. This is in the range of total Hg concentration in the emissions of 1.9 -5.6 µg/Nm³. Hg balance were obtained from two units (1 and 2) at Duvha Power Plant in this study, however , a series of long-term and comprehensive study is required to evaluate the reliable Hg mass distribution and behaviour in a coal fired power plant.

6.7 Conclusions

The following conclusions were deduced from the study of the emissions and Hg speciation carried out at Duvha Power Station (units 1 and 2) equipped with fabric filter devices:

- The Hg balance for both units varied from 74.36% to 74.57% of the input coal Hg
- The predominant form of Hg after the fabric filter devices was Hg^{2+} , due to the oxidation of Hg^0 to Hg^{2+} as the flue gas temperature decreases
- A series of long-term and comprehensive study is required to evaluate the reliable Hg mass distribution and behaviour in a coal fired power plant.

CHAPTER 7

AIR QUALITY MONITORING OF MERCURY SPECIES

AROUND POWER PLANTS

This chapter presents results of sampling and Hg speciation measured at Elandsfontein Air Quality Monitoring (AQM) station and at the flare discharge of Majuba Underground Coal Gasification (UCG) plant. Hg speciation was determined using the established techniques for Hg speciation used in Chapter 6. Total gaseous mercury (TGM) was measured using Tekran 2537B automated mercury monitor. Some content (results) in this chapter has been submitted for publication: Jongwana L.T. and Crouch A.M. Air Quality Monitoring of Mercury species at Elandsfontein in South Africa. South African Journal of Science, SAJS-2013-0243. The sampling for Hg speciation was conducted in accordance with the ASTM method of Ontario Hydro (OH) sampling.

The main objectives are the same as those given in Chapter 6, but with one additional aim here, namely, to compare the total value of mercury species with the TGM as measured using the Tekran 2537B at Elandsfontein AQM station.

7.1 Sampling for mercury speciation

At Elandsfontein AQM station, the sampling was carried out over a period of 10 days in winter (5 days winter 2010 and 5 days winter 2011) and 10 days in summer (5 days summer 2011 and 5 days summer 2012). The sampling by OH method and the TGM measurements using the Tekran 2537 B were carried out at the same place. At Majuba UCG plant, the sampling was carried out over a period of 5 days in summer 2012 and 5 days winter 2012.

7.1.1 Total gaseous Hg measurement

The TGM was measured using the Tekran 2537B system. The instrument collects total gaseous Hg concentrations on gold traps within the system, which is equipped with a 45-mm diameter Teflon pre-filter (pore size 0.2 mm). The following experimental conditions applied: flow rate 1 l/min, total flow through the denuder and particulate filter assembly 7 l/min. The instrument samples air, and traps Hg vapour onto patented cartridges containing an ultra-pure gold adsorbent. The amalgamated Hg is thermally desorbed and detected using cold vapour atomic fluorescence spectrometry (CVAFS). The Tekran 2537B instrument was routinely subjected to automated daily calibrations using an internal permeation Hg vapour standards from National Institute of Standards and Technology standard. Two-point calibrations (zero and span) were performed separately for each pure gold cartridge. The detection limit for TGM was 2 pg/m³.

7.1.2 Atmospheric Hg speciation

The OH method was used obtain Hg⁰ and Hg²⁺ samples from the atmosphere at the Elandsfontein AQM station for Hg speciation. Samples were taken over a period of 2.5 h, using a vacuum pump to suck air through seven chilled impingers. The first three impingers contained 100 ml KCl (1 M) solution. These impingers capture Hg²⁺ from air. The fourth impinger contained 100 ml of a mixture of 5% (v/v) HNO₃ and 10% (v/v) H₂O₂. The fifth and sixth impingers contained 100 ml of a mixture of 4% KMnO₄ and 10% H₂SO₄. These impingers (5 and 6) capture Hg⁰ from air. The last impinger contained silica gel to capture the remaining moisture from the air. The measurements by the Tekran instrument and OH method were made at the same place at time. A total flow rate of 7 l/min of air passing through the impingers was measured

by a flow meter. The sampling height at Elandsfontein AQM station was 3 m. The samples were collected into amber/brown glass bottles using the ‘clean hands dirty hands’ procedure (EPA method 1669) (see Section 4.3.1) and preserved as explained for the OH method. The sampling train glassware and tubing were cleaned, daily, following the OH procedure, to avoid trace metal contamination.

7.1.3 Sampling at Majuba UCG flare

At the UCG plant, atmospheric Hg speciation was carried out using the OH method. The sample train was placed 5 m away from the flare and 0.5 m above the ground. Samples were taken over a period of 2.5 h using a vacuum pump to suck air through seven chilled impingers. Approximately 7 l/min of air sample passed through the impingers for 2.5 h. After each sampling event, the samples were transferred to amber/brown glass bottles using the ‘clean hands dirty hands procedure’ (EPA method 1669) and preserved as required by the OH method. The sampling train glassware and tubing were cleaned, daily, following the OH procedure, to avoid trace metal contamination.

7.2 Site descriptions of sampling points

7.2.1 Elandsfontein AQM station

Figure 7.1 shows where the Elandsfontein AQM station is situated. It is situated 25 km east of Kriel and Matla Power Stations, 38 km south of Duvha Power Station and 50 km south-southeast of Witbank, Central Mpumalanga. The primary industrial activities around Elandsfontein AQM station in the Mpumalanga Highveld are electrical power generation involving coal-fired power plants, as well as coal mining, maize meal farming and an oil refinery.

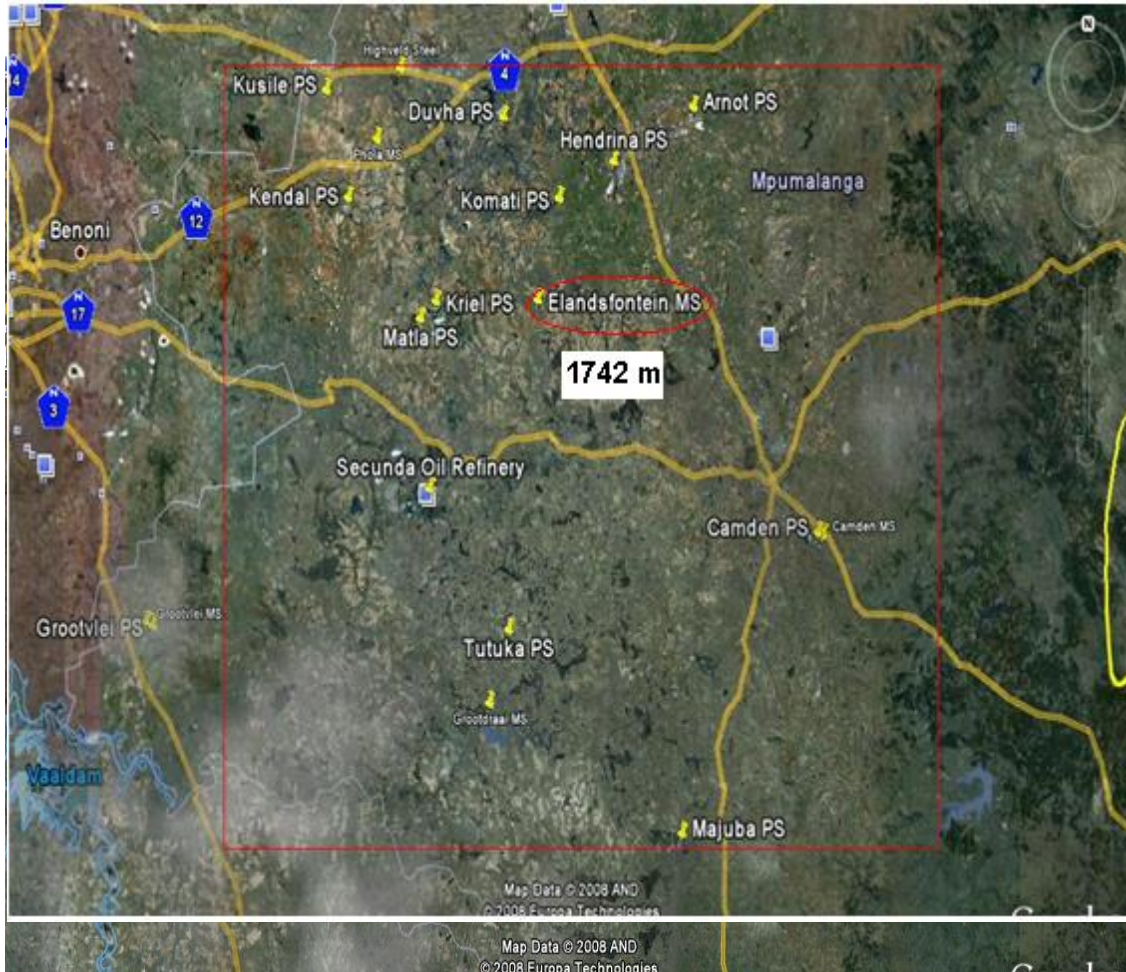


Figure 7.1: Google map for sampling location and regional power plants around Elandsfontein AQM station [with permission of Google Earth (26.2453S, 29.4173E)].

7.2.2 Wind rose at Elandsfontein AQM station

The atmospheric dispersion potential at Elandsfontein AQM station was determined using hourly meteorological data. The data set spanned the period from January 2009 to December 2011 [Thomas and Watson, 2008]. Figure 7.2 depicts the wind rose and wind class frequency distribution graphs that were extracted from the data provided. The Elandsfontein AQM station is associated mostly with winds originating from a north-westerly, northerly, south-easterly and easterly direction, as is depicted by the wind rose [http://www.eskom.co.za]. The field flowing from all directions is

characterized by high wind speeds of >10 m/s, which suggests that pollution emanating from the facility could be dispersed for large distances towards the Elandsfontein AQM station. Calm winds (winds of <0.5 m/s) are noted to occur 0.2% of the time. Consequently, the resultant flow field is from the north-west.

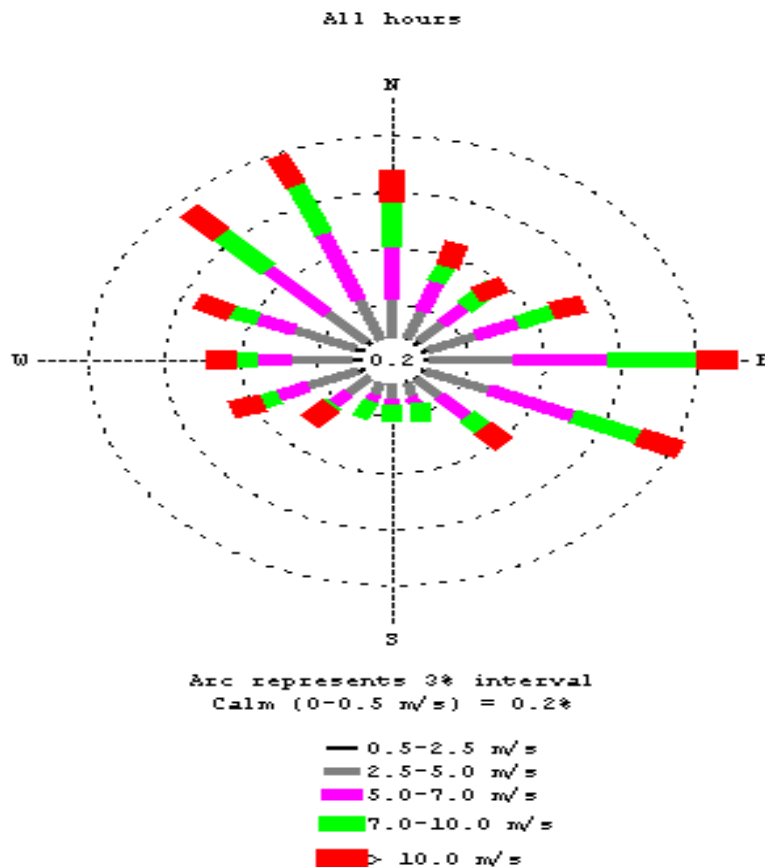


Figure 7.2: Wind rose from Elandsfontein AQM station [Thomas and Watson, 2008].

7.2.3 Majuba UCG plant flare

The UCG plant is situated south-east of the Majuba Power Station. It is approximately 13 km south-west of Amersfoort and west of the N11 national road between Amersfoort and Volksrust. The position of the Majuba Power Station is shown in Figure 7.1. A burning flare is shown in Figure 7.3.



Figure 7.3: Majuba Power Station with UCG plant (bottom right) and burning flare in the foreground (bottom left).

7.2.4 Wind rose at Majuba UCG flare

The wind direction on the sampling day determines the position of the sampling train from the flare because of the atmospheric dispersion potential. The atmospheric dispersion potential at the UCG plant was determined using hourly meteorological data sourced from the UCG Pilot Plant Weather Station. The data set spanned the period from October 2006 to August of 2007 [Thomas and Watson, 2008]. Figure 7.4 depicts the wind rose and wind class frequency distribution graphs that were extracted from the data provided. The dispersion potential of the area is briefly described by the wind rose and wind class frequency distribution graph presented in Figure 7.4. The Majuba UCG plant is associated mostly with winds originating from a westerly and easterly direction as is depicted by the wind rose. The field flowing from the west is

characterized by high wind speeds greater than 8 m/s, which suggests that pollution emanating from the proposed facility, could be dispersed for large distances eastward from the site. Winds from the east are also noted to occur for 33% of the time, which have a potential to distribute pollutants from the proposed facility in a westerly direction. Calm winds (winds <0.5 m/s) are noted to occur 0.6% of the time. Consequently the resultant flow field is from west.

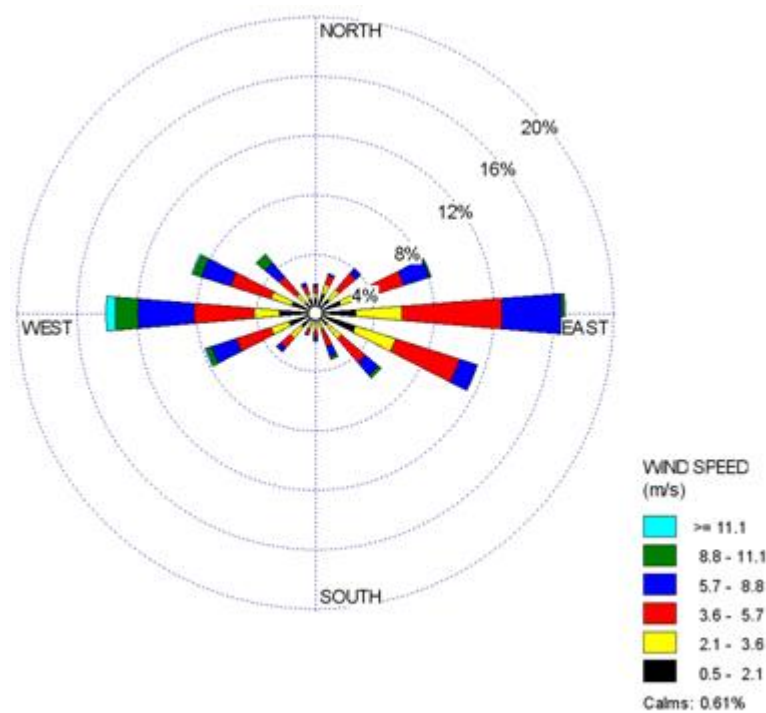


Figure 7.4 Wind rose from Majuba Power Station [Thomas and Watson, 2008].

7.3 Analysis

The atmospheric Hg speciation samples collected according to the OH method were analysed by the following methods: capillary electrophoresis coupled with a photodiode array detector (CE-PDA); high-performance liquid chromatography with amperometric detection (HPLC-AD) and atomic fluorescence spectroscopy (AFS) methods.

7.4 Results and discussion

7.4.1 Hg speciation at Elandsfontein AQM station.

Table 7.1: Summary of Hg speciation measurements and TGM at Elandsfontein AQM station, June 2010 to January 2012

Days	Winter				Summer				Winter				Summer				
	Samples	Tekran 2537B (ng/m ³)	CE (ng/m ³)	HPLC-AD (ng/m ³)	AFS (ng/m ³)	Tekran 2537B (ng/m ³)	CE (ng/m ³)	HPLC-AD (ng/m ³)	AFS (ng/m ³)	Tekran 2537B (ng/m ³)	CE (ng/m ³)	HPLC-AD (ng/m ³)	AFS (ng/m ³)	Tekran 2537B (ng/m ³)	CE (ng/m ³)	HPLC-AD (ng/m ³)	AFS (ng/m ³)
1	Hg ²⁺		0.518	0.517	0.518		0.245	0.241	0.241		0.465	0.466	0.465		0.261	0.261	0.261
	Hg ⁰		0.410	0.412	0.412		0.342	0.345	0.344		0.388	0.389	0.389		0.379	0.378	0.381
	Total Hg	1.080	0.932	0.929	0.930	0.743	0.587	0.586	0.585	1.108	0.853	0.855	0.854	0.843	0.64	0.639	0.642
2	Hg ²⁺		0.503	0.505	0.503		0.352	0.352	0.352		0.414	0.414	0.412		0.243	0.244	0.245
	Hg ⁰		0.385	0.385	0.388		0.518	0.520	0.519		0.364	0.366	0.367		0.329	0.331	0.332
	Total Hg	1.071	0.888	0.890	0.891	1.103	0.87	0.872	0.871	1.010	0.778	0.780	0.779	0.784	0.572	0.575	0.577
3	Hg ²⁺		0.504	0.504	0.504		0.385	0.386	0.385		0.424	0.423	0.425		0.295	0.298	0.299
	Hg ⁰		0.392	0.394	0.391		0.490	0.500	0.508		0.325	0.325	0.326		0.419	0.420	0.421
	Total Hg	1.121	0.896	0.898	0.895	0.964	0.875	0.886	0.893	0.985	0.749	0.748	0.751	0.953	0.714	0.718	0.72
4	Hg ²⁺		0.465	0.468	0.466		0.385	0.388	0.385		0.432	0.431	0.434		0.271	0.273	0.273
	Hg ⁰		0.374	0.374	0.375		0.428	0.423	0.431		0.367	0.369	0.370		0.402	0.405	0.408
	Total Hg	1.011	0.839	0.842	0.841	1.101	0.813	0.811	0.816	1.080	0.799	0.80	0.804	0.873	0.673	0.678	0.681
5	Hg ²⁺		0.502	0.504	0.501		0.337	0.338	0.337		0.459	0.460	0.459		0.289	0.289	0.287
	Hg ⁰		0.388	0.386	0.392		0.428	0.432	0.429		0.358	0.356	0.357		0.391	0.392	0.394
	Total Hg	1.142	0.890	0.890	0.893	1.020	0.765	0.770	0.766	1.120	0.817	0.816	0.816	0.932	0.680	0.681	0.681
	% quality uncertainty	±1.1%	±0.31%	±1.8%	±0.82%												

Table 7.1 shows the speciated atmospheric Hg concentrations measured with the analytical techniques mentioned above and total gaseous Hg measured by Tekran 2537B at Elandsfontein AQM station for 10 days in winter (5 days winter 2010 and 5 days winter 2011) and 10 days in summer (5 days summer 2011 and 5 days summer 2012). Two species, namely, Hg^0 and Hg^{2+} , were detected by all the analytical methods used (CE, HPLC-AD and AFS). Very good correlation in results for the various analytical methods was observed.

Figures 7.5 a, b, c and d show the different patterns observed during the sampling period. TGM concentrations measured by Tekran 2537B were found to be slightly higher (~20%) than the total of the Hg species. The latter was calculated as follows:

$$Total = Hg^0 + Hg^{2+}$$

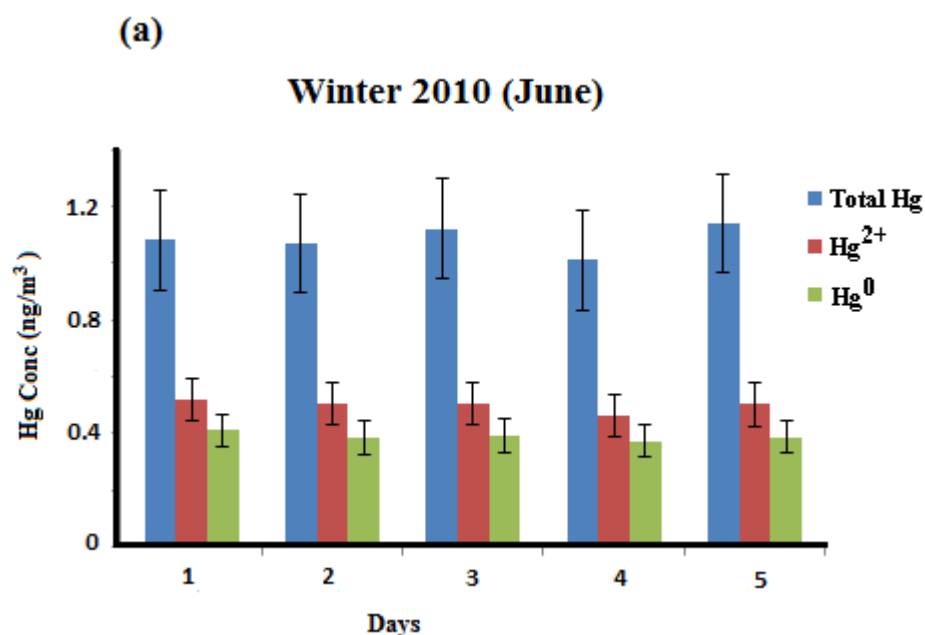


Figure 7.5a: Patterns of speciated Hg and TGM at Elandsfontein AQM station observed during the sampling period (21- 25 June 2010).

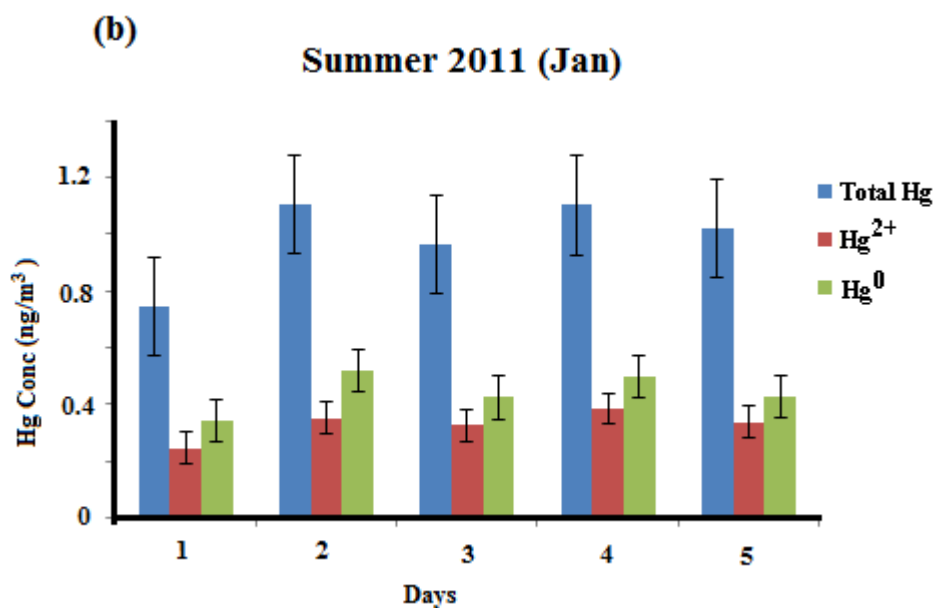


Figure 7.5b: Patterns of speciated Hg and TGM at Elandsfontein AQM station observed during the sampling period (17 – 21 January 2011).

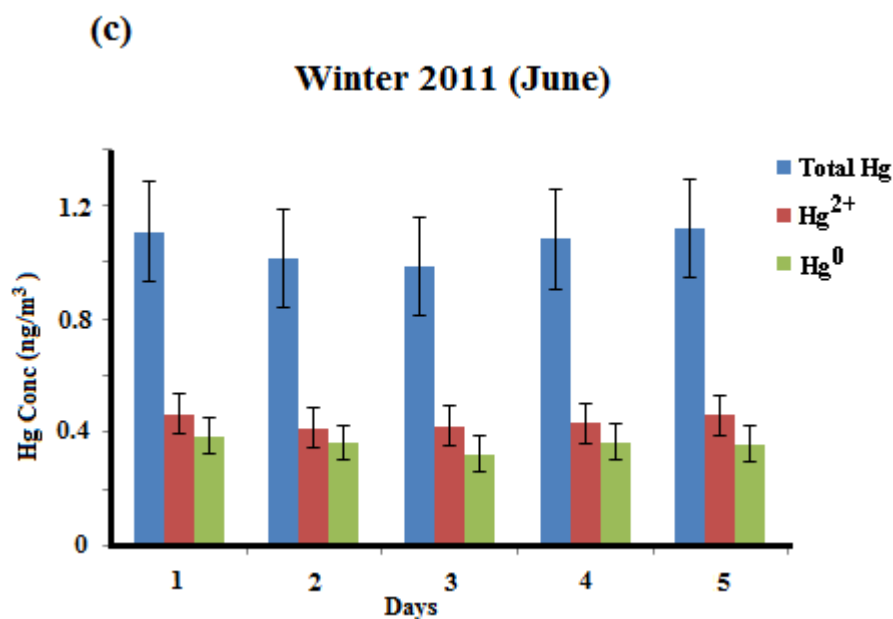


Figure 7.5c: Patterns of speciated Hg and TGM at Elandsfontein AQM station observed during the sampling period (20-24 June 2011).

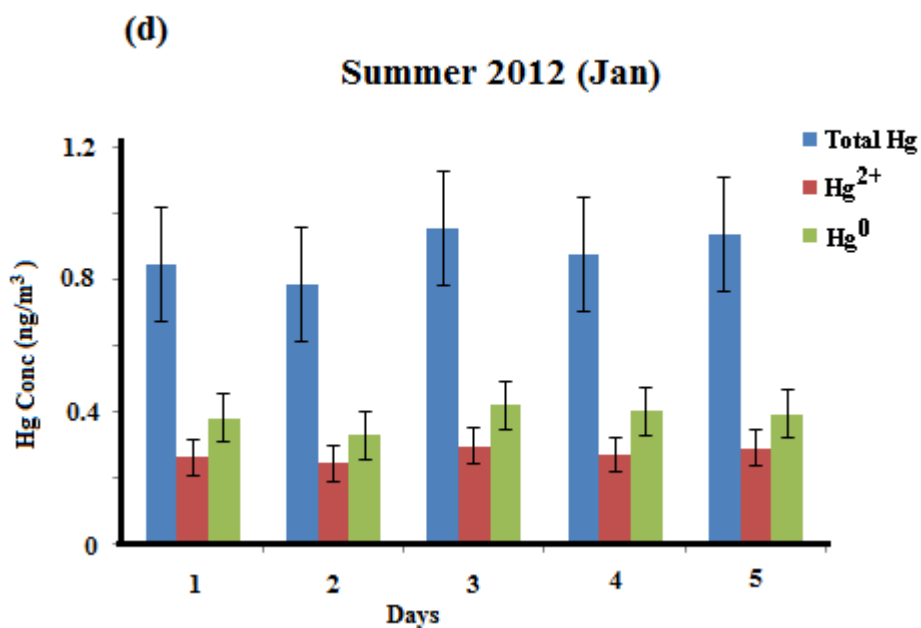


Figure 7.5d: Patterns of speciated Hg and TGM at Elandsfontein AQM station observed during the sampling period (16 – 20 January 2012).

The total gaseous Hg concentrations measured by Tekran 2537B at the Elandsfontein AQM station over the sampling period were in the range 0.734–1.142 ng/m³. The highest value measured was 1.142 ng/m³ in June 2010.

The speciation results at Elandsfontein AQM station, recorded during the sampling periods, suggest that Hg²⁺ is the predominant Hg species in the winter whereas in summer Hg⁰ is the predominant species. In the case of the Elandsfontein AQM station during the winter period, it has been suggested that Hg⁰ emitted from anthropogenic sources is oxidized by ozone (O₃); a hydroxyl radical (OH[•]); nitrate (NO₃); hydrogen peroxide (H₂O₂); and/or halogen containing compounds (Cl[•], Br[•], ClO, BrO, ClBr) [Raofie and Ariya, 2004]. In atmospheric Hg concentrations and speciation studies from 2004–2007, conducted by Peterson et al. (2009) in Reno, Nevada (USA) it was observed that O₃ concentrations were slightly correlated with Hg²⁺ concentrations in the atmosphere.

The Mpumalanga Highveld area during the time of winter sampling was very misty and windy. This could suggest that Hg⁰ released into the atmosphere may be deposited on the

cloud or mist droplets. Chemical reactions occur in aqueous phase (cloud droplets)—the following can take place: oxidation of Hg^0 to Hg^{2+} and reduction of Hg^{2+} to Hg^0 . The most important reactions in this aqueous reduction–oxidation balance are thought to be the oxidation of Hg^0 with ozone, reduction of Hg^{2+} by sulphite (SO_3^{2-}) ions, or complexation of Hg^{2+} with soot to form particulate Hg (Hg_p). This is illustrated in Figure 7.6. The Hg^{2+} produced from oxidation of Hg^0 by ozone can be reduced back to Hg^0 by sulphite; however, the oxidation of Hg^0 by ozone is much faster than the reduction of Hg^{2+} by sulphite [Lindqvist *et al.*, 1991]. Therefore, there will be a build-up of Hg^{2+} in the atmosphere. Due to windy conditions experienced at the Mpumalanga Highveld during winter, the build-up of Hg^{2+} in the atmosphere is thus evident from the results obtained from the Elandsfontein AQM station at the time.

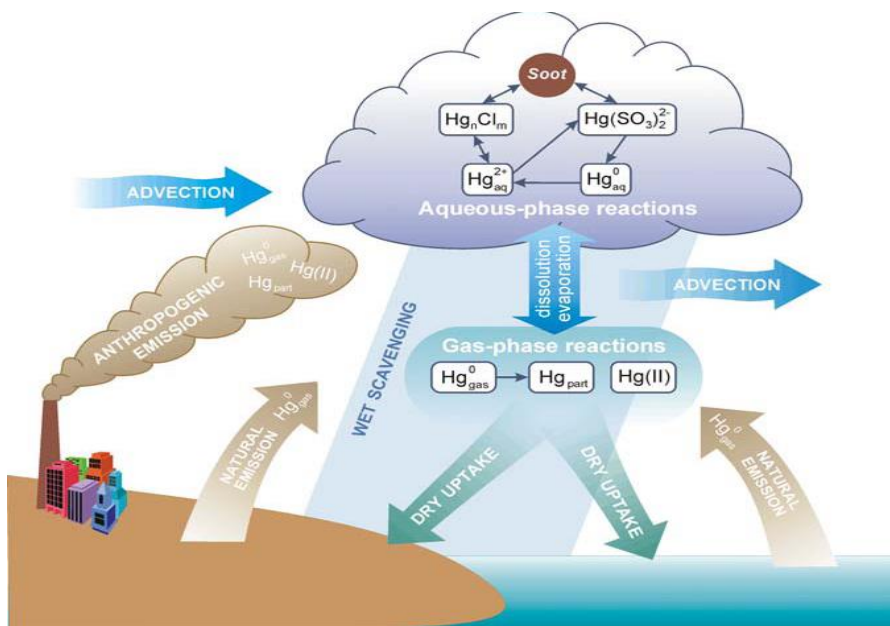


Figure 7.6: Summary of some of the important physical and chemical transformations of Hg in the atmosphere. (Figure adapted from Shia *et al.*, 1999)

During the summer sampling period, however, the Mpumalanga Highveld was sunny and hot, with less windy conditions. As shown in Table 7.1, the prominent species during this season was Hg^0 , unlike during winter, when the Hg^{2+} species was more prominent. A possible reason for this is that the Hg^0 emitted from anthropogenic sources is oxidized, but may be reduced to

Hg^0 in the presence of UV radiation. Furthermore, the oxidation may be very slow due to lack of heterogeneous interactions with aerosols, clouds and wind flux, which can convert Hg from one species to another.

The different patterns of Hg^0 and Hg^{2+} concentrations in the atmosphere observed at Elandsfontein AQM station are different to seasonal patterns observed by Peterson et al. (2009) in Reno, Nevada (USA). Peterson et al. (2009) on the study conducted between 2004 and 2007 observed that Hg^0 concentration was the predominant species in winter and Hg^{2+} was the predominant species in summer. The elevated Hg^0 concentrations in winter were associated with a period of cold and stagnant air, whereas the elevated Hg^{2+} can be explained by in situ oxidation of gaseous Hg^0 or mixing of Hg^{2+} derived from free troposphere to the surface. Holmes et al. (2006) observed similar oxidation of Hg^0 to Hg^{2+} as a potential sink for Hg^0 in the middle and upper troposphere where low temperatures can favour this chemistry.

7.4.2 Hg speciation at the flare of the Majuba UCG plant.

Table 7.2 shows the speciated Hg concentrations measured at the flare of the Majuba UCG plant. Both Hg^0 and Hg^{2+} species were detected by all the speciation methods (CE, HPLC-AD and AFS). Hg^{2+} was collected in impingers containing a chilled aqueous potassium chloride solution. Hg^0 was collected in subsequent impingers (one impinger containing a chilled aqueous acidic solution of hydrogen peroxide and three impingers containing chilled aqueous acidic solutions of potassium permanganate).

Table 7.2: Summary of Hg speciation measurements at Majuba UCG plant flare

Days	Samples	Summer			Winter		
		Jan-12			Jun-12		
		CE	HPLC-UV-AD	AF	CE	HPLC-UV-AD	AF
		(ng/m ³)	(ng/m ³)	(ng/m ³)	(ng/m ³)	(ng/m ³)	(ng/m ³)
1	Hg ²⁺	0.005	0.004	0.005	0.142	0.141	0.144
	Hg ⁰	0.009	0.009	0.01	0.006	0.006	0.005
	Total Hg	0.014	0.013	0.015	0.148	0.147	0.149
2	Hg ²⁺	0.005	0.004	0.005	0.014	0.013	0.013
	Hg ⁰	0.008	0.009	0.01	0.001	0.002	0.003
	Total Hg	0.013	0.013	0.015	0.015	0.015	0.016
3	Hg ²⁺	0.005	0.004	0.004	0.002	0.003	0.003
	Hg ⁰	0.01	0.009	0.01	0.002	0.001	0.001
	Total Hg	0.015	0.013	0.014	0.004	0.004	0.004
4	Hg ²⁺	0.006	0.006	0.005	0.091	0.091	0.089
	Hg ⁰	0.012	0.01	0.012	0.006	0.005	0.006
	Total Hg	0.018	0.016	0.017	0.097	0.096	0.095
5	Hg ²⁺	0.004	0.005	0.005	0.128	0.128	0.13
	Hg ⁰	0.012	0.009	0.01	0.006	0.005	0.005
	Total Hg	0.016	0.014	0.015	0.134	0.133	0.135
	% quality uncertainty	±0.31%	±1.8%	±0.82%			

The total Hg concentrations measured by all the analytical techniques were found to be in the range 0.004–0.018 ng/m³. This is in the range of Hg concentrations of 0.0048–0.156 ng/m³ measured at the Hanna II UCG flare discharge (Wyoming, United States of America) [Radian Corporation, 1976]. Days 4 and 5 in January 2012 were very windy and the direction of the wind was towards the UCG flare from Majuba Power Station. That may explain higher total

Hg concentrations on those days. Both Hg^{2+} and Hg^0 species were detected as expected, since the measurement was done close to the source and wind direction was from the east. As explained in Figure 7.4, wind from the east occurs 33% of the time, which suggests that pollution emanating from the proposed facility could be dispersed for short distances westward from the site. Hence both species, Hg^0 and Hg^{2+} , were detected.

7.5 Conclusions

7.5.1 Hg speciation at Elandsfontein AQM station

Different trends of results were obtained for the specific sampling period. During winter sampling, Hg^{2+} was the predominant species as compared to Hg^0 that was predominant species during summer sampling. The total Hg concentrations measured by all the analytical techniques used for the period were found to be in the range 0.734–1.142 ng/m^3 .

Variation patterns in the resulting data suggest that Hg emitted from the anthropogenic sources is oxidised or reduced depending on the phase transitions, biodegradation, and surface and heterogeneous interactions with aerosols and clouds. Physical mechanisms such as wind flux, runoff, and dry and wet deposition transport elemental and oxidized Hg species from one place to another.

7.5.2 Hg speciation at Majuba UCG flare

Based on the results that were obtained, it is evident that Hg emitted from power plants in different chemical species, with each species have different fate in the atmosphere. Climate, wind direction and terrain also play a role in the transport of Hg emissions. For this, it is difficult to predict the transport patterns of emissions. However, with correct measuring equipment and modeling, the patterns of emissions should be able to be predicted.

CHAPTER 8

THE USE OF MODELLING PROCESSES TO PREDICT MERCURY SPECIATION AT DUVHA POWER STATION AND IN AMBIENT AIR

8.1 Modelling of Hg in flue gas at Duvha Power Station

In the combustion zone, Hg in coal evaporates and exists as Hg^0 , which is cooled by passage through the downstream of the flue gas flow and can be oxidized by flue gas components such as HCl, SO_2 , H_2O and fly ash, finally, forming an oxidized form of Hg (Hg^{2+}) such as HgCl_2 , HgO , etc. [Laudal *et al.*, 2000; Lee *et al.*, 2004; Meij *et al.*, 2002; Zhang *et al.*, 2013]. This oxidation can occur by both homogeneous and heterogeneous reactions, resulting in the formation of Hg_p , Hg^{2+} and Hg^0 . Galbreath and Zygarlicke (2000) also reported that chlorine content in coal can significantly influence formation of Hg^{2+} . Attempts to understand Hg transformation were made by Qiu *et al.* (2003) and Wilcox *et al.* (2004). The authors focused on the effect of flue gas components and operating parameters of power stations. Eight-step mechanism for homogeneous Hg oxidation by chlorine to predict Hg oxidation under coal combustion conditions were proposed by Widmer *et al.* (2004):

- (i) $\text{Hg} + \text{Cl} + \text{M} \leftrightarrow \text{HgCl} + \text{M}$
- (ii) $\text{Hg} + \text{Cl}_2 \leftrightarrow \text{HgCl} + \text{Cl}$
- (iii) $\text{Hg} + \text{HCl} \leftrightarrow \text{HgCl} + \text{H}$
- (iv) $\text{Hg} + \text{HOCl} \leftrightarrow \text{HgCl} + \text{OH}$
- (v) $\text{HgCl} + \text{Cl} + \text{M} \leftrightarrow \text{HgCl}_2 + \text{M}$
- (vi) $\text{HgCl} + \text{Cl}_2 \leftrightarrow \text{HgCl}_2 + \text{Cl}$
- (vii) $\text{HgCl} + \text{HCl} \leftrightarrow \text{HgCl}_2 + \text{H}$
- (viii) $\text{HgCl} + \text{HOCl} \leftrightarrow \text{HgCl}_2 + \text{OH}$

This homogeneous reaction mechanism was tested on a bench scale by Krishnakumar and Helble (2007). The authors used reaction kinetics data that was theoretically calculated by Wilcox et al. (2004) using a quantum chemistry approach for three of the eight reactions. Good correlation of the results between experimental and kinetic calculations was observed. In this study, the values of Hg concentrations measured at the flue gas using the Ontario Hydro (OH) method in units 1 and 2 at Duvha Power Station were used as a data set for comparison with the predicted values using a kinetic reaction model of Hg oxidation by chlorine. The main aim was to determine whether the oxidation of Hg could be explained by the chlorine content in coal. The Chemked model was used to perform kinetic calculations at Duvha Power Station units 1 and 2 using the data measured at the stack.

8.1.1 Chemked – A program for chemical kinetics of gas-phase reactions

Chemked [Jelezniak and Jelezniak, (2009)] is a program designed for creating and editing thermodynamic and chemical kinetics databases, for the creation of reaction mechanisms and simulation of problems of complex gas-phase chemistry. The program uses thermodynamic data and chemical reactions that have the CHEMKIN-II description [<http://www.chemked.com>]

The information is collected in databases that are stored in files of the Microsoft Excel type. The data are displayed in the tables and can be easily handled. Chemked has multiple document interfaces and can simultaneously process several reaction databases connected with a thermodynamic database. The program provides numerical and graphical information on thermodynamic functions and reaction rate constants.

Chemked incorporates a solver for integration of differential equations of gas-phase chemical kinetics at constant pressure or constant volume (density) without mass and heat transfer. The

necessary information on thermodynamics and reactions is provided for the solver directly from the databases under consideration. The solver output contains numerical and graphical information on mixture-averaged as parameters and species concentrations.

8.2 Result of modelling Hg in flue gas

The eight-step homogeneous Hg oxidation mechanism of Widmer et al. (2004), with reaction rate constants of Wilcox et al. (2004) and Qiu et al. (2003), were used to perform the kinetic calculations. A high quench temperature (440 K/s) profile and low Hg concentration (0.1 ppm) were used for the modelling. Chemked did not include reactions between Hg and interhalogen species.

Three reactions from the mechanism were found to have an impact on the formation of HgCl_2 . The level of oxidation increases if the reaction $\text{HgCl} + \text{HCl} = \text{HgCl}_2 + \text{H}$ is turned off. Oxidation completely ceased if either $\text{Hg} + \text{Cl} + \text{M} = \text{HgCl} + \text{M}$ or $\text{HgCl} + \text{Cl}_2 = \text{HgCl}_2 + \text{Cl}$ was removed. Removing the reaction $\text{HgCl} + \text{HCl} = \text{HgCl}_2 + \text{H}$ promoted oxidation because the reverse reaction consumes HgCl_2 . Results indicated that mercury oxidation by chlorine is a two-step process that is controlled by the reactions $\text{Hg} + \text{Cl} + \text{M} = \text{HgCl} + \text{M}$ and $\text{HgCl} + \text{Cl}_2 = \text{HgCl}_2 + \text{Cl}$, and the formation of HgCl is the rate-controlling step. Analysis of the rate of production of the reactions involving HgCl_2 in Figure 8.1 shows that the reaction $\text{HgCl} + \text{Cl}_2 = \text{HgCl}_2 + \text{Cl}$ contributes more to the formation of the main oxidation product, HgCl_2 . The reaction $\text{Hg} + \text{Cl} + \text{M} = \text{HgCl} + \text{M}$ is the main source of HgCl .

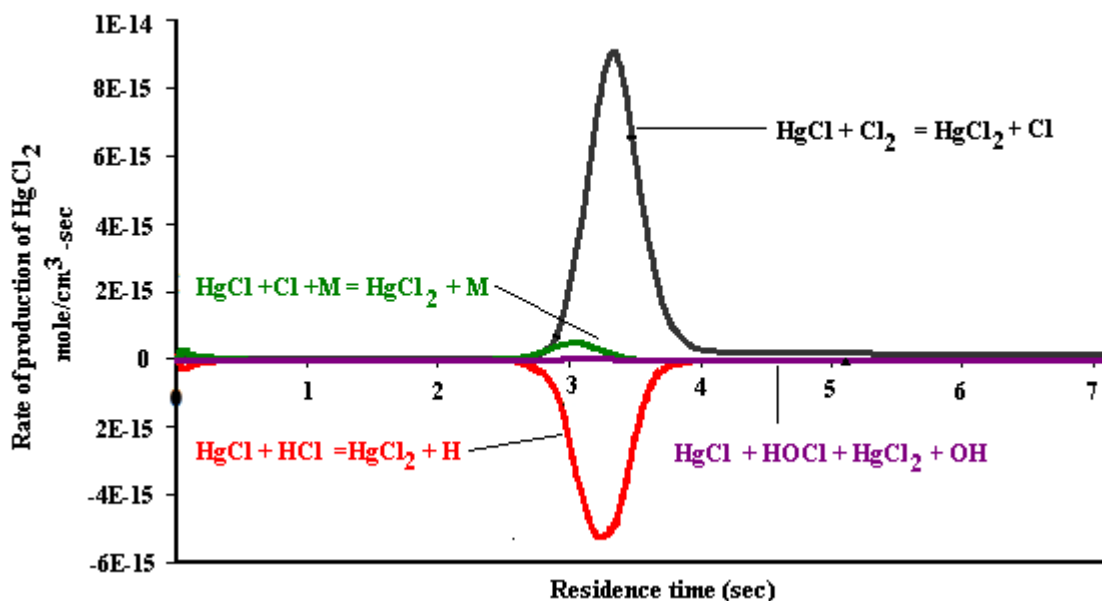


Figure 8.1: Model predictions for the rate of production of the reactions involving HgCl₂.

Table 8.1 shows the results of kinetic calculations for Hg²⁺ and Hg⁰ and the actual power station measurements. Previous studies by (Shah et al. (2010)) confirmed that with an increasing concentration of chlorine in the reactions, the model predicts that the level of Hg oxidation steadily increases. Because the measurements were taken in flue gas from large power stations and South African coal contains low concentrations of chlorine (~8.2 ppm) [Wagner and Hlatswayo, 2005], factors other than chlorine content might have influenced the speciation of Hg in the flue gas. Such factors could be the SO₂, NO₂ and O₂ content in flue gas. Previous studies have reported the significant influence of SO₂, NO₂ and O₂ on Hg oxidation in flue gas [Tao *et al.*, 2010].

Table 8.1: Comparison of measurements of Hg speciation at Duvha unit 1 and 2 compared to predicted values using a Chemked for Hg oxidation by chlorine.

Units	Measured Hg ⁰ in flue gas (%)	Measured Hg ²⁺ in flue gas (%)	Hg ⁰ as predicted by the model (%)	Hg ²⁺ as predicted by the model (%)
1	11.1	88.1	15	95
2	11.2	88.0	7.7	92.3

The difference between predicted values and real measurement values may possibly be due to various factors namely, inaccuracy measurements of Hg content under power station conditions, loss of Hg due to its volatility during combustion and the lack of heterogeneous reaction mechanisms in the kinetic model.

8.2.1 Comparison of results obtained in this study to international studies

In this study, the total Hg concentration in flue gas passing the FF was $3.8 \mu\text{g}/\text{Nm}^3/\text{s}$ in species. Since South African coal contains $<100 \text{ ppm Cl}$ ($\sim 8.2 \text{ ppm}$), Hg^0 will be the predominant species at the inlet of FF at Duvha Power Station units 1 and 2 [Zhang *et al.*, 2013]. Therefore, chlorine will have less influence on the oxidation of Hg^0 and its influence cannot be reliably predicted by a homogeneous kinetic model. This results explain why the Hg^0 concentrations in flue gases from units 1 and 2 at Duvha Power Station are in the lower range when compared to those reported international studies [He *et al.*, 2007; Gou *et al.*, 2007; Lee *et al.*, 2006; Wang *et al.*, 2009], *viz*, presumably because of coals with lower Hg concentration being used for combustion. Because units 1 to 3 at Duvha Power Station are equipped with fabric filters, a larger proportion of Hg^{2+} is likely to be released into the atmosphere via stack emissions and this may cause the deposition of Hg in the vicinity of power stations.

8.3 Modelling of Hg at Elandsfontein Air Quality Monitoring Station

The patterns observed at Elandsfontein Air Quality Monitoring Station (AQM) station are not adequate for modelling because of lack of proper dispersion or transport model for this purpose. Hg speciation at Elandsfontein AQM station was carried out in order to test the developed techniques on environmental samples. Therefore, for making any important deduction from the patterns, a more comprehensive data is needed. Such data should include source characteristics, environmental conditions (local and regional meteorology, terrain,

nearby structures), as well as accurate atmospheric chemistry (reaction kinetics, thermodynamics, gas and aqueous phase chemistry) and removal and deposition process (precipitation, dry deposition). Therefore, further studies of the atmospheric processes should be carried out.

CHAPTER 9

SUMMARY, CONCLUSIONS AND RECOMMENDATIONS FOR FUTURE RESEARCH

9.1 Summary

This study focuses on the development and validation of analytical methodologies that are capable of differentiating between the different forms of mercury in environmental samples (air, liquids and solids) from coal-fired power plants. Capillary electrophoresis with amperometric detection, high performance liquid chromatography with amperometric detection, and atomic fluorescence spectrometry methods were developed for mercury speciation. Total mercury in solids (coal and ash) was measured by direct mercury measurement using a well-established method, involving the use of the automatic mercury analyzer LECO AMA-254. Total gaseous mercury was measured using the Tekran 2537B system. Very low detection limits observed using the methods that were developed are attractive for the monitoring of mercury in the environment.

The speciation of Hg in environmental samples (air, liquids and solids) using newly developed analytical methodologies was achieved. Mercury speciation in South African coal after acid extraction showed that although South African coal contains mainly inorganic mercury small quantities of organic mercury are also present. Different trends in Hg speciation results at the Elandsfontein Air Quality Monitoring (AQM) station were observed over the sampling period. During winter sampling, Hg^{2+} was the predominant species, while Hg^0 was predominant the species during summer sampling. Mercury speciation carried out at Duvha Power Station (units 1 and 2), equipped with fabric filter devices, revealed that the predominant form of Hg after the fabric filter devices was Hg^{2+} . Mercury speciation at the Majuba Underground Coal Gasification flare revealed that although mercury is emitted from

power plants in the form of different chemical species, with each species have a different fate in the atmosphere.

9.2 Conclusions

The following conclusions were deduced from this study:

- Validated analytical methodologies with very low detection limits that are capable of differentiating between the different forms of mercury in environmental samples were developed.
- Direct Hg analysis using an automatic mercury analyzer (AMA 254 Mercury Analyzer) is the suitable method for total Hg analysis in coal
- Chapter 6 and 7 show that OH method is the suitable for sampling Hg species in ambient air and in flue gases at coal fired power plant stack
- On application to environmental samples, very good correlations in results were observed between the different methods.
- The patterns observed and data recorded at the Elandsfontein AQM station and Duvha Power Station, respectively, were however, insufficient to permit accurate modelling.

9.3 Recommendations

Continuous measuring of Hg concentrations in coals combusted; the influence of emission control devices on Hg reductions; and species composition of Hg emitted from power plants is needed. The data measured will provide an inventory of Hg speciation at coal-fired power plants. This will improve the understanding of Hg transformation during combustion and the estimates of Hg emission.

A seasonal intensive field campaigns focusing on specific Hg processes occurring at various seasons, and in highly sensitive ecosystems around Mpumalanga Highveld is important. The purpose will be to observe all forms of Hg in the ambient air and in both wet and dry deposition. The data measured will establish the links between changes in atmospheric Hg, tropospheric chemistry and climate. This study would form basis for implementing long-term monitoring programme that will focus on the changes in Hg and other air pollutants in the physical and chemical state of Hg in the lower atmosphere; in particular to provide the means to discern and understand the causes of such changes.

Also further works to build measurement sites that permit a careful investigation of inter-hemispheric transport and trends in background concentrations. This approach will produce verified data sets for testing and improving regional models for atmospheric Hg.

REFERENCES

Agraz, R., Sevilla, M.T. and Hernandez, L. (1995). Voltammetric quantification and speciation of mercury compounds. *Journal of Electroanalytical Chemistry*, 390:45

AMAP/UNEP (2008). Technical background report to the global atmospheric mercury assessment. Tech. rep., Arctic Monitoring and Assessment Programme/UNEP, Chemicals Branch, pp.136

Balarama Krishna, M.V., Ranjit, M., Karunasagar, D. and Arunachalam, J. (2005). A rapid ultrasound-assisted thiourea extraction method for the determination of inorganic and methyl mercury in biological and environmental samples by CVAAS. *Talanta*, 67:70.

Baldwin, P. (2000). Electrochemical determination of carbohydrates: Enzyme electrodes and amperometric detection in liquid chromatography and capillary electrophoresis. *Electrophoresis*, 21:4017

Baker, P.G.L., Brunke, E-G., Slemr, F. and Crouch, A.M. (2002). Atmospheric mercury measurement at Cape Point, South Africa. *Atmospheric Environment*, 36:2459

Bettmer, J., Cammann, K. and Robecke, M. (1993). Determination of organic ionic lead and mercury species with high-performance liquid chromatography using sulphur reagents. *Journal of Chromatography A*, 654:177

Bloom, N. and Fitzgerald, W.F. (1988). Determination of volatile mercury species at the picogram level by low-temperature gas chromatography with cold-vapour atomic fluorescence detection. *Analytica Chimica Acta*, 208:151

Brenner, I.J. (2010) ICPMS Applications. *Encyclopedia of Spectroscopy and Spectrometry* (Second edition), pp 991

Cai, Y. (2000). Speciation and analysis of mercury, arsenic, and selenium by atomic fluorescence spectrometry. *Trends in Analytical Chemistry*, 19:1

Cammann, K., Robecke, M. and Bettner J. (1994). Simultaneous determination of organic ionic lead and Mercury species using HPLC. *Fresenius' Journal of Analytical Chemistry*, 350:30

Constantinou, E. and Seigneur, C. (1993). A mathematical model for multimedia health risk assessment. *Environmental Software*, 8:231

Craig, P.J. (1986). *Organometallic Compounds in the Environment*. John Wiley and Sons, New York

Dabrowski, J.M., Ashton, P.J., Murray, K., Leaner, J.J. and Mason, R.P. (2008). Anthropogenic Mercury emissions in South Africa: Coal combustion in power plants. *Atmospheric Environment*, 42:6620

Dabek-Zlotorzynska, E., Lai, E.P.C. and Timerbaev, A.R. (1998). Capillary Electrophoresis the state-of-the-art in metal speciation studies. *Analytica Chimica Acta*, 359:1

Dale, L. and Riley, K. (1995). Standard analytical methods for trace elements in coal. Australian Coal Association Research Program, Project number: C5063

Ebinghaus, R., Turner, R.R., de Lacerda L.D., Vasilier, O. and Salomons, W. (1999). *Mercury Contaminated Sites*. Springer, Berlin, pp. 538

Eder, B.K., Coventry, D.H., Clark, T.L. and Bollinger, C.E. (1986). RELAMAP: A Regional Lagrangian Model of Air Pollution – user's guide. EPA/600/8-86/013. Project Report. U.S. Environmental Protection Agency, Research Triangle Park, NC.

Eliassen, A. and Saltbones, J. (1983). Modelling of long-range transport of sulphur over Europe: A two-year model run and some model experiments. *Atmospheric Environment*, 17:1457

Environmental Research and Technology (ERT) (1984). ADOM/TADAP model development program, Vol 1–7, ENSR, Acton, MA

EPA Method 1669. ‘Clean Hands/Dirty Hands Basic Sampling Procedure’, excerpted from EPA Method 1669. WI DNR Total Mercury Monitoring Procedures (5/21/03 draft)

EPRI TR-107695 (1996). Final Report. Mercury in the Environment: A research update. Environment & Renewable Energy, Technical Report, Chapter 6, <http://www.epri.com>

Feng, X. and Hong, Y. (1999). Modes of occurrence of Mercury in coals from Guizhou, People’s Republic of China. *Fuels*;78:1181

Galbreath, K.C. and Zygarlicke, C.J. (2000). Mercury transformations in coal combustion flue gas. *Fuel Process Technology*, 65:289

Gao, Y., Shi, Z., Long, Z., Wu, P., Zheng, C. and Hou, X. (2012). Determination and speciation of mercury in environmental and biological samples by analytical atomic spectrometry. *Microchemical Journal*, 103:1

Goodarzi, F. (2002). Mineralogy, elemental composition and modes of occurrence of elements in Canadian feed-coals. *Fuels*, 81:1199

Guo, X., Zheng, C.G. and Xu, M.H. (2007). Characterization of Mercury emissions from a coal-fired power plant. *Energy Fuels*, 21:898

Gupta, R.C. (2007). *Veterinary Toxicology: Basic and Clinical Principles*, Elsevier, USA

Hardy, S. and Jones, P. (1997). Capillary electrophoresis determination of methylmercury in fish and crab meat after extraction as the dithizone sulphonate complex. *Journal of Chromatography A*, 765:345.

Harrington, C.F. and Catterick, T. (1997). Problems encountered during the development of a method for the speciation of mercury and methylmercury by high-performance liquid

chromatography coupled to inductively coupled plasma mass spectrometry. *Journal of Analytical Atomic Spectrometry*, 12:1053

Harrington, C.F. (2000). The speciation of mercury and organomercury compounds by using high-performance liquid chromatography. *Trac-Trends in Analytical Chemistry*, 19:167

He, B., Cao, Y., Romero, C. E., Bilirgen, H., Sarunac, N., Agarwal, H. and Pan, W. (2007). Comparison and validation of OHM and SCEM measurements for a full-scale coal-fired power plant. *Chemical Engineering Communications*, 194:1596

Heiger, D.N., Cohen, A.S., Karger, B.L. (1990). Separation of DNA restriction fragments by high performance capillary electrophoresis with low and zero cross linked polyacrylamide using continuous and pulsed electric fields. *Journal of Chromatography*, 516:33

Hempel, M., Hintelmann, H. and Wilken, R.D. (1992). Determination of organic mercury species in soil by high performance chromatography with ultraviolet detection. *Analyst*, 117:667

Hill, S.J. and Fisher, A.S. (1999). Atomic fluorescence, methods and instrumentation. *Encyclopedia of Spectroscopy and Spectrometry (Second edition)*, pp. 78

Hoffart, A., Seames, W., Kozliak, E., Riedinger, S., Francini, J. and Carlson, C. (2006). A two-step acid mercury removal process for pulverized coal. *Fuel*, 85:1166

Holland, P.T. (1996). IUPAC Pesticides report .36. Glossary of terms relating to pesticides (IUPAC Recommendations 1996). *Pure and Applied Chemistry*, 68:1167

Holmes, C. D., Jacob, D. J. and Yang, X. (2006). Global lifetime of elemental mercury against oxidation by atomic bromine in the free troposphere, *Geophysical Research Letters* 33, art. no. L20808

Holmes, C. D., Jacob, D. J., Mason, R.P and Jaffe, D.A. (2009). Sources and deposition of reactive gaseous mercury in the marine atmosphere. *Atmospheric Environment*, 43:2278

Hua, L. and Tan, S.N. (2000). Amperometric detection of cytochrome by capillary electrophoresis at a sol–gel carbon composite electrode. *Analytical. Chimica. Acta*, 403:179.

Huggins, F.E. (2002). Overview of analytical methods for inorganic constituents in coal. *International Journal Coal Geology*, 50:169

<http://www.ceandcec.com/> accessed June 2012

<http://www.chem.unep.ch/> accessed January 2013

http://www.eqb_dqe.cciw.ca/ modelling/ accessed May 2012

<http://www.eskom.co.za/> accessed December 2012

<http://www.GoogleEarth.com/> 26.2453S, 29.4173E last viewed June 2012

<http://www.leco.com/> accessed November 2011

<http://www.pca.state.mn.us/> accessed March 2012

<http://www.en.wikipedia.org/wiki/Mercury/> accessed January 2012

http://en.wikipedia.org/wiki/Duvha_Power_Station/ accessed 10 April 2014

Jelesniak, M. and Jelesniak, I. (2009). Chemked – A program for chemical kinetics of gas-phase reactions. <http://www.chemked.com> accessed 13 September 2012

Jones, A.B. and Slotton, D.G. (1996). Mercury effects, Sources and control measures. A special study of the San Francisco Estuary Regional Monitoring Program. San Francisco Estuary Institute. Richmond, CA. RMP Contribution no.20

Jongwana, L.T. and Crouch, A.M. (2012). Mercury speciation in South African coal. *Fuel* 94:234

Kellie, S., Duan, Y., Cao, Y., Chu, P., Mehta, A., Carty, R., Liu, K., Pan, W. and Riley, J. T. (2004). Mercury emissions from a 100-MW wall-fired boiler as measured by semicontinuous mercury monitor and Ontario Hydro Method. *Fuel Processing Technology*, 85:6

Kohl, F. (2011). Mercury sorbents that allow continued use of fly ash in concrete. 8th Mercury Emissions from Coal (MEC8) Working Group; 18–20 May 2011, Kruger Gate, South Africa.

Kolker, A., Senior ,C.L. and Quick J.C. (2006). Mercury in coal and the impact of coal quality on mercury emissions from combustion systems. *Applied Geochemistry*, 21:1821

Krishnakumar, B. and Helble, J. (2007). Understanding mercury transformations in coal-fired power plants: Evaluation of homogeneous Hg oxidation mechanisms. *Environmental Science and Technology*, 41 (22):7870

Kubán, P., Houserová, P., Kubán, P., Hauser P.C. and Kubán, V. (2007). Mercury speciation by CE: A review. *Electrophoresis*, 28:58

Lai, E.P.C., Zhang, W., Trier, X., Georgi, A., Kowalski, S., Kennedy, S., MdMuslim, T. and Dabek-Zlotorzynska, E. (1998). Speciation of mercury at ng/ml concentration levels by CE with amperometric detection. *Analytical. Chimica Acta*, 364:63

Landers, J.P. (1997). *Handbook of CE (Second edition)*, CRC Press, Boca Raton, Florida

Laudal, D.L., Brown, T.D. and Nott, B.R. (2000). Effects of flue gas constituents on mercury speciation. *Fuel Processing Technology*, 65–66:157–165

Leermakers, M., Baeyens, W., De Gieter, M., Smedts, B., Meert, C., De Bisschop, H.C., Morabito, R. and Quevauviller, Ph. (2006). Toxic arsenic compounds in environmental samples: Speciation and validation. *Trends in Analytical Chemistry*, 25:1

Leaner, J.J., Dabrowski, J.M., Mason, R.P., Resane, T., Richardson, M., Ginster, M., Gericke, G., Petersen, C.R., Masekoameng, E., Ashton, P.J. and Murray, K. (2009). Mercury emissions from point sources in South Africa. *Mercury Fate and Transport in the Global Atmosphere*. 113

Lee, S. J., Seo ,Y-C., Jung, J., Hong, J.H., Park, J.W., Hyun, J.E. and Lee, T.G. (2004). Mercury emissions from selected stationary combustion sources in Korea. *Science of the Total Environment*, 325:155

Lee, S.J., Seo, Y-C., Jang, H-N., Park, K-S., Baek, J-I,., An, H-S. and Song, K-C. (2006). Speciation and mass distribution of Mercury in a bituminous coal-fired power plant. *Atmospheric Environment*, 40:2215

Li, S. F. Y. (1992). Capillary electrophoresis: principles, practice and applications, Elsevier Science, Amsterdam. 2. Heftmann, E.

Liang, L., Horvat, M., Cernichiari, E., Gelein, B. and Balogh, S. (1996). Simple solvent extraction technique for elimination of matrix interferences in the determination of methylmercury in environmental and biological samples by ethylation gas chromatography cold vapor atomic fluorescence spectrometry. *Talanta*, 43:1883

Lin, C-J. and Pehkonen S.O. (1999). The chemistry of atmospheric Mercury: A review. *Atmospheric Environment*, 33:2067

Lindqvist, O., Johansson, K., Astrup, M., Anderson, A., Bringmark, L., Hovsenius, G., Hakanson, L., Iverveld,t A., Meili, M. and Trim, B. (1991). Mercury in the Swedish environment: Recent research on causes, consequences and corrective methods. *Water, Air and Soil Pollution*, 55:1

Liu L., Duan, Y., Wang, Y., Wang, H. and Yin, J. (2010). Experimental study on mercury release behaviour and speciation during pyrolysis of two different coals. *Journal of Fuel Chemistry and Technology*, 38(2):134

Lourens, A.S., Beukes, J.P., van Zyl, P.G., Fourie, G.D., Burger, J.W., Pienaar, J.J., Read, C.E. and Jordaan, J.H. (2011). Spatial and temporal assessment of gaseous pollutants in the Highveld of South Africa. *South African Journal of Science*, 107(1/2):269

Lu, J.Y., Schroeder, W.H., Berg, T., Munthe, J., Schneeberger, D. and Schaedlich, F. (1998). A device for sampling and determination of total particulate mercury in ambient air. *Analytical Chemistry*, 70:2403

Lu, Y., Rostam-Abadi, M., Chang, R., Richardson, C. and Paradis, J. (2007). Characteristics of fly ashes from full-scale coal-fired power plants and their relationship to mercury adsorption. *Energy Fuels*, 21:2112

Maa, Y.F., Hyver, K.J., Swedberg, S.A. (1991). Impact of wall modifications on protein elution in high performance capillary electrophoresis. *Journal of High Resolution Chromatography*, 14: 65

Martin, L.G., Jongwana, L.T. and Crouch, A.M. (2010). Capillary electrophoretic separation and post-column electrochemical detection of mercury and methylmercury and applications to coal samples. *Electrochimica Acta*, 55:4303

Masekoameng, E., Leaner, J.J. and Dabrowski, J.A., (2010). Trends in anthropogenic mercury emissions estimated for South Africa during 2000 to 2006, *Atmospheric Environment*, 44:3007

Medina, I., Rubí, E., Mejuto, M.C. and Cela, R. (1993). Speciation of organomercurials in marine samples using capillary electrophoresis. *Talanta*, 40:1631

Meij, R. (1994). Trace element behavior in coal-fired power plants. *Fuel Processing Technology* 39:199

Meij, R., Vredendregt, L.H.J. and Winkel H. (2002). The fate and behavior of mercury in coal-fired power plants. *Journal of the Air and Waste Management Association*, 52:917

Morita, M., Yoshinaga, J. and Edmonds, J.S. (1998). The determination of mercury species in environmental and biological samples. *Pure and Applied Chemistry*, 70(8):1585

MRA (Mining Review Africa) (2003). Eskom projects 2% annual growth in its coal uptake. <http://www.miningreview.com> last visited on February 2012

Niksa, S., Fujiwara, N., Fujita, Y., Tomura, K., Moritomi, H., Tuji, T., and Takasu, S. (2002) A mechanism for mercury oxidation in coal-derived exhausts. *Journal of Air Waste Management Associations*, 52:894

Pai, P., Karamchandani, P.K. and Venkatram, A. (1996). Performance of a flux conserving and a semi-Lagrangian advection scheme in simulating a photochemical episode, in: Gryning and Schiermeier (Eds.), Air Pollution Modeling and its Application XI, Plenum Press, New York, pp. 311

Pai, P., Karamchandani, P.K. and Seigneur C. (1997). Simulation of the regional atmospheric transport and fate of mercury using a comprehensive Eulerian model. Atmospheric Environment, 99:108

Pacyna, E.G., Pacyna, J.M., Steenhuisen, F. and Wilson, S. (2006). Global anthropogenic mercury emission inventory for 2000. Atmospheric Environment, 40:4048

Pacyna, E.G., Pacyna, J.M., Sundseth, K., Munthe, J., Kindbom, K., Wilson, S., Steenhuisen, F. and Maxson, P. (2010). Global emission of mercury to the atmosphere from anthropogenic sources in 2005 and projections to 2020. Atmospheric Environment, 44:2487

Páger, C.S. and Gáspár, A. (2000). Possibilities of determination of Mercury compounds using capillary zone electrophoresis. Fresenius' Journal of Analytical Chemistry, 366:466

Palvish, J.H.; Holmes, M.J.; Galbreath, K.C.; Zhuang, Y. and Palvish, B.M. (2003). Pilot scale investigation of mercury control technologies for utilities burning lignite coal. In combined power plant air pollutant control mega symposium, 19–22 May 2003, Washington DC

Pavlish, J.H., Hamre, L.L. and Zhuang, Y. (2010). Mercury control technologies for coal combustion and gasification systems. Fuel, 89:838

Pavlish, J.H. (2011). Enhancing mercury capture to meet global mercury reductions with sorbent enhancement additives. 8th Mercury Emissions from Coal (MEC8) Working Group; 18–20 May 2011, Kruger Gate, South Africa

Petersen, G., Schneider, B., Eppel, D., Grass, H., Iverfeldt, A., Misra, P.K., Bloxam, R., Wong, S., Schroeder, W.H., Voldner, E. and Pacyna, J. (1991). Numerical modelling of the

atmospheric transport, chemical transformations, and deposition of mercury: Air pollution modelling and its applications VIII, Van DopH and Steyn D.G (Eds.), Plenum Press, New York, pp. 215

Petersen, G., Iverfeldt, A. and Munthe, J. (1995). Atmospheric mercury species over central and northern Europe. Model calculations and comparison with observation from Nordic air and precipitation network for 1987 and 1988. *Atmospheric Environment*, 29:47

Peterson, C., Gustin, M. and Lyman, S. (2009). Atmospheric mercury concentrations and speciation measured from 2004 to 2007 in Reno, Nevada, USA. *Atmospheric Environment* 43:4646

Pirrone, N. (2001). Mercury research in Europe: towards the preparation of the New Europe Air Quality Directives. *Atmospheric Environment*, 35:2979

Pirrone, N., Cinnirella, S., Feng, X., Finkelman, R.B., Friedli, H.R., Leane, J., Mason, R., Mukherjee, A.B., Stracher, G.B., Streets, D.G. and Telmer, K. (2010). Global mercury emissions to the atmosphere from anthropogenic and natural sources. *Atmospheric Chemistry and Physics*, 10:5951

Pleijel, K. and Munthe, J. (1995). Modelling the atmospheric mercury cycle-chemistry in fog droplets. *Atmospheric Environment*, 29:1441

Porcella, D., (1994). Mercury in the environment: biogeochemistry. In: Watras, C.J., Huckabee, J.W. (Eds.), *Mercury Pollution: Integration and synthesis*. CRC Press, Boca Raton, FL, pp. 3

Qiu, J., Helble, J. J. and Sterling, R. (2003). Proceedings of the 12th International Conference on Coal Science, Cairns, Queensland, Australia, 2003

Qvarnström, J. and Frech, W (2002). Mercury species transformations during sample pre-treatment of biological tissues studied by HPLC-ICP-MS. *Journal of Analytical Atomic Spectrometry*, 17(11):1486

Radian Corporation (1976). Monitoring of an in-situ gasification test of the linked vertical well concept. Report No. 200-138-04

Raofie, F. and Ariya, P.A. (2004). Product study of the gas-phase BrO-initiated oxidation of Mercury: Evidence for stable Hg¹⁺ compounds. *Environmental Science & Technology*, 38:4319

Sable, S., Jong, W. and Spliethoff, H. (2008). Combined homo- and heterogeneous model for mercury speciation in pulverized fuel combustion flue gases. *Energy & Fuels*, 22:321

Scifres, J., Wasko, M., McDaniel, W. and Cheema, V. (1995). Determination of ultra-level total mercury in sediment and tissue by microwave digestion and atomic fluorescent detection. American Environmental Laboratory

Seigneur, C., Wrobel, J. and Constantinou, E. (1994). A chemical kinetic mechanism for atmospheric inorganic mercury. *Environmental Science and Technology*, 28:1589

Senior, C.L., (2001). Power production in the 21st Century: Impacts of fuel quality and operations. Engineering Foundation Conference, Snowbird, UT, 28 October–2 November 2001

Shah, P., Strezov, P. and Nelson, P.F. (2010). Speciation of mercury in coal-fired power station flue gas. *Energy Fuels*, 24:205

Shannon, J.D. (1985). User's Guide for the Advanced Statistical Trajectory Regional Air Pollution (ASTRAP) model. EPA/600/8-85/106 (NTIS PB 85-236783/XAB), US Environmental Protection Agency

Shia, R.-L., Seigneur, C., Pai, P., Ko, M. and Sze, N.D. (1999). Global simulation of atmospheric mercury concentrations and deposition fluxes. *Journal of Geology and Research*, 104(D19): 23747

Schoeder, W.H., Yarwood, G. and Niki, H. (1991). Transformation processes involving mercury species in the atmosphere. *WASP56*: 653

Schoeder, W.H. and Munthe, J. (1998). Atmospheric mercury: An overview. *Atmospheric Environment*, 32:809

Silva da Rocha, M., Soldado, A.B., Blanco-Gonzalez, E and Sanz-Medel, A. (2000). Speciation of mercury compounds by capillary electrophoresis coupled on line with quadrupole and double-focusing inductively coupled plasma mass spectrometry. *Journal of Analytical Atomic Spectrometry*, 15:513

Slemr, F., Brunke, E.G., Ebinghaus, R., Temme, C., Munthe, J., Wängberg, I., Schroeder, W., Steffen, A. and Berg, T. (2003). Worldwide trend of atmospheric mercury since 1977. *Geophysical Research Letters*, 30(10):1516

Spiro, T.G. and Stagliani, T.G. (1996). *Chemistry of the Environment*, New York, Prentice Hall

Subir, M., Ariya, P.A. and Dastoor, A.P. (2012). A review of the sources of uncertainties in atmospheric mercury modeling II. Mercury surface and heterogeneous chemistry: A missing link. *Atmospheric Environment*, 46:1

Swedberg, S.A. (1990). Use of non-ionic and zwitterionic surfactants to enhance selectivity in high performance capillary electrophoresis. An apparent micellar electrokinetic capillary chromatography mechanism. *Journal of Chromatograph*, 503:449

Tao, Y., Zhuo, Y., Zhang, L., Chen, C. and Xu, X., (2010). Impact of flue gas species and temperature on mercury oxidation. *Tsinghua Science and Technology*, 15:418

TEKRAN (1998). Model 2357A: Principles of Operation. Tekran Inc., Ontario, Canada

Timerbaev, A.R. and Shpigun, O.A. (2000). Analysis of highly saline samples by capillary zone electrophoresis: Enhanced direct UV detection of inorganic anions using on-capillary preconcentration and clean-up techniques. *Electrophoresis*, 21:4179

Timerbaev, A.R. (2002). Recent advances and trends in capillary electrophoresis of inorganic ions. *Electrophoresis*, 23:3884

Timerbaev, A.R. (2013). Element Speciation Analysis Using Capillary Electrophoresis: Twenty Years of Development and Applications. *Chemical Reviews*, 113: 778

Thomas, R. and Watson, R.M. (2008). Air quality scoping impact assessment for the proposed new Majuba combined cycle gas turbine (CCGT) power plant in the Amersfoort area, Mpumalanga province. Project carried out on behalf of Bohlweki Environmental (Pty) Ltd Project Reference No: E01.JNB.000179 Rev 2, Date of Issue: 31 January 2008

Thorsrud, B.A. and Faqi, A.S. (2011). Developmental and reproductive toxicity of TCDD, lead and mercury. *Encyclopedia of Environmental Health*, 36

UNEP (2008). United Nations Environment Programme. Global Atmospheric Mercury Assessment: Sources, Emissions and Transport, Geneva, 2008 Available at: www.chem.com accessed on January 2012

Uria, J.E.S. and Sanz-Medel, A. (1998). Inorganic and methylmercury speciation in environmental samples. *Talanta*, 47:509

US EPA (1997). Mercury Study Report to Congress, Vol 111, Fate and transport of mercury in the environment. EPA 452/R-97-005

US EPA (1999). Mercury Study Report to Congress. Vol V: Health Effects of Mercury and Mercury Compounds. EPA-452/R-97-007

US EPA (2000). Control of Mercury emissions from coal fired electric utility boilers, EPA 600/R-01-109

U.S. EPA (2005a). Federal Regulations, 40 CFR, Part 63: Revision of December 2000 Regulatory Finding on the Emissions of Hazardous Air Pollutants from Electric Utility Steam Generating Units and the Removal of Coal- and Oil-Fired Electric Utility Steam Generating

Units from the Section 112(c) (Clean Air Mercury Rule (CAMR)). List; Final Rule, Code of Fed Regist, 70 (59):15993

U.S. EPA (2005b). 40 CFR Parts 51, 72, et.al. Rule to Reduce Interstate Transport of Fine Particulate Matter and Ozone (Clean Air Interstate Rule); Revisions to Acid Rain Program; Revisions to the NO_x SIP call; Final Rule; U.S. Environmental Protection Agency: Washington, DC,

Virginia, M. (2002). Chemical Incident Response service, Number 26

Vogt, C. and Conradi, S. (1994). Complex equilibria in capillary zone electrophoresis and their use for the separation of rare earth metal ions. *Analytica Chimica Acta*, 294:145

Wang, Y., Duan, Y., Yang, L., Zhao, C., Shen, X., Zhang, M., Zhuo, Y. and Chen, C. (2009). Experimental study on mercury transformation and removal in coal-fired boiler flue gases. *Fuel Processing Technology*, 90 (5): 643

Wagner, N.J. and Hlatshwayo, B. (2005). The occurrence of potentially hazardous trace elements in five Highveld coals, South Africa. *International Journal of Coal Geology*; 63:228

Wallingford, R. and Ewing, A.G. (1988). Retention of ionic and non-ionic catechols in capillary zone electrophoresis with micellar solutions. *Journal of Chromatography*, 44(1):299

Weinberger, R. (2000). *Practical Capillary Electrophoresis* (Second edition), Academic Press, NYC

Widmer, N. C., West, J. and Cole, J. A. (2004). Proceedings of Air and Waste Management Association's 93rd Annual Conference and Exhibition, Pittsburgh, Pa, 2004

Wilcox, J., Robles, J., Marsden, D.C. and Blowers, P. (2004). Theoretically predicted rate constants for mercury oxidation by hydrogen chloride in coal combustion flue gases. *Environmental Science and Technology*, 37:4199

Wong, Y.C. and Whang, C.W. (1993). High-performance liquid-chromatography of inorganic mercury and organomercury with 2-mercaptobenzthiazole. *Journal of Chromatography*, 628:133

Yan, D., Zhang, J. and Schwedt, G. (1989). Ion-chromatographic trace analysis of mercury, cadmium and zinc by post-column derivatisation with a water-soluble porphyrin. *Fresenius' Journal of Analytical Chemistry*, 334:507

Zhang, L., Daukoru, M., Torkamani, S., Wang, A., Hao, J. and Biwwas, P. (2013). Measurements of mercury speciation and fine particle size distribution on combustion of China coal seams. *Fuel*, 104:732

Zhou, J. and Lunte, S.M. (1995). Simultaneous detection of thiols and disulfides by CE-electrochemical detection using a mixed-valence ruthenium cyanide-modified microelectrode. *Analytical Chemistry*, 67:13

APPENDICES

APPENDIX 1:

Electropherograms for analysis of coal samples from different power stations

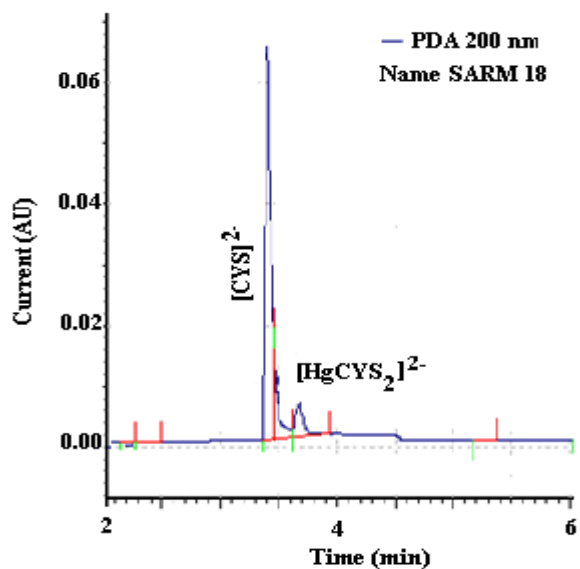


Figure A1.1: Electropherogram of SARM 18 coal complexed with cysteine: buffer 0.025 M sodium borate, pH 9.35, voltage = +25 kV, UV = 200 nm.

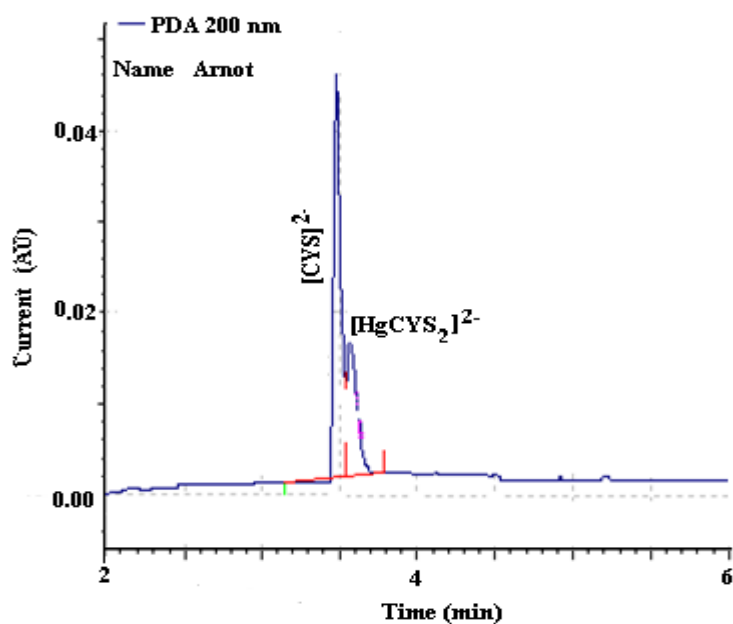


Figure A1.2 Electropherogram of Arnot coal complexed with cysteine: buffer 0.025 M sodium borate, pH 9.35, voltage = +25 kV, UV = 200 nm.

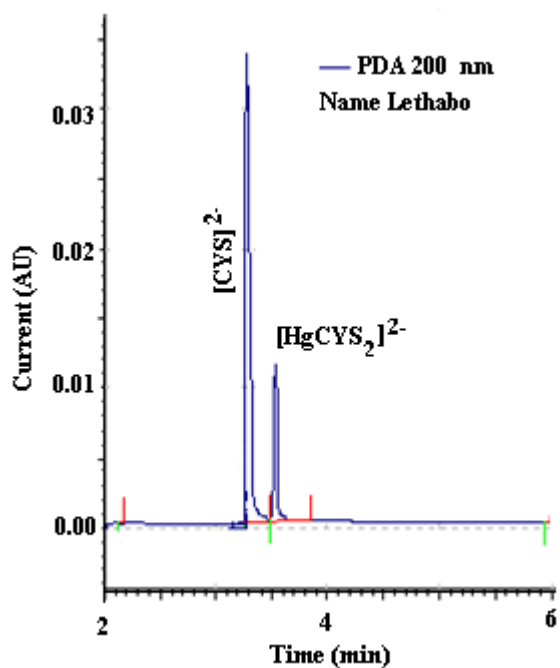


Figure A1.3: Electropherogram of Lethabo coal complexed with cysteine: buffer 0.025 M sodium borate, pH 9.35, voltage = +25 kV, UV = 200 nm.

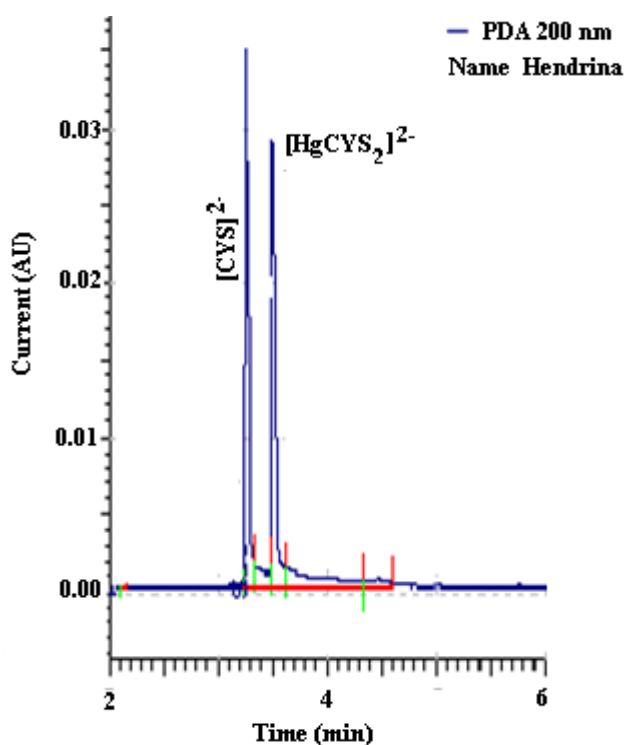


Figure A1.4: Electropherogram of Hendrina coal complexed with cysteine: buffer 0.025 M sodium borate, pH 9.35, voltage = +25 kV, UV = 200 nm.

APPENDIX 2:

Photographs of analytical instruments used



Figure A2.1: Beckman Coulter P/ACE MDQ instrument for capillary electrophoresis.

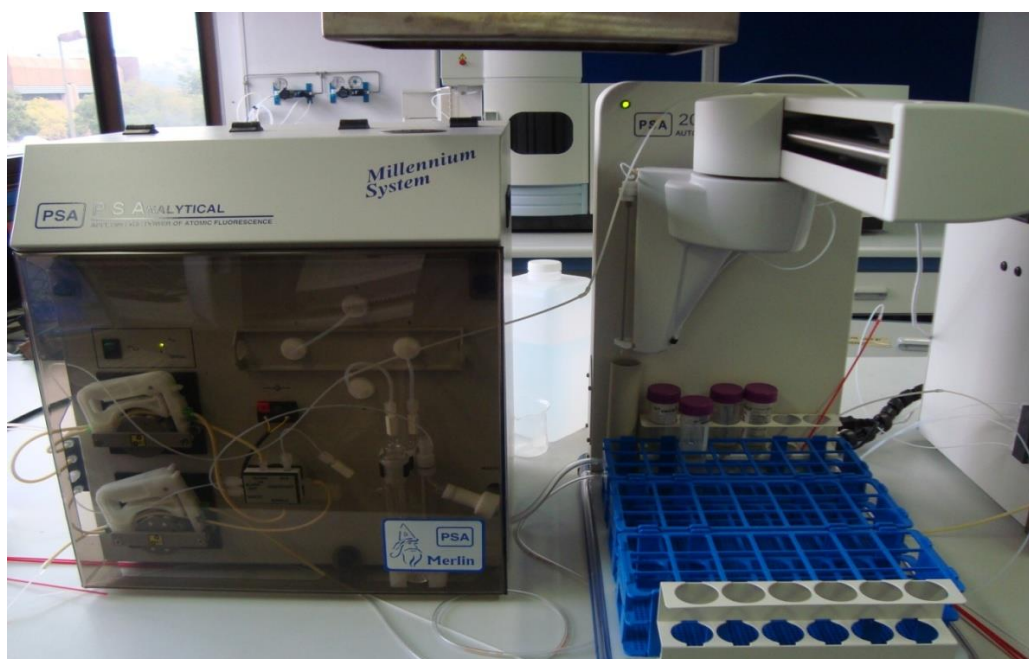


Figure A2. 2: Millennium Merlin atomic fluorescence spectrometer system.



Figure A2.3: Leco AMA 254 mercury analyzer for direct Hg analysis.

APPENDIX 3

Copyright Clearance to use the publications information.

A3.1: Capillary electrophoretic separation and post-column electrochemical detection.

ELSEVIER LICENSE TERMS AND CONDITIONS

Sep 06, 2013

This is a License Agreement between Lulamile T Jongwana ("You") and Elsevier ("Elsevier") provided by Copyright Clearance Center ("CCC"). The license consists of your order details, the terms and conditions provided by Elsevier, and the payment terms and conditions.

All payments must be made in full to CCC. For payment instructions, please see information listed at the bottom of this form.

Supplier	Elsevier Limited The Boulevard, Langford Lane Kidlington, Oxford, OX5 1GB, UK
Registered Company Number	1982084
Customer name	Lulamile T Jongwana
Customer address	Eskom Research center, Germiston, Gauteng 2022
License number	3222981302385
License date	Sep 06, 2013
Licensed content publisher	Elsevier
Licensed content publication	Fuel
Licensed content title	Mercury speciation in South African coal
Licensed content author	Lulamile T. Jongwana, Andrew M. Crouch
Licensed content date	April 2012
Licensed content volume number	94
Licensed content issue number	
Number of pages	6
Start Page	234
End Page	239
Type of Use	reuse in a journal/magazine
Requestor type	author of new work
Intended publisher of new work	Other
Portion	full article
Format	electronic
Are you the author of this Elsevier article?	Yes
Will you be translating?	No
Order reference number	
Title of the article	Capillary electrophoretic separation and post-

Publication new article is in	column electrochemical detection
Publisher of the new article	Electrochimica Acta Elsevier
Author of new article	Lynwill G. Martin, Lulamile T. Jongwana, Andrew M. Crouch
Expected publication date	Nov 2013
Estimated size of new article (number of pages)	6
Elsevier VAT number	GB 494 6272 12
Permissions price	0.00 USD
VAT/Local Sales Tax	0.0 USD / 0.0 GBP
Total	0.00 USD
Terms and Conditions	

INTRODUCTION

1. The publisher for this copyrighted material is Elsevier. By clicking "accept" in connection with completing this licensing transaction, you agree that the following terms and conditions apply to this transaction (along with the Billing and Payment terms and conditions established by Copyright Clearance Center, Inc. ("CCC"), at the time that you opened your Rightslink account and that are available at any time at <http://myaccount.copyright.com/>).

GENERAL TERMS

2. Elsevier hereby grants you permission to reproduce the aforementioned material subject to the terms and conditions indicated.

3. Acknowledgement: If any part of the material to be used (for example, figures) has appeared in our publication with credit or acknowledgement to another source, permission must also be sought from that source. If such permission is not obtained then that material may not be included in your publication/copies. Suitable acknowledgement to the source must be made, either as a footnote or in a reference list at the end of your publication, as follows:

“Reprinted from Publication title, Vol /edition number, Author(s), Title of article / title of chapter, Pages No., Copyright (Year), with permission from Elsevier [OR APPLICABLE SOCIETY COPYRIGHT OWNER].” Also Lancet special credit - “Reprinted from The Lancet, Vol. number, Author(s), Title of article, Pages No., Copyright (Year), with permission from Elsevier.”

4. Reproduction of this material is confined to the purpose and/or media for which permission is hereby given.

5. Altering/Modifying Material: Not Permitted. However figures and illustrations may be altered/adapted minimally to serve your work. Any other abbreviations, additions, deletions and/or any other alterations shall be made only with prior written authorization of Elsevier

Ltd. (Please contact Elsevier at permissions@elsevier.com)

6. If the permission fee for the requested use of our material is waived in this instance, please be advised that your future requests for Elsevier materials may attract a fee.

7. **Reservation of Rights:** Publisher reserves all rights not specifically granted in the combination of (i) the license details provided by you and accepted in the course of this licensing transaction, (ii) these terms and conditions and (iii) CCC's Billing and Payment terms and conditions.

8. **License Contingent Upon Payment:** While you may exercise the rights licensed immediately upon issuance of the license at the end of the licensing process for the transaction, provided that you have disclosed complete and accurate details of your proposed use, no license is finally effective unless and until full payment is received from you (either by publisher or by CCC) as provided in CCC's Billing and Payment terms and conditions. If full payment is not received on a timely basis, then any license preliminarily granted shall be deemed automatically revoked and shall be void as if never granted. Further, in the event that you breach any of these terms and conditions or any of CCC's Billing and Payment terms and conditions, the license is automatically revoked and shall be void as if never granted. Use of materials as described in a revoked license, as well as any use of the materials beyond the scope of an unrevoked license, may constitute copyright infringement and publisher reserves the right to take any and all action to protect its copyright in the materials.

9. **Warranties:** Publisher makes no representations or warranties with respect to the licensed material.

10. **Indemnity:** You hereby indemnify and agree to hold harmless publisher and CCC, and their respective officers, directors, employees and agents, from and against any and all claims arising out of your use of the licensed material other than as specifically authorized pursuant to this license.

11. **No Transfer of License:** This license is personal to you and may not be sublicensed, assigned, or transferred by you to any other person without publisher's written permission.

12. **No Amendment Except in Writing:** This license may not be amended except in a writing signed by both parties (or, in the case of publisher, by CCC on publisher's behalf).

13. **Objection to Contrary Terms:** Publisher hereby objects to any terms contained in any purchase order, acknowledgment, check endorsement or other writing prepared by you, which terms are inconsistent with these terms and conditions or CCC's Billing and Payment terms and conditions. These terms and conditions, together with CCC's Billing and Payment terms and conditions (which are incorporated herein), comprise the entire agreement between you and publisher (and CCC) concerning this licensing transaction. In the event of any conflict between your obligations established by these terms and conditions and those established by CCC's Billing and Payment terms and conditions, these terms and conditions shall control.

14. **Revocation:** Elsevier or Copyright Clearance Center may deny the permissions described in this License at their sole discretion, for any reason or no reason, with a full

refund payable to you. Notice of such denial will be made using the contact information provided by you. Failure to receive such notice will not alter or invalidate the denial. In no event will Elsevier or Copyright Clearance Center be responsible or liable for any costs, expenses or damage incurred by you as a result of a denial of your permission request, other than a refund of the amount(s) paid by you to Elsevier and/or Copyright Clearance Center for denied permissions.

LIMITED LICENSE

The following terms and conditions apply only to specific license types:

15. **Translation:** This permission is granted for non-exclusive world **English** rights only unless your license was granted for translation rights. If you licensed translation rights you may only translate this content into the languages you requested. A professional translator must perform all translations and reproduce the content word for word preserving the integrity of the article. If this license is to re-use 1 or 2 figures then permission is granted for non-exclusive world rights in all languages.

16. **Website:** The following terms and conditions apply to electronic reserve and author websites:

Electronic reserve: If licensed material is to be posted to website, the web site is to be password-protected and made available only to bona fide students registered on a relevant course if:

This license was made in connection with a course,

This permission is granted for 1 year only. You may obtain a license for future website posting,

All content posted to the web site must maintain the copyright information line on the bottom of each image,

A hyper-text must be included to the Homepage of the journal from which you are licensing at <http://www.sciencedirect.com/science/journal/xxxxx> or the Elsevier homepage for books at <http://www.elsevier.com/> , and

Central Storage: This license does not include permission for a scanned version of the material to be stored in a central repository such as that provided by Heron/XanEdu.

17. **Author website** for journals with the following additional clauses:

All content posted to the web site must maintain the copyright information line on the bottom of each image, and the permission granted is limited to the personal version of your paper. You are not allowed to download and post the published electronic version of your article (whether PDF or HTML, proof or final version), nor may you scan the printed edition to create an electronic version. A hyper-text must be included to the Homepage of the journal from which you are licensing at <http://www.sciencedirect.com/science/journal/xxxxx> . As part of our normal production process, you will receive an e-mail notice when your article appears on Elsevier's online service ScienceDirect (www.sciencedirect.com). That e-mail will include the article's Digital Object Identifier (DOI). This number provides the electronic link to the published article and should be included in the posting of your personal version. We ask that you wait until you receive this e-mail and have the DOI to do any posting.

Central Storage: This license does not include permission for a scanned version of the

material to be stored in a central repository such as that provided by Heron/XanEdu.

18. **Author website** for books with the following additional clauses: Authors are permitted to place a brief summary of their work online only. A hyper-text must be included to the Elsevier homepage at <http://www.elsevier.com/> . All content posted to the web site must maintain the copyright information line on the bottom of each image. You are not allowed to download and post the published electronic version of your chapter, nor may you scan the printed edition to create an electronic version.

Central Storage: This license does not include permission for a scanned version of the material to be stored in a central repository such as that provided by Heron/XanEdu.

19. **Website** (regular and for author): A hyper-text must be included to the Homepage of the journal from which you are licensing at <http://www.sciencedirect.com/science/journal/xxxxx>. or for books to the Elsevier homepage at <http://www.elsevier.com>

20. **Thesis/Dissertation**: If your license is for use in a thesis/dissertation your thesis may be submitted to your institution in either print or electronic form. Should your thesis be published commercially, please reapply for permission. These requirements include permission for the Library and Archives of Canada to supply single copies, on demand, of the complete thesis and include permission for UMI to supply single copies, on demand, of the complete thesis. Should your thesis be published commercially, please reapply for permission.

21. Other Conditions:

v1.6

If you would like to pay for this license now, please remit this license along with your payment made payable to "COPYRIGHT CLEARANCE CENTER" otherwise you will be invoiced within 48 hours of the license date. Payment should be in the form of a check or money order referencing your account number and this invoice number RLNK501106790. Once you receive your invoice for this order, you may pay your invoice by credit card. Please follow instructions provided at that time.

Make Payment To:

Copyright Clearance Center

Dept 001

P.O. Box 843006

Boston, MA 02284-3006

For suggestions or comments regarding this order, contact RightsLink Customer Support: customer@copyright.com or +1-877-622-5543 (toll free in the US) or +1-978-646-2777.

Gratis licenses (referencing \$0 in the Total field) are free. Please retain this printable license for your reference. No payment is required.

-5555		0016-2361			false
printableLicense			4357407	/App/Includes/Pri	/App/PrintableLic
/App/Includes/No	1378460116044	MsW5sWqOIMCO	unknow n	unknow n	

A3.2: Mercury speciation in South African coal.

ELSEVIER LICENSE TERMS AND CONDITIONS

Sep 06, 2013

This is a License Agreement between Lulamile T Jongwana ("You") and Elsevier ("Elsevier") provided by Copyright Clearance Center ("CCC"). The license consists of your order details, the terms and conditions provided by Elsevier, and the payment terms and conditions.

All payments must be made in full to CCC. For payment instructions, please see information listed at the bottom of this form.

Supplier	Elsevier Limited The Boulevard, Langford Lane Kidlington, Oxford, OX5 1GB, UK
Registered Company Number	1982084
Customer name	Lulamile T Jongwana
Customer address	Eskom Research center, Germiston, Gauteng 2022
License number	3222980969742
License date	Sep 06, 2013
Licensed content publisher	Elsevier
Licensed content publication	Fuel
Licensed content title	Mercury speciation in South African coal
Licensed content author	Lulamile T. Jongwana, Andrew M. Crouch
Licensed content date	April 2012
Licensed content volume number	94
Licensed content issue number	
Number of pages	6
Start Page	234
End Page	239
Type of Use	reuse in a journal/magazine
Requestor type	author of new work
Intended publisher of new work	Other
Portion	full article
Format	electronic
Are you the author of this Elsevier article?	Yes
Will you be translating?	No
Order reference number	
Title of the article	Mercury speciation in South African coal
Publication new article is in	Fuel
Publisher of the new article	Elsevier
Author of new article	Lulamile T. Jongwana, Andrew M. Crouch

Expected publication date	Nov 2013
Estimated size of new article (number of pages)	6
Elsevier VAT number	GB 494 6272 12
Permissions price	0.00 USD
VAT/Local Sales Tax	0.0 USD / 0.0 GBP
Total	0.00 USD

Terms and Conditions

INTRODUCTION

1. The publisher for this copyrighted material is Elsevier. By clicking "accept" in connection with completing this licensing transaction, you agree that the following terms and conditions apply to this transaction (along with the Billing and Payment terms and conditions established by Copyright Clearance Center, Inc. ("CCC"), at the time that you opened your Rightslink account and that are available at any time at <http://myaccount.copyright.com/>).

GENERAL TERMS

2. Elsevier hereby grants you permission to reproduce the aforementioned material subject to the terms and conditions indicated.

3. Acknowledgement: If any part of the material to be used (for example, figures) has appeared in our publication with credit or acknowledgement to another source, permission must also be sought from that source. If such permission is not obtained then that material may not be included in your publication/copies. Suitable acknowledgement to the source must be made, either as a footnote or in a reference list at the end of your publication, as follows:

“Reprinted from Publication title, Vol /edition number, Author(s), Title of article / title of chapter, Pages No., Copyright (Year), with permission from Elsevier [OR APPLICABLE SOCIETY COPYRIGHT OWNER].” Also Lancet special credit - “Reprinted from The Lancet, Vol. number, Author(s), Title of article, Pages No., Copyright (Year), with permission from Elsevier.”

4. Reproduction of this material is confined to the purpose and/or media for which permission is hereby given.

5. Altering/Modifying Material: Not Permitted. However figures and illustrations may be altered/adapted minimally to serve your work. Any other abbreviations, additions, deletions and/or any other alterations shall be made only with prior written authorization of Elsevier Ltd. (Please contact Elsevier at permissions@elsevier.com)

6. If the permission fee for the requested use of our material is waived in this instance, please be advised that your future requests for Elsevier materials may attract a fee.

7. Reservation of Rights: Publisher reserves all rights not specifically granted in the combination of (i) the license details provided by you and accepted in the course of this

licensing transaction, (ii) these terms and conditions and (iii) CCC's Billing and Payment terms and conditions.

8. License Contingent Upon Payment: While you may exercise the rights licensed immediately upon issuance of the license at the end of the licensing process for the transaction, provided that you have disclosed complete and accurate details of your proposed use, no license is finally effective unless and until full payment is received from you (either by publisher or by CCC) as provided in CCC's Billing and Payment terms and conditions. If full payment is not received on a timely basis, then any license preliminarily granted shall be deemed automatically revoked and shall be void as if never granted. Further, in the event that you breach any of these terms and conditions or any of CCC's Billing and Payment terms and conditions, the license is automatically revoked and shall be void as if never granted. Use of materials as described in a revoked license, as well as any use of the materials beyond the scope of an unrevoked license, may constitute copyright infringement and publisher reserves the right to take any and all action to protect its copyright in the materials.

9. Warranties: Publisher makes no representations or warranties with respect to the licensed material.

10. Indemnity: You hereby indemnify and agree to hold harmless publisher and CCC, and their respective officers, directors, employees and agents, from and against any and all claims arising out of your use of the licensed material other than as specifically authorized pursuant to this license.

11. No Transfer of License: This license is personal to you and may not be sublicensed, assigned, or transferred by you to any other person without publisher's written permission.

12. No Amendment Except in Writing: This license may not be amended except in a writing signed by both parties (or, in the case of publisher, by CCC on publisher's behalf).

13. Objection to Contrary Terms: Publisher hereby objects to any terms contained in any purchase order, acknowledgment, check endorsement or other writing prepared by you, which terms are inconsistent with these terms and conditions or CCC's Billing and Payment terms and conditions. These terms and conditions, together with CCC's Billing and Payment terms and conditions (which are incorporated herein), comprise the entire agreement between you and publisher (and CCC) concerning this licensing transaction. In the event of any conflict between your obligations established by these terms and conditions and those established by CCC's Billing and Payment terms and conditions, these terms and conditions shall control.

14. Revocation: Elsevier or Copyright Clearance Center may deny the permissions described in this License at their sole discretion, for any reason or no reason, with a full refund payable to you. Notice of such denial will be made using the contact information provided by you. Failure to receive such notice will not alter or invalidate the denial. In no event will Elsevier or Copyright Clearance Center be responsible or liable for any costs, expenses or damage incurred by you as a result of a denial of your permission request, other than a refund of the amount(s) paid by you to Elsevier and/or Copyright Clearance Center for denied permissions.

LIMITED LICENSE

The following terms and conditions apply only to specific license types:

15. **Translation:** This permission is granted for non-exclusive world **English** rights only unless your license was granted for translation rights. If you licensed translation rights you may only translate this content into the languages you requested. A professional translator must perform all translations and reproduce the content word for word preserving the integrity of the article. If this license is to re-use 1 or 2 figures then permission is granted for non-exclusive world rights in all languages.

16. **Website:** The following terms and conditions apply to electronic reserve and author websites:

Electronic reserve: If licensed material is to be posted to website, the web site is to be password-protected and made available only to bona fide students registered on a relevant course if:

This license was made in connection with a course, This permission is granted for 1 year only. You may obtain a license for future website posting,

All content posted to the web site must maintain the copyright information line on the bottom of each image,

A hyper-text must be included to the Homepage of the journal from which you are licensing at <http://www.sciencedirect.com/science/journal/xxxxx> or the Elsevier homepage for books at <http://www.elsevier.com/>, and

Central Storage: This license does not include permission for a scanned version of the material to be stored in a central repository such as that provided by Heron/XanEdu.

17. **Author website** for journals with the following additional clauses:

All content posted to the web site must maintain the copyright information line on the bottom of each image, and the permission granted is limited to the personal version of your paper. You are not allowed to download and post the published electronic version of your article (whether PDF or HTML, proof or final version), nor may you scan the printed edition to create an electronic version. A hyper-text must be included to the Homepage of the journal from which you are licensing at <http://www.sciencedirect.com/science/journal/xxxxx>. As part of our normal production process, you will receive an e-mail notice when your article appears on Elsevier's online service ScienceDirect (www.sciencedirect.com). That e-mail will include the article's Digital Object Identifier (DOI). This number provides the electronic link to the published article and should be included in the posting of your personal version. We ask that you wait until you receive this e-mail and have the DOI to do any posting.

Central Storage: This license does not include permission for a scanned version of the material to be stored in a central repository such as that provided by Heron/XanEdu.

18. **Author website** for books with the following additional clauses: Authors are permitted to place a brief summary of their work online only. A hyper-text must be included to the Elsevier homepage at <http://www.elsevier.com/>. All content posted to the web site must maintain the copyright information line on the bottom of each image. You are not allowed to download and post the published electronic version

of your chapter, nor may you scan the printed edition to create an electronic version.

Central Storage: This license does not include permission for a scanned version of the material to be stored in a central repository such as that provided by Heron/XanEdu.

19. **Website** (regular and for author): A hyper-text must be included to the Homepage of the journal from which you are licensing at <http://www.sciencedirect.com/science/journal/xxxxx>. or for books to the Elsevier homepage at <http://www.elsevier.com>

20. **Thesis/Dissertation**: If your license is for use in a thesis/dissertation your thesis may be submitted to your institution in either print or electronic form. Should your thesis be published commercially, please reapply for permission. These requirements include permission for the Library and Archives of Canada to supply single copies, on demand, of the complete thesis and include permission for UMI to supply single copies, on demand, of the complete thesis. Should your thesis be published commercially, please reapply for permission.

21. Other Conditions:

v1.6

If you would like to pay for this license now, please remit this license along with your payment made payable to "COPYRIGHT CLEARANCE CENTER" otherwise you will be invoiced within 48 hours of the license date. Payment should be in the form of a check or money order referencing your account number and this invoice number RLNK501106787. Once you receive your invoice for this order, you may pay your invoice by credit card. Please follow instructions provided at that time.

Make Payment To:
Copyright Clearance Center
Dept 001
P.O. Box 843006
Boston, MA 02284-3006

For suggestions or comments regarding this order, contact RightsLink Customer Support: customercare@copyright.com or +1-877-622-5543 (toll free in the US) or +1-978-646-2777.

Gratis licenses (referencing \$0 in the Total field) are free. Please retain this printable license for your reference. No payment is required.

-5555	ELS	0016-2361			false
printableLicense			4357407	/App/Includes/Pri	/App/PrintableLic
/App/Includes/No	1378460263833	7i2djKMuoK2N1E5	unknow n	unknow n	